TITLE A STUDY ON OXYHALIDE GLASSES

AUTHOR M.R. SAHAR

INSTITUTION and DATE University of Warwick 1990

REDUCTION X 20

CAMERA 6

A STUDY ON OXYHALIDE GLASSES

by

M.R.SAHAR

For submission for the
degree of Doctor of Philosophy

University of Warwick
Department of Physics
March 1990

DECLARATION

This dissertation is submitted to the University of Warwick in support of my application for admission to the degree of Doctor of Philosophy. It is an account of my work carried out in the Department of Physics, University of Warwick during the period October 1986 to October 1989 and, except where specifically acknowledged in the text, is a result of my own independent research. No part of this thesis has been submitted in respect of a degree to this or any other university.

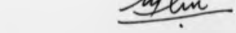

MARCH 1990

M.R.SAHAR

ACKNOWLEDGEMENT

I would like to record my thanks to my supervisor, Dr. Diana Holland, for her continued interest and guidance throughout the course of this work and for the careful reading of the manuscript. Also, of great technical assistance were H. Mathers, B. Lamb and the other members of the glass ceramics group, S.York and G. Smith for their aid with the scanning electron microscopy.

My thanks also to the University Technology of Malaysia and to the Public Services Department of Malaysia who jointly provided financial support.

Finally, my thanks go to my wife, Sabariah, for her encouragement, and for her care and attention to my daughters, Sarah and Asmida, throughout the period of this work.

LIST OF CONTENTS

CHAPTER 4 : RESULTS

ABSTRACT

Oxychloride glasses in the ternary system Sb_2O_3 - $PbCl_2$ - $ZnCl_2$ have been prepared. The thermal properties and the crystallisation behaviour of these glasses have been investigated by differential scanning calorimetry, viscometry, x - ray diffraction, scanning electron microscopy with energy dispersive x - ray analysis and infra - red spectroscopy.

Thermal stability gaps, $T_c - T_g$ up to 149 °C are observed. The predominant crystal phases formed, depending on composition, are $ZnCl_2$, Sb_2O_3 and a lead antimony oxychloride Sillen phase whose stoichiometry varies with glass composition from $PbSb_2O_{3.5}Cl_3$ to $PbSb_2O_{3.5}Cl$. Relative crystal growth rates for the glasses have also been measured and values up to 0.16 μm sec^{-1} are observed. These values are found to be strongly dependent on the chlorine content of the glasses as are also the viscosity characteristics.

The chemical durability of the glasses has also been studied under various conditions. Initial water dissolution rates between 10^{-2} to 10^{-4} gm cm^{-2} day^{-1} were observed. The corrosion rates were found to be chlorine content dependant and reaction mechanisms are suggested.

The introduction of a heavy metal chloride such as $BiCl_3$ or $TlCl$, as a fourth component, was found to increase the chlorine content without much affecting the thermal stability. However, an excessive amount of chlorine makes the glass less durable.

LIST OF FIGURES

LIST OF TABLES

LIST OF ABBREVIATIONS

JCPDS - Joint Committee For Powder Diffraction Standards.

DSC - Differential Scanning Calorimetry.

SEM - Scanning Electron Microscopy.

XRD - X - Ray Diffraction.

IR - Infra red

EDX - Energy Dispersive X-ray Analysis.

TEM - Transmission Electron Microscopy.

RH - Relative Humidity.

UV - Ultra violet

DTA - Differential Thermal Analysis

CHAPTER 1 : INTRODUCTION

1.1 Introduction

Glasses are mostly isotropic, homogeneous materials and thus highly suited to the transmission of light, and hence useful in making optical fibres. The best glasses are those that show a high percentage of transmission at the required wavelength. The factors affecting transmission are scattering and absorption losses, which are classified into extrinsic and intrinsic. Extrinsic scattering losses are caused by such imperfections as bubbles or microcrystals, while extrinsic absorption losses originate from impurities such as OH ions or rare metal ions. Impurities can be eliminated by purification while defects can be minimised by optimised processing. Thus, only intrinsic losses would remain. These are composed of Rayleigh scattering, UV and IR absorption. Rayleigh scattering is caused by microfluctuations in the refractive index, while UV absorption originates from the electronic bandgap transitions. Both factors decrease with increased wavelength. The IR absorption, which is due to multiphonon absorption, increases with wavelength and can be related to the material properties by the equation $\nu \propto (k/\mu)^{1/2}$ (1) where ν is the vibration frequency, k is the force constant and μ is the reduced mass of the vibrating unit. Hence, high

IR transmission is favoured by glass formers which contain heavy elements (high reduced mass), interacting by weak force constants (low field strength and bond strength). On the other hand, light masses and strong force constants lead to high strength, high melting point and low thermal expansion.

Oxides such as SiO_2 - based glasses belong to the latter category which reflect their high thermal stability (2). However, their IR transmission is restricted to less than 4.5 µm, due to Si-O vibration (3). Also, the presence of an OH absorption band is observed around 3 - 4 µm (4). GeO_2 - based glasses give better IR transmission, up to 5.7 µm (5), presumably due to higher reduced mass, but, their application is not only limited by Ge-O absorption band (6) but also by the high solubility of these glasses in water (7). TeO_2 - based glasses also encounter the same problems (8). In summary, oxide glasses are only useful in the near IR to mid IR region (less than 5 µm). For longer wavelengths, other systems have to be developed.

Halides have been considered to have the most appropriate optical properties (for optical fibre design) because of their low intrinsic loss and thus reasonable IR transmission characteristic. $ZnCl_2$ - based glasses often show IR transmission beyond 10 µm (9) but exploitation is highly limited by the hygroscopicity of the glasses even if the composition is modified by additional chloride (10). BeF_2 easily forms a glass on cooling from the molten state (11).

However, this glass was reported to be highly toxic and too hygroscopic for practical handling and use (12). ZrF_4 - based glasses are probably the most promising group of new glasses (13). IR transmission up to 7 um in the far IR region (14) and thermal stability up to 100 °C (12) were observed. The most limiting factor is their low durability (15) and the fact that fibre drawing conditions often lead to devitrification (16). In summary, most halide glasses show considerable IR transmission but their chemical durability is low as a consequence of the weak M-X bond (X = halide) (8). This limits their practical usage.

Because of the problems encountered both by oxide and halide glasses, it is of interest to develop other IR transmitting materials which will show characteristics intermediate between these glasses. This led to the development of oxyhalide glasses, originally intended for ultra low loss optical fibres in the mid to far IR region. Until recently, the dominant systems were of the oxychloride glass systems (17,18,19). These glasses exhibit some promising characteristics especially for longer wavelength usage. They are stable in air (17), have high IR transmission and wide glass formation ranges (18) and should provide a compromise in properties between those of oxide and pure halide glasses (18).

Thus, oxychloride glasses can be potential candidates for IR transmitting materials. However, the lack of information on their thermal and chemical stability has restricted

interest in these materials. It was therefore important that a systematic study of these systems be carried out in order to provide more information.

1.2 Aims Of The Project.

A group of oxychlorides which form stable glasses and have wide formation ranges has been prepared. In order to provide more information on thermal and chemical properties, the following studies were carried out :-

1. Analytical and microstructural study.

The aim of this study is to establish the nature of the phase development in the glasses. This is important since any information on the crystal phase may be related to the structural units in the glass and the thermal stability of the glass. In doing so, the techniques of DSC, XRD, SEM and IR spectroscopy will be employed.

2. The study of the relationship of glass viscosity and crystal growth behaviour to glass composition.

This study will provide information on the thermal behaviour of the glass which is crucial when it comes to real applications, especially fibre drawing. The relation between crystal growth or viscosity and the glass

composition will indicate how thermal behaviour is controlled by the glass structure. The uncontrolled growth of crystals is an important contribution to extrinsic scattering loss behaviour.

3. A study on chemical durability under various conditions.

This is important in that it will show how chemically stable the glasses are under a variety of application conditions. Furthermore, the variation of durability with glass composition will provide an indication of the changes in glass structure.

4. The effect of heavy halides in the systems.

As heavy elements will increases the reduced mass (and, in theory, shift the phonon edge to longer wavelength), it is of particular interest to see their effect on thermal and chemical characteristics of the glasses.

1.3 Choice Of Systems

To achieve the aims of the project, a series of oxychloride glass systems were chosen. They are :-

Binary :

- $(1-x)\ Sb_2O_3 - x\ ZnCl_2$ $\quad 0.2 < x < 0.6$
- $(1-x)\ Sb_2O_3 - x\ PbCl_2$ $\quad 0.3 < x < 0.5$

Ternary :

- $(0.7-x)\ Sb_2O_3$ - $0.3\ PbCl_2$ - $x\ ZnCl_2$ $\quad 0.1 < x < 0.5$
- $(0.7-x)\ Sb_2O_3$ - $0.3\ PbCl_2$ - $x\ TlCl$ $\quad 0.05 < x < 0.1$
- $(0.7-x)\ Sb_2O_3$ - $0.3\ PbCl_2$ - $x\ BiCl_3$ $\quad 0.05 < x < 0.1$

Quaternary :

- $(0.4-x)\ Sb_2O_3$ - $0.3\ PbCl_2$ - $0.3\ ZnCl_2$ - $x\ TlCl$ $\quad 0.05 < x < 0.1$

Oxychlorides of these groups were chosen not only to remedy the lack of information in the literature, but also because these glasses are transparent up to 8.8 μm and have Tc - Tg gaps up to 149 °C, ie; potentially good for IR fibres. The choice of TlCl and $BiCl_3$ as heavy halide candidates is simply because they have similar chemical properties to $PbCl_2$. Hence, any difference in their effect, will partly be attributable to their higher atomic number. These halides will also contribute to the amount of chlorine in the systems. This could be an interesting subject.

1.4 Thesis Plan

The contents of the thesis will be divided into chapters as follows :-

Chapter 2 reviews the background of current knowledge regarding some of the infra-red transmitting glasses, in particular halide and oxyhalide glasses. The concept of glass stability will also be reviewed. This chapter also surveys (in general) several methods for viscosity measurement. Finally, this chapter gives an account of the theory of normal growth rate.

Chapter3 describes the experimental techniques employed in the research programme. These will include glass preparation, thermal analysis, SEM and IR analysis. In the case of crystal growth rates, their calculation using an averaging method will also be indicated. The indentation method for viscosity measurement is described. Finally, chemical durability studies are outlined.

Chapter 4 contains all the experimental results obtained from the investigation on thermal behaviour, microstructural and phase development , and chemical durability characteristics of the glasses.

Chapter 5 discusses the overall experimental findings, with emphasis on the correlation between the chlorine content in the glass with the observed changes in thermal and chemical behaviour of the glasses. This chapter will also discuss the effect of introducing heavy metal halides into the glass with respect to the chlorine content. The corrosion

mechanism will also be discussed and a reaction mechanism suggested. A section is devoted to describing the finding of new Sillen phase compositions.

Chapter 6 summarizes the conclusions which can be drawn from the above discussion.

Suggestions for future work will be made in chapter 7.

Appendix 1 gives an account of the calculation on glass constituents obtained from EDX data.

References

1. Kittel, C. ; Intro. To Solid State Physics, John Wiley and Sons. Inc. 6 th. ed. (1986).
2. Mazurin, O.V., Streletsina, M.V. and Shvaiko - Shvaikovskya, T.P. ; Handbook Of Glass Data, vol 1, Elsvier, (1983).
3. Donald, I.W. and McMillan, P.W. ; J. Mater. Sci. 13 (1978) 1151-1176.
4. Florence, J.M., Glaze, F.W., and Black, M.H. ; J. Res. Nat. Bur. Stand. 50 (1947) 703.
5. Cleek, G.W. and Hamilton, H.E. ; US Patent 3 119 (1964) 703.
6. Murthy, M.K. and Kirby, E.M. ; Phys. Chem. Glasses, 5 (1964) 144.
7. Murthy, M.K. and Hill, H. ; J. Amer. Ceram. Soc. 48 (1965) 109.
8. Ulrich, D.R. ; J. Amer. Ceram. Soc. 47 (1964) 595.
9. Lucas, J. ; Halide Glass, in Glass ...Current Issue, ed. A.F. Wright and J. Dupuy, Martinus Nijhoff Pub. (1985).
10. Savage, J.A. ; Int. Sym. Hal. and Non-Oxide Glass 1, Cambridge, UK (1982).
11. Sun, K.H. ; US Patent 2 466 507 (1949).
12. Miyashita, T. and Manabe, T, ; IEEE, J. Quant. Elect. QE-18, 10 (1982) 1432.
13. Poulain, M. and Poulain, M. ; Mater. Res. Bull. 10 (1975) 243-246.

14. Takahashi, S., Shibata, S., Kanamori, T., Mitachi, S. and Manabe, T. ; Physics For Fibre Optic, in Advances In Ceramics, vol 2, ed. B.Bendow and S.S.Mitra (1981) 74-82.

15. Simmons, C.J. and Simmons, J.H. ; J.Amer. Ceram. Soc. 69(9) (1986) 681-69.

16. Lau, J., Nakata, A.M. and Mackenzie, J.D. ; J. Of Non-Cryst. Sol. 70 (1985) 233-242.

17. Dubois, B., Aomi, H., Videau, J.J, Portier, J. and Hagenmuller, P. ; Mat. Res. Bull. 19 (1984) 1317.

18. Ahmed, M.M and Holland, D. ; Mater. Sci. Forum (1987) 19-20.

19. Ahmed, M.M. and Holland, D. ; Glass Tech. Vol 28, no3 (1987) 141.

CHAPTER 2 : BACKGROUND

2.1 Introduction

The ASTM defines a glass as " an inorganic product of fusion which has been cooled to a rigid condition without crystallising " or, a glass is a material formed by cooling from normal liquid state which has shown no discontinous change at any temperature but has become more or less rigid through a progressive increase in its viscosity. This describes what could be called the classical formation from the melt.

Glass formation has been observed in a very large number of inorganic systems. Until recently, glass chemistry has been largely dominated by oxide systems, the most common being silicate glasses which are based on SiO_2, whilst others include glasses based on B_2O_3, P_2O_5, GeO_2 and As_2O_3. These materials provide a very strong tridimensional (3D) covalent network which is needed to form a glass and are the so - called " glass - formers". If we consider melts made from two or more components, the range of oxide glasses is enormously extended, for example melting any glass - forming oxide with an alkali metal oxide.

Halide glasses based on BeF_2 were first identified by Goldschmidt (1), while Heyne (2) prepared the fluoroberyllate glasses. At about the same time, Warren and Hill (3) found that BeF_2 has the same tetrahedral type of

structure as vitreous SiO_2. This work has been continued intensively by Sun and co - workers (4 - 8). $ZnCl_2$ based glasses were first discovered by Maier (9). The glass forming ability of this material has been attributed in part to its low bond ionicity (10) and low melting temperature (11). The binary $ZnCl_2$ glasses containing an alkali halide component were found to be more stable than vitreous $ZnCl_2$ (12). Formation of ZrF_4 based glasses was first reported by Poulain et. al (13). This compound has been characterised as a " glass network former " to which other compounds are added in order to prepare a vitreous material. These include " network modifiers " such as BaF_2 (14,15) and intermediate compounds such as ThF_4 (16) and HfF_4 (17,18). Other less important halide glasses have been reported over the years. Some of them are glasses based on AgCl, AgI and $PbBr_2$ (19), $PbCl_2$-$BaCl_2$ (20), TlCl (21), $SnCl_2$. PbI_2 (22) and many others. Information on these systems is limited and the glass forming regions are unknown.

Oxyhalide glass systems based on Sb_2O_3 were first reported by Dubois et. al (23). The work was based on the general formula of (1-x) Sb_2O_3 - xRX_2 (X = F, Cl, Br or I), where RX_2 is a halide chosen from MnF_2, $MnCl_2$, $MnBr_2$, PbCl2, $PbBr_2$, PbI_2, $SrCl_2$ or $BaCl_2$. The report also presented the glass - forming limits of each system. Dubois (24) also reported a structural study of the above system. A similar system has been reported by Ahmed and Holland (25). The same authors also reported the preparation of the PbO - GeO_2 -

$PbCl_2$ glass system (26). The glass forming tendency of a oxyhalide system has particularly been studied by Ota and Soga (27) using the $NaPO_3$ - $MnCl_2$ glass composition. Other oxyhalide glass system such as PbO - $PbCl_2$ (28), Sb_2O_3 - $SbCl_3$ / $CdCl_2$ (29) have also been prepared. However, it should be noted that mixtures of $ZnCl_2$ with Na_2SO_4 or K_2SO_4 (12) would not form a glass.

Most of the glass systems provide a wide glass - forming region including the halide and oxyhalide systems. These glasses may provide characteristics which suit some applications although a compromise must be made between the stability and optical transmission of such systems.

2.2 Infra - Red Transmitting Glasses

In 1951, Kapany (30) made the first serious study of the transmission of images along uncoated and plastic coated aligned bundles of flexible oxide glass fibres. In fact, he was the first to apply the term " fibre optics " defining it as the art of active and passive guidance of light rays in the spectral regions (UV, V and IR) along transparent fibres over a predetermined path. Of the three regions mentioned above, the infra red region is of most interest because of its wide range of applications. The main application is in communications especially for very long, repeaterless, communication links (31). Others include infra

- red lenses, new optical - fibre sensors, infra - red laser components and related laser surgery (32), a very good prospect for electro - chemical devices (33) and many others such as windows and domes that protect detection systems from the environment. Depending on the field of application other factors such as mechanical properties, thermal and chemical stability are also matters of great concern.

The most important criteria in the selection of an infrared fibre material are that it can be formed into a homogeneous fibre of considerable length and that it will have low optical loss. The loss mechanisms consist of absorption and scattering which are classified into intrinsic and extrinsic factors. The intrinsic losses consist of UV absorption, Rayleigh scattering and IR absorption .

The UV absorption coefficient (α_{uv}) may be expressed by the relation (34):

$$\alpha_{uv} = A \exp (B / \lambda)$$

where A and B are constants and λ is the wavelength.

The probability of interaction (ie: increased absorption) is maximum at short wavelength and decreases as the wavelength increases. At longer wavelengths (ie: visible or infrared regions), the possibility becomes small although not zero. This absorption is due to electronic transitions between electron states and is a function of the energy gap of the material.

The dependence of Rayleigh scattering on wavelength is expressed as (34):

$$\alpha_{sc} = C / \lambda^4$$

where C is a constant which depends on the material. As we know, glass is not purely homogeneous. There exist regions of higher and lower density, resulting in a small variation of refractive index and therefore of light velocity. The effect is more significant for shorter wavelengths.

The IR absorption coefficient (α_{ir}) which is due to multiphonon absorption can be described as (34):

$$\alpha_{ir} = D \exp (- E / \lambda)$$

where D and E are constants. Because of thermal excitation, atoms and molecules are constantly in motion. As these motions occur, they define a stationary vibrational system with a certain level of energy. For the simplest mode of vibration of a linear diatomic molecule consisting of two point masses, M_1 and M_2, the vibrational frequency average ($\bar{\nu}$) according to this model is given by the Szigeti relation (35) :

$$\bar{\nu} = 1/2\pi (f/\mu)^{1/2}$$

where the reduced mass $\mu = (M_1 M_2 / M_1 + M_2)$ and f is the force constant. This means that heavier ions and weaker bonding forces are preferable for the IR absorption to be located at sufficiently long wavelength.

The combination of these three loss mechanisms leads to theoretical curves as shown in fig 2.1 (38). The total loss decreases as the operational transmittance wavelength increases until a cross - over point is reached where the total loss again increases, because at longer wavelength the loss is dominated by the multiphonon absorption .

The V - curve (fig 2.1) is a useful quantitative tool for assessing infrared optical materials as candidates for optical fibres. This curve determines the theoretical lowest limit of attenuation at a certain wavelength. For the low loss required by telecommunications, the attenuation for an infrared fibre should approach the lowest limit determined by this curve.

In this figure, the effect of increasing atomic weight of the cation and / or anion in promoting extended transmittance into the infrared is clearly seen. Thus, it is clear that silicates are only useful in the near infrared and that it is necessary to resort to heavy metal halide or oxyhalide materials for the mid and far infrared wavebands.

The extrinsic absorption losses have a noticeable contributions from impurities in the glass matrix. Factors which may produce refractive index inhomogeneity such as

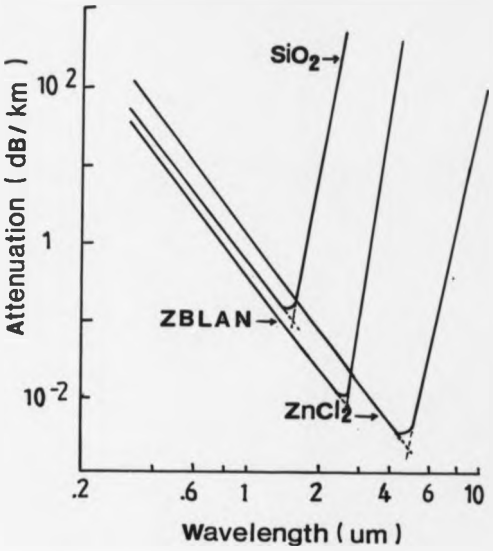

Fig. 2.1 : Intrinsic loss for some glasses (36)

defects, bubbles, local variation in composition and others are sources of extrinsic scattering losses. However, normally, optical glasses are in principle free from such defects and the only losses should come from various impurities such as hydroxyl ions (OH^-), transition metal ions (Fe^{2+}, Cr^{3+}, ...) and other complex anions. Each of these ions may contribute adsorption bands of different shapes, intensity and position.

The materials used for infrared transmitting fibres fall into two categories: crystalline and glass. Crystalline materials from which fibre can be prepared practically are limited while glass material is very suitable for the fabrication of optical fibre although a suitable composition needs to be selected to form a sufficiently stable glass without devitrification during the fibre fabrication.

2.2.1 Oxide Glasses

Oxide glasses especially SiO_2 based or containing B_2O_3, P_2O_5, V_2O_5 have been reported extensively (37) especially for IR optical fibres. However, silica glass has an intrinsic limit mainly caused by the fundamental Si-O vibration and absorption bands at shorter wavelength due to the presence of OH^- or due directly to the effect of additives on the silica network. Work has been done (38,39) to eliminate the presence of OH-bands as well as weakening

the Si-O bond by use of additives in the system. Glasses based on B_2O_3 and P_2O_5 exhibit very limited infra - red transmission due to their high vibrational frequencies associated with B-O and P-O bonds respectively. Many workers also have tried using heavy metal oxide based glasses such as GeO_2, TeO_2, Bi_2O_3, Sb_2O_3 and others. Work has been done on GeO_2 based glass (40-41) but most of the glasses still show prominent hydroxyl absorption. Furthermore, vitreous GeO_2 powder is very soluble in water (42). Glasses based on TeO_2 have been prepared (for instance by Ulrich (43)). All the glasses transmitted well in the infrared up to 6.3 μm, but an absorption band was observed at 3.5 μm which reduced transmission from 80 % to 65 % , and this was attributed to the presence of water in the glass. Glass forming compositions of Sb_2O_3-Al_2O_3-R_2O were examined by Hedden et al. (44). The glass transmitted to 5.4 μm, with 10 % transmission up to 6 μm. Dumbaugh (45) has reported stable glasses in Bi_2O_3 based systems. However, they exhibit relatively low softening points and were observed to crystallise if heated below this point.

2.2.2 Halide Glasses

Many workers have successfully prepared halide glass systems for infra red optical purposes. Generally, there are two categories of halide glasses. The first consist of fluoride glasses and the second consist of chloride glasses. Fluoride

glasses have been prepared based on a variety of glass formers such as BeF_2, ZrF_4, HfF_4 and combinations such as AlF_3-BeF_2. Many investigations of fluoroberyllate glasses have been reported (46). These show very good refractive indices and appear good for use as I-R transmitting fibres. However, the cost and toxicity of beryllium could limit practical applications. Also, these glasses are very sensitive to water. Zirconium fluoride - based glasses were developed by Poulain et al. (13,47). Studies show that these glasses exhibit some optical characteristics which are attractive for optical fibre design (46). Their transmission range is continous from 0.2 μm in the UV up to 7 μm in IR region. However, the glass melts cannot be cooled down slowly, otherwise crystallisation occurs, while on the other hand, slow cooling is needed to produce homogeneous glass or large sample size. Additionally, these glasses undergo some surface attack when exposed to water.

The replacement of ZrF_4 by HfF_4 has also been reported (48) and it shows the same chemical behaviour but is heavier implying that at a certain wavelength, the absorption coefficient for HfF_4 - based glass should be lower than for ZrF_4 - based glass. Other fluoride glasses which have been developed are multicomponent AlF_3 or ZnF_2 glasses (50). Most of them show basic properties similar to fluorozirconate glasses with some differences in durability and optical transmission.

Chloride glasses would be alternative candidates for IR fibres although they are known to be hygroscopic. Only $ZnCl_2$ has been drawn (51) but its optical loss characteristics have not been measured. Other chloride glasses such as fluorochloride cadmium glasses (52) have also been reported. These glasses show extended IR transmission but are very hygroscopic and may easily devitrify.

2.2.3 Chalcogenide Glasses

Chalcogenide glasses containing the elements of As, Ge, P and S, Se and Te are available with stable vitreous states and wide transmission ranges (53). However, it has not been possible to reduce optical losses to the level required for telecommunication. The main problem lies in the removal of extrinsic impurities and has not yet been solved.

2.3 Oxyhalide Glasses

In recent years, researchers have tried to find alternatives to the above three types of IR transmitting glass. Many considerations have been taken into account in order to achieve a compromise between the oxide glass properties and the halide glass behaviour. As a result of this a combination of oxide and halide compositions was made to produce a so-called oxyhalide glass system.

As we have mentioned earlier, oxyhalide glasses based on Sb_2O_3 were first prepared by Dubois et al. (23) and then followed by Ahmed and Holland (25,26,29) and Ota et al. (27). All of the systems show considerable attractive optical properties. They are transparent from about 0.43 μm up to 6.5 μm. In the system Sb_2O_3-$PbCl_2$-$ZnCl_2$ (25), the I-R edge is at ≈ 6.8 μm and decreases slightly to ≈ 6.0 μm in Sb_2O_3-$SbCl_3$ / $CdCl_2$ glasses (26). However, there are broad bands between 500 cm^{-1} and 669 cm^{-1} which are believed to be due to the Sb-O-Sb stretching vibration (54). This dominates the absorption edge which may limit practical applications.

2.3.1 Oxyhalide Glass Structure

There is little information available in the literature about the structure of oxyhalide glasses.

The structure of a crystalline oxychloride, namely mendipite ($Pb_3O_2Cl_2$) has been studied in detail by Gabrielson (55). He showed that the Pb atoms are both in sixfold and sevenfold coordination, the coordination sphere being made up of both oxygen and chlorine ions. Rao and Rao (28) studied the structure of PbO-$PbCl_2$ glasses using an X-ray diffraction technique. They found that the structure of the glasses is dominated by the chemical tendencies of the ions, covalent Pb-O-Pb linkages being crucial to the glass formation. They also found that Pb atoms are likely to be

octahedrally coordinated with two oxygens and four chlorines and such model features account successfully for the experimental pair distribution functions. The structure of the Sb_2O_3-$PbCl_2$ glass system has been studied by Dubois et al. (24). The study was carried out by means of X-ray diffraction as well as Raman investigation and comparison was made with Sb or As based glasses. It was found that the glass was built from the SbO_3 trigonal pyramid structural unit when the amount of $PbCl_2$ is low and changes to SbO_4 square based pyramids when the amount of $PbCl_2$ is higher. In the SbO_4 structural unit regime, the Pb atoms occupy the common site of two square based pyramids, one formed by O atoms and the other one by Cl atoms which produce the structure of $PbSbO_2Cl$ (see figure 2.2), a so called " Sillen type " phase. A study of the vitreous Sb_2O_3 structure by Hasegawa et al. (56) has also suggested that the Sb_2O_3 glass contains a structural unit of SbO_3 pyramids similar to that of valentinite, one of the crystal form of Sb_2O_3.

2.3.2 Glass forming system

Most of the oxyhalide glasses systems known have a wide range of glass formation (23 - 29) and comprise not only binary but also ternary and even quaternary systems. Most of the glasses can be formed by additions of up to 60 mol % of alkali halide (23,24,27).

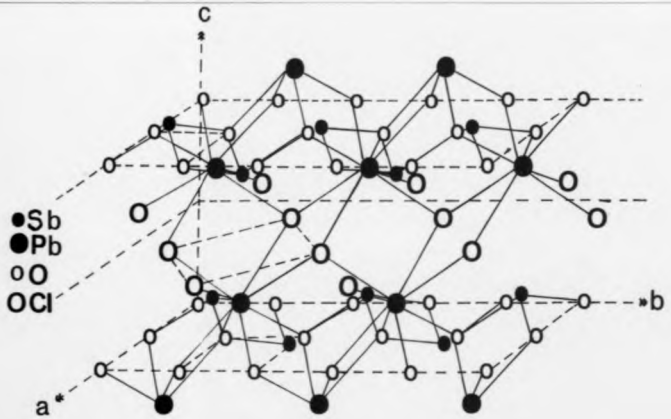

Fig. 2.2 : Crystal structure of $PbSb_2OCl$ (24).

2.3.3 Oxyhalides as IR transmitting glasses

To be a good candidate for IR transmitting glass, glass must show good transparency at longer wavelengths, which means that it has low losses due to scattering. As discussed earlier, most oxyhalide glass system exhibit considerable transparency in the IR region. An example of this is a glass of a composition Sb_2O_3-$PbCl_2$-$ZnCl_2$ which shows transparency up to 8.8 μm. Others are from the PbO-GeO_2-$CdCl_2$ system where the transparency is up to 6.0 um while a system of Sb_2O_3-PbI_2 shows a transparency up to 6.0 um. The loss due to absorption is expected to be in between pure halide glass and oxide glass while the refractive indices are around 1.5. In conclusion, oxyhalide glasses can be alternatives for IR transmission. However, other factors such as thermal stability or chemical durability of the glass should also be considered.

2.4 Glass stability

Some authors emphasize glass stability based on the crystallisation rate during cooling or reheating; some refer to the relaxation process near the glass transition (55) and some even refer to the chemical durability of the glass. While it is only by direct observation that glasses can be shown to exhibit the required stability, it is attractive

to have some quantitative scale of glass stability. In practice, many researchers, obtain their glass stability data by using DSC or by doing some durability test. In general, the investigations of glass stability can be divided into two categories:-

1. Thermal
2. Chemical

2.4.1 Thermal stability

A glassy state is metastable and tends to transform continously towards the more stable states. This transformation process occurs by two processes, namely structural relaxation and crystallisation. The structural relaxation process is driven by the considerable strain frozen-in during glass formation. During the process of annealing, the material relaxes towards the internal equilibrium state of the liquid from which it was obtained, mostly controlled by atomic diffusion (see eg. ref. 57). The crystallisation process depends on kinetic and thermodynamic factors and proceeds by two important processes namely nucleation and growth. DTA (Differential Thermal Analysis) or DSC can provide parameters such as Tg (Transformation temperature), T_x (onset of crystallisation), crystallisation temperature Tc (exotherm maximum) and Tm (melting temperature).

A glass forming ability or thermal stability range may be evaluated from the difference between Tc and Tg although some glass scientists weight this difference by 1/Tg leading to the factor Tc - Tg / Tg which is dimensionless.

Another glass stability scale was given by Hruby's criterion H_r (58) defined as :

$$H_r = (Tc - Tg) / (Tm - Tc)$$

Basically, this equation gives the same criteria as Tc - Tg but it varies more quickly when the crystallisation peak shifts. It also takes into account the melting temperature, Tm, although this may not be significant as it always correlates with Tg. All these stability scales have been used successfully by various workers.
Another stability scale which combines all the parameters involved is given by Saad et al.(59) :

$$S = (Tc - Tx)(Tc - Tg) / Tg$$

where S is expressed in Kelvins. However, this new criterion required the samples to be heated at the same heating rate in all cases. Also, the location of the crystallisation peak is dependent on grain size, as some surface crystallisation

is always involved, and similar particle sizes should be used.

So far, at least, there are four known criteria used to determine the thermal stability. Of these four, the first ie: thermal stability range T = To - Tg or Tx - Tg are most frequently used.

The thermal stabilities of silicate and other oxide glasses are well known. Most of the binary silicate systems have values of Tg more than 400 °C (see eg. ref. 60,61) and values of To higher than 550 °C (see eg. ref. 62,63) and much higher for pure silica glass (see eg. ref. 64). The values of Tg and To of other oxide glasses also indicate that most of them are stable.

The thermal stability ranges of halide glasses are best known for the heavy halide systems. Pure $ZnCl_2$ glass has a relatively low stability range where T = To -Tg = 70 °C (65) although this value may vary, mainly because of the effect of the difference in water content (66,67). However, some reported that binary glasses containing an alkali halide component such as KCl, KBr or KI are more stable than the vitreous $ZnCl_2$ itself with the mixture of $ZnCl_2$-KI being the most stable (12). Other chloride glasses such as $BiCl_3$-KCl and $ThCl_4$-NaCl-KCl have also been studied (65) but most of them are very hygroscopic. The typical temperatures for $BiCl_3$ are Tg = (30 - 50) °C and Tm = (180 - 200) °C and

for $ThCl_4$ glasses, Tg = 130 °C and Tm = 290 °C. With such properties, these glass systems are not of interest for exploitation. Evidence of glass forming ability in fluoride glasses is very interesting. Included in this class are glasses based on BeF_2, AlF_3, ZrF_4 and a combination of them or with alkali metal flourides. Of all of them, the glasses based on ZrF_4 are the most promising. The various combinations give Tc - Tg ranging from 47 °C (ZrF_4-BaF_2 system) to 80 °C (in ZrF_4-BaF_2-LaF_3-AlF_3 glasses) (65). But with addition of NaF (known as ZBLAN glass), the values of Tc - Tg are improved. Parker et al.(68) reported the gap up to 93 °C. Others have reported the Tc - Tg value to be 115 °C (69) and 116 °C (70) and this value is the best so far reported. Work has also been done to combine the ZBL (ZrF_4-BaF_2-LaF_3) with chlorides such as $ZnCl_2$ and $BiCl_3$ but it was found that the value of Tc - Tg is about 55 °C (71), even lower than that of vitreous $ZnCl_2$.

In recent years, research on oxyhalide glasses has been developed progressively. They have been reported to exhibit glass stability ranges Tc - Tg of as low as 40 °C in oxybromide glasses up to 93 °C in the binary system of Sb_2O_3-$PbCl_2$ glasses (23). With the introduction of $ZnCl_2$ as a third component, the stability range seems to be much improved to about Tc - Tg = 149 °C (25). Ternary systems such as PbO-GeO_2-$PbCl_2$ glasses have shown reasonable glass stability ranges with Tc - Tg = 143 °C (26). This value

certainly shows that the oxyhalides from this ternary system can form very stable glasses. The binary oxyhalide system of Sb_2O_3-$MnCl_2$ has also been prepared and has a value of Tg = 328 °C and Tc = 472 °C (23). When the Sb_2O_3 was replaced by $NaPO_3$, the value of Tg was reported to be more than 420 °C (27). Other binary oxyhalides from the PbO-$PbCl_2$ glass system have also been reported by Rao et al. (72). The report showed that the glass was reasonably stable and the Tc - Tg value is up to 93 °C. The glasses from the TeO_2-$ZnCl_2$ binary system have also been prepared (73) but unfortunately, no thermal properties have been reported.

So, it has been shown that in terms of thermal stability, oxyhalide glasses can have a stability range which is better than some other well known glasses. This indicates that oxyhalide glasses might be very good prospects for some practical applications. But other factors such as chemical durability of the glasses must also be taken into account.

2.4.2 Chemical Stability

There is no infallible method of prediction that one glass is more chemically stable than another except after both have experienced similar experimental conditions. Scientific studies of the chemical durability of glass have been in progress for many years but a complete understanding of the

process has not yet been achieved. Many attempts have been made to clarify this. Paul (74) for example, tried to understand the chemical durability of glasses by means of a thermodynamic approach. Others like Scholze (75) use a physico-mathematical treatment in order to understand the mechanisms for silicate glasses. Some workers have also tried to predict the chemical durability of glasses from their compositions. Probably, Weberbauer (76) was the first to do so, followed by Hifte and Newton (77) and many others subsequently (78,79).

The other way to study chemical durability is by experiment. In general, most of the tests expose glass to water and make some assessment of how much damage has been produced. The choice of water as a test substance is reasonable since it is everywhere, cheap and glass will inevitably be exposed to it. Normally, there are three conditions under which glass will be tested. One is in water itself, secondly under normal atmospheric humidity and finally in some degrees of relative humidity (RH). In most cases, temperature also plays a significant role. Other test methods such as the powder test (80), dimming test (81), long exposure test (82) and many others are basically similar to those three basic conditions mentioned above.

The reaction of glass with water has been studied by hundreds of workers (eg. 83 - 85). The detailed mechanisms involved in the reaction between glass and water are given by Rana and Douglas (86) and by Doremus (87). The effect of

humidity on weathering of glass was studied in detail by Walters and Adams (88). In their study, levels of 30% RH up to 98% RH were employed at 50 °C. The authors also did some experiments with cyclic and static conditions of RH and reported that the cycling condition was found to be less severe than static 98% RH.

2.4.2.1 Oxide (silicate) Glasses

The durability of silica glass was studied by Ito and Tomozawa (89). Depending on the applied water pressure, the result show that silica glass dissolves in water after a few hours. The durability of binary silica glass was studied in detail by Dubrovo et al.. The study was conducted in water (90), in acid solution (91), in alkaline solution (92) and also in salt solution (93). The experiments were conducted at temperatures from 25 °C up to 100 °C in water and with varying time of exposure. The result show that under all the conditions, the binary silicate dissolves easily. However, the durability of silicate glasses can be improved by adding other components such as Al_2O_3 (94) and ZrO_2 (95). The high water content of silicate glasses was studied in detail by Tomozawa et al. (96) in terms of their hygroscopicity. The results show that the diffusion of water in the glass is very fast for glasses with high water content.

The chemical durability of other oxide glasses has also been studied. For example, B_2O_3 glasses were examined by Southard

(97), GeO_2 based glasses by Takahashi et al. (98), glasses based on P_2O_5 by Kanazawa et al. (99) and many others. Most of them used powders with a particle size range from 0.1 - 0.5 mm, with different time duration and temperature. In the case of $CaO-P_2O_5$ glasses (100) the solubility of glass in basic solvents indicates that the glass is more stable when the percentage of CaO is increased.

2.4.2.2 Halide Glasses

Halide glasses and crystalline compounds are extensively attacked by water which means that, either in water or in normal atmosphere, halide glasses are in danger of corrosion. This is a result of a very poor M-X chemical bond (X = Cl^-, Br^-, I^-) which is unstable with respect to the hydrated cation $M(H_2O)_n$.

The chemical durability of fluorozirconate glasses has been reported by many workers. Poulain et al. (47) reported that the $ZrF_4-BaF_2-ThF_4$ glass system is stable in wet atmosphere up to 350 °C . However they also noted that the glass surface is attacked by water after a few hours at 20 °C. Further, it was reported (48) that the dissolution rate of this glass in boiling water was about 4.7×10^{-5} gm cm^{-2} min^{-1} (ie; 10^2 time faster than typical silicate glasses). The study of reactions of this glass with water was carried out further in more detail by Simmons and Simmons (101). As for previous workers, they also found that the

fluorozirconate glasses leached rapidly in water, a very thick hydrated layer being formed on the glass surface which absorbs a large amount of water.

2.4.2.3 Oxyhalide Glasses

There are few reports of the chemical durability of oxyhalide glasses in the literature except a few remarks by Dubois et al .(23). They reported that most oxyhalide glasses based on Sb_2O_3 are generally resistant to atmospheric attack except for Sb_2O_3-LiCl and Sb_2O_3-KF glass systems which are attacked after about one month. However, they also reported that most of these glasses will react with hot water.
The study of chemical durability of oxyhalides is still in progress.

As we have mentioned earlier, most silicate glasses and non-silicate oxide glasses, are, in general, chemically stable although in some applications such as optical fibres , they are less attractive (due to absorption losses caused by scattering), than many halide glasses such as the fluorozirconate glass system. On the other hand, many halide glasses are less chemically durable especially in the water condition. So, obviously, some compromises should be made between these two characteristics. Oxyhalide glass might provide the better solution.

It is however difficult to make general statements about the durability of one glass compared with another. Not only do the results depend on various factors such as temperatures, glass compositions, solution pH, they are also affected by relatively small differences in sample preparation, experimental techniques and apparatus used. It is therefore quite impossible to propose a standard test for chemical durability.

2.5 Viscosity

One of the most important criteria in glass forming is viscosity. The way in which the viscosity of a glass melt varies with temperature is very important in determining the shaping process which leads to a glass article. Further, the connection between viscosity and other properties of the glass might lead to a better understanding of glass structure.

2.5.1 Definition Of Viscosity

The viscosity which is actually referred to, shear viscosity or coefficient of shear viscosity, is defined as follows:- Suppose there is a liquid which is confined between two parallel plates with the upper moving with a velocity v, and the lower stationary (Figure 2.3). The distance between the plates remains constant. For a large number of liquids,

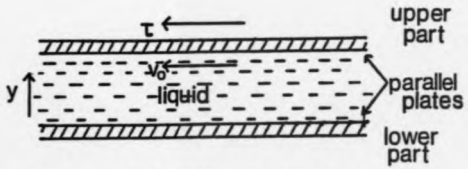

Fig. 2.3: Definition of viscosity

the velocity in the liquid varies linearly with distance between the plate. In order to maintain this motion, a force should be applied to the upper plate in the direction of its motion, to overcome the force of friction within the liquid. The force per unit area (known as the shear stress, τ) is proportional to the velocity gradient in the liquid dv/dy. Thus,

$$\tau = \Pi \cdot dv/dy$$

where Π is the proportionality constant or viscosity. However this equation is only valid when v_o is below a certain value. If v_o is high enough, turbulent flow may develop. Fortunately, this flow is never encountered in glass melts because of their high viscosity. The equation is also only valid for newtonian fluids which is normally true for glasses above the transformation range. The unit of Π in the SI system is N s m^{-2} or Pa s which in cgs are dyne s cm^{-2} or P (Poise). This unit has been used extensively in glass literature where the conversion is 1 P = 0.1 Pa s = 1 d Pa s.

With industrial glasses, the viscosity which is required by many technological practices is in the range of 10^2 P to $10^{14.5}$ P. During melting and refining the glass melt, the viscosity should decrease down to 10^2 P, forming requires viscosities of 10^3 P to 10^7 P. Annealing of the glass takes place at viscosities 10^{13} P to $10^{14.5}$ P while working with a flame requires a viscosity of about 10^4 P to 10^9 P (102). So

called reference points of viscosity have been set internationally and are described in detail by Hlavac (102). The viscosity of glasses depends very strongly on composition. However, it is difficult to describe the relation between viscosity and composition since individual components may increase the viscosity in one type of glass and may decrease it in another. Of course it also depends on how much of the individual component is present in the glass. In silicate glasses, oxides such as Al_2O_3 and SiO_2 will increase the viscosity while PbO and modifiers will reduce it. B_2O_3 decreases viscosity at the melting temperature, while increasing it at lower temperatures (up to 15% B_2O_3). These effects of individual component have been studied by Gehloff et al.(103) and later reviewed by Scholze (104). The book by Mazurin et al. (105), a collection of data on two and three component of oxide glasses, is a very useful source of information.

In halide glasses such as BeF_2, the addition of LiF substantially decreases the viscosity (106) while other halides such as AlF_3 or KF reduce the viscosity only slightly. The study of viscosity and the effect of other halides has been limited.

Moreover, reports of the effect of oxide or halide on the behaviour of oxyhalide glasses are virtually none.

2.5.2. Methods of Viscosity Measurement

As mentioned earlier, the range of viscosity which is of interest in manufacturing and use of glass is very wide, so it is quite impossible to measure the whole range of viscosity using only one method.

One of the most important factors is the measurement of temperature. The thermocouple used to measure the temperature must be as close to the glass as possible. The viscometer furnace must be designed such that the glass temperature is constant and adequate time for the glass to come to thermal equilibrium must be given before the temperature reading is taken. Calibration using a standard glass must also be made so that the reading will be accurate. Changes in the characteristics of the furnace and thermocouple will seriously affect the accuracy of the data. Some of the methods for measuring viscosity are described below. The range of the viscosity measurement and the equations involved will be stated where available.

2.5.2.1 Rotating Cylinder Viscometer

This is the most widely used method for measuring viscosity especially for higher temperatures over the range of 10 P to 10^8 P. The apparatus and the measurement technique have been described well by Dietzel et al. (107). The equation

involved in the final form after some arrangement is;

$$\eta = (T/ 4\pi\Omega l_e).(r_o^2 - r_i^2) / (r_i^2 r_o^2)$$

where T is the torque which caused the twist, Ω is the angular velocity, l_e is the effective length and r_o , r_i are external and internal radii of the cylinders respectively. The range can be extended to higher viscosity with some modification of the apparatus and this has been done by Napolitano et al. (108) who were able to measure viscosities over the range of 10 P to 10^9 P.

2.5.2.2 Parallel Plate Viscometer

This method of measurement has been describe in detail by Hagy (108) and Fontana (110). This method uses a circular disc of glass which is sandwiched between metal plates. When the force is applied normal to the plate surfaces, the change in the distance between the plates was measured. The equation of the viscosity can be written as follows;

$$Ft/3\eta v = (1/h - 1/h_o) + v/8\pi (1/h^4 - 1/h_o^4)$$

where F is the force applied, t is the time interval, v is the volume of the specimen, h_o, h are the initial and the

final thicknesses of the specimen respectively. This method gives an accurate result over the viscosity range of 10^{6} P to $10^{10.5}$ P.

2.5.2.3 Penetration Viscometer

This method, also known as the indentation method was probably first used by Cox (111), using a sphere to penetrate the glass surface. Later, Hynes and Rawson (112) used a vertical alumina rod with Nimonic indenter to penetrate the glass. However, both of these methods need the sample to be withdrawn from the furnace and cooled down before another experiment can be done and so limits the practical usage. Douglas et al.(113) described a more suitable penetration viscometer, followed by Meikhail (114) using a Linear Voltage Displacement Transducer (LVDT) to measure the indenter displacement. Viscosities over the range of 10^{8} P to 10^{11} P can be measured with an experimental accuracy of about ± 2% . After some mathematical treatment, the viscosity equation can be written as;

$$\eta = 9/32\ Pt\ (\ 2R\ )^{-1/2}.l^{-3/2}$$

where P is the applied force, t is the time taken during the experiment, R is the indenter radius and l is the penetration depth.

Some modifications have been made to this apparatus to extend the range of viscosity measurement by Whetton and Hall (115) who describe a balance - type, computer - linked, penetration viscometer, claimed to be capable of measuring the viscosity over the range of 10 P to 10^{12} P. This range is of course much better than any other techniques previously used with an error of less than ± 1%. The range covered is virtually the whole range of interest to the glass technologist.

2.6.3 Fibre Drawing

An important product of the glass industry is glass fibre. Because of its viscosity - temperature behaviour, where viscosity decreases gradually with temperature, a rod of glass can be drawn down in diameter into a fibre of the size required by the manufacturer. In fibre fabrication, a " preform " is drawn into a fibre on a fibre - drawing machine, as describe in the literature (116,117). Fibre drawing needs a very low viscosity, in the range of 10^{3} P to 10^{4} P.

The drawing force necessary to produce a fibre depends on the viscosity of the glass as it emerges from the orifice. If the temperature of the glass is too high (very low viscosity), then the drawing force is insufficient to balance the surface tension acting upwards at the side of the orifice and therefore the process is no longer possible.

So, there must be an upper limit of temperature to supply an adequate viscosity for fibre drawing. There is of course a lower temperature limit determined by two factors. First, if the glass is too viscous, the drawing force becomes high enough to break a fibre, and secondly, if the temperature of the orifice is too low, devitrification may take place inside the orifice which also might break the fibre. Provided that the temperature of the orifice is high enough (above the liquidus temperature) there will be no danger of devitrification since the rate of cooling after the glass has left the orifice is very rapid.

In summary, the viscosity - temperature characteristics of the glass are very important in the process of fibre drawing. In the present work, viscosity measurements have been made over a limited range to indicate the dependence on composition, however no fibre drawing has been attempted.

2.6 Crystal Growth Rate

There are many theories of growth such as normal growth theory, surface nucleation growth or screw dislocation growth. Since our calculation will be based on the first theory, it will therefore be describe in detail.

2.6.1 Normal Growth Theory

After formation of stable nuclei in the parent phase, crystallisation proceeds by growth of the new phase. For normal growth, all atoms arriving at the crystal - liquid interface can either join the crystal to become solid or may leave the crystal surface (it is assumed that this occurs uniformly all over the crystal surface). In order that atoms may cross the interface between crystal and surrounding liquid, they must acquire an activation energy, ΔG_a. Once the atom has crossed the interface to the crystal, its free energy is reduced. Thus for an atom to leave the crystal surface, it needs a higher activation energy, equal to $(\Delta G_a + v \Delta G / v_m)$ where ΔG is the free energy difference per unit volume between liquid and crystal at temperature T, v is the volume occupied by an atom and v_m is the molar volume of the crystalline phase. The growth rate is proportional to the difference in the particle flux from the liquid to the crystal and vice versa. In simplified form, the growth rate, U, is given by (118):

$$U = \lambda \nu_a \exp (-\Delta G_a / kT) [1 - \exp (- v\Delta G / v_m kT) \quad (2.1)$$

where λ is approximately one interatomic spacing and ν_a is the frequency at which each atom vibrates due to thermal energy.

Since $v / v_o k = 1 / R$, where R is the gas constant, equation (2.1) can be rewritten in the final form as;

$$U = \lambda v_o \exp (-\Delta G_o / kT) (1 - \exp (-\Delta G / RT) \quad (2.2)$$

The variation of U and temperature can be seen in figure 2.4.

In the low temperature region, $\Delta G >> RT$. Thus, the last term of equation (2.2) is negligible and,

$$U = \lambda v_o \exp (- \Delta G_o / kT) \quad (2.4)$$

Thus, U could be controlled by many factors such as molecular reorientation or by transport properties.
In the higher temperature region, $\Delta G << RT$. Thus, the last expression,

$$1 - \exp (- \Delta G / RT) \cong \Delta G / RT$$

So, equation (2.2) can be rewritten to give,

$$U = \lambda v_o \Delta G / RT [\exp (- \Delta G_o / kT)] \quad (2.5)$$

Thus, U is directly proportional to the thermodynamic driving force, ΔG.

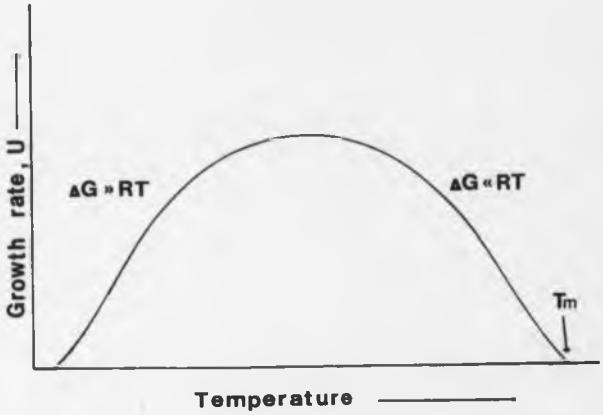

Fig. 2.4 : Dependance of growth rate on temperature.

In summary, for normal nucleation and growth, at large undercooling, the growth is controlled by many factors while at small undercooling, the growth rate is controlled by thermodynamic driving force.

References

1. Goldschmidt, V.M. ; Skrifter Norska Vid. Akad.(Oslo) 8 (1926) 127.
2. Heyne, G.; Angew. Chem. 46 (1933) 473.
3. Warren, B.F. and Hill, C.F.,; Z. Krist. 89 (1934) 481.
4. Sun, K.H. and Callear, T.E., ; US Patent 2 466 506 (Apr.5 (1949).
5. Sun, K.H. ; US Patent 2 466 507 (Apr.5 1949).
6. Sun, K.H. ; US Patent 2 466 508 (Apr.5 1949).
7. Sun, K.H. ; US Patent 2 466 509 (Apr.5 1949).
8. Sun,K.H. and Huggin, M.L., ; US Patent 2 511 224 (June 13 1950).
9. Maier, L.G. ; US Bureau Of Mines, Tech. Paper (1925)360.
10. Balta, P. and Balta, E. ; Introduction To The Physical Chemistry Of Vitreous State, Abacus, Kent, England, 1961.
11. Vallet, C.E. and Braunstein, J. ; J.Am.Ceram.Soc.60 (1977) 315.
12. Schultz, I. ; Naturwissenschaftes 44 (1975) 536.
13. Poulain, M.,Poulain, M. and Lucas, J. ; Mat.Res.Bull. 10 (1975) 243.
14. Aliaga, N., Fonteneau, G. and Lucas, J. ; Ann. Chim. Fr.3 (1978) 51.

15. Lecoq, A. and Poulain, M. ; J. Non. Cryst. Sol. 34 (1979) 101.

16. Poulain, M. and Lucas, J. ; Verres Refract. 32 (1975) 505.

17. Lucas, J., Poulain, M. and Poulain, M. ; Ger. Patent 2, 726 (1977) 170.

18. Drexhage, M.G., Moynihan, C.T. and Saleh, M. ; Mat. Res. Bull. 15 (1980)213.

19. Sun, K.H. ; Glass Ind. 27 (1946) 552.

20. Mellor, J.E. ; Comprehensive Treatise On Inorganic And Theoretical Chemistry, vols.VII and IX , Longmans, Green & Co. Lond. 1929 .

21. Moynihan, C.T. ; Ionic Interactions, ed.S.Petrucci.(Acad. N.York 1971) 261.

22. Winter, A. ; J. Am. Ceram. Soc. 40 (1957) 54.

23. Dubois, B., Aomi, H., Videau, J.J, Portier, J. and Hagenmuller, P. ; Mat. Res. Bull. vol. 19 (1984) 1317-1323.

24. Dubois, B., Videau, J.J., Couzi, M. and Portier, J. ; J. Non-Cryst. Sol.88 (1986) 355-365.

25. Ahmed, M.M. and Holland, D. ; Glass tech. vol.28, no 3, (June1987) 141-144.

26. Ahmed, M.M. and Holland, D. ; Mat. Sci. Forum, vol.5 (1985)175-188.

27. Ota, R. and Soga, N. ; J. Non-Cryst. Sol.95&96 (1987) 465-472.

28. Rao,B.G and Rao, K.J. ; Phy. Chem. Glass. Vol.25,no1, (Feb 1984) 11-15.

29. Ahmed, M.M. and Holland, D. ; Mat.Sci.Forum ,vol 19-20 (1987) 87.

30. Kapany, N.S. ; Fibre Optics. Principles And Application., Acad. Press, N.York 1967.

31. Kao, K.C. and Hockham, G.A. ; Proc.Inst.Elect. Eng.113 (1966) 1151.

32. Maze, G., ; Fluoride Glasses, ed: Comyns A.E., John Wiley & Sons (1989).

33. Leroy, D., Lucas, J., Poulain, M. and Ravine, D. ; Mat. Res. Bull. 13 (1978) 1125.

34. Poulain, M. ; Endeavour, New Series, vol 11,no 1 (1987) 25 - 28.

35. Szigeti, B. ; Proc.Roy.Soc.A204 (1950) 51.

36. Nishimura, M. ; Photonics Spectra (June 1986) 109.

37. Donald, I.W. and McMillan, P.W. ; J.Mat.Sci.13 (1978) 2301 - 2312.

38. Keck, D.B., Maurer, R.D. and Schultz, P.C. ; Appl. Phy. Lett. 22 (1973) 307

39. Newn, G.R., Pantelis, P., Wilson, J.L., Uften, R.W. and Worthington, R. , Optoelectronics 5 (1973) 595.

40. Reibling, E.F. ; J. Mater. Sci. 7 (1972) 40.

41. Topping, J.A., Cameron, N. and Murthy, M.K. ; J. Amer. Ceram. Soc. 57 (1972) 519.

42. Murthy, M.K. and Hill, H. ; J.Amer. Ceram.Soc. 48 (1965) 109.

43. Ulrich, D.R. ; J. Amer. Ceram. Soc. 47 (1964) 595.

44. Heddan, W.A. and King, B.W. ; J.Amer.Ceram.Soc.43 (1960) 387.

45. Dumbaugh, W.H. ; US Patent 3,723 (1973) 141.

46. Baldwin, C.M., Almeida, R.M. and Mackenzie, J.D. ; J.Non - Cryst.Sol.43 (1981) 309.

47. Poulain, M., Chanthanasinh, M. and Lucas, J. ; Mat. Res. Bull. 12 (1977) 151.

48. Lucas, J., Chanthanasinh, M., Poulain, M., Brun, P. and Weber, M.J. ; J. Non - Cryst. Sol. 27 (1978) 273.

49. Drexhage, M.G., El-Bayoumi O.H. and Moynihan C.T. ; Advances in IR Fibres, Tech. Dig. SPIE, Los Angles, CA , Jan.1982,paper 320-06.

50. Lucas, J. ; Advances in IR Fibres, Tech. Dig. SPIE, Jan. 1982. paper 320-05.

51. Uitert, L.G.V. and Wemple, S.H. ; App. Phy. Lett. vol 33 (July 1988) 57-59

52. Matecki, M., Poulain, M. and Poulain, M. ; J. Non-Cryst. Sol. 56 (1983) 81.

53. Hilton, A.R., Jones, C.E. and Brau, M. ; Phys. Chem. Glass. vol 7, no 4, (1966) 105-112.

54. Miller, P.J. and Cody, C.A. ; Spectrochim. Acta 38A (1982) 555.

55. Gabrielson, O. ; Ark. Miner. Geol. 2 (1957) 299.

56. Hasegawa, H., Sone, M. and Imaoka, M. ; Phys. Chem. Glass. 19 (1978) 28.

57. McMillan, P.W. ; Glass - Ceramic, 2nd ed. Acad. Press, Lond. 1979.

58. Hruby. A. ; J. Phys. (Czech) B 32 (1972) 1187.

59. Saad, M. and Poulain, M. ; Proc. 4th Int. Symp. On Halide Glasses, California, USA, Jan. 26-29, 1987.

60. Boesch L.P. and Moynihan C.T. ; J. Non-Cryst. Sol. 17,1,(1975) 44-60.

61. James, P.F. ; Phys. Chem. Glasses, 15, 4 (1974) 95-105.

62. Morley, J.G. ; Glass. Tech. 6, 3 (1961) 68-89.

63. Matusita, K. and Tashiro, M. ; Phys. Chem. Glasses, 14, 4 (1973) 77-80.

64. Mazurin, O.V., Leko, V.K. and Komrova, L.A. ; J. Non-Cryst. Sol. 18,1 (1975) 1-9.

65. Lucas, J.; Glass.,...Current Issue, ed. Wright, A.F and Dupuy, J., Martinus Nijhoff Pub. 1985.

66. Goldstein, M. and Nakonecznyj, M. ; Phys. Chem. Glass. 6 (1965) 126.

67. Eisenberg, A., Farb, H. and Cool, L.G. ; J. Poly.Sci. Pat A-2 4 (1966) 855.

68. Parker, J.M., Seddon, A.B. and Clare, A.G. ; Phys. Chem. Glass. 28, 1 (Feb. 1987) 4-10.

69. Busse, L.E., Lu, G., Tran, D.C. and Sigel, G.H.Jnr. ; Mat. Sci. Forum, 5 (1985) 219.

70. Shah, W.H. ; PhD Thesis, Univ. Of Sheffield 1989.

71. Zhonghong, J., Xinyuan, H., Xiuyu, S. and Xiangshu, Z. ; J. Non-cryst. Sol. 56 (1983) 69-74.

72. Rao, K.J., Rao, B.G. and Elliot, S.R. ; J. Mat. Sci. 20 (1985) 1678-1682.

73. Bridge, B., Bavins, T.E., Woods, D. and Woolven, T. ; J. Non-cryst. Sol. 88 (1986) 262-70.

74. Paul, A. ; J. Mat. Sci. 12 (1977) 2246-68.

75. Scholze, H. ; J. Non-Cryst. Sol. 52 (1982) 91-103.

76. Webberbaur, A. ; Glastech. Ber. 10 (1932)361-426.

77. Iliffe, C.J.A. and Newton, R.G. ; Verres Refract. 30 (1976) 30-34.

78. Peddle, C.J. ; Defect In Glass, Glass Pub. Ltd. Lond (1927).

79. Turner, W.E.S. ; J. Soc. Glass. Tech. 1 (1917) 213-222.

80. Peddle, C.J. ; J. Soc. Glass. Tech. 4 (1920) 3-20T.

81. Zchimmer, E. ; Z. Electrchem. 11 (1905) 828-838.

82. Peddle, C.J. ; J. Soc. Glass. Tech. 4 (1920) 299-310T.

83. Paul, A. ; Chemistry Of Glasses, Chapman & Hall, Lond. 1982.

84. Tomozawa, M. ; J. Non-Cryst. Sol. 73 (1985) 197-204.

85. Hench, L.L. and Clark, D.E. ; J. Non-Cryst. Sol. 28 (1978) 83-105.

86. Rana, M.A. and Douglas, R.W. ; Phys. Chem. Glass. 2, 6 (Dec 1961) 196-205.

87. Doremus, R.H. ; Reactivity Of Solids, eds: Mitchel J.W., De Vries R.C., Roberts R.W. and Cannon P., Wiley,N.York, 1969, p.667.

88. Walter, H.V. and Adams, P.B. ; J. Non-Cryst. Sol. 19 (1975) 183-99.

89. Ito, S. and Tomozawa, M. ; J. Amer. Ceram. Soc. 64, 11 (1981) C160.

90. Dubrovo, S.K., Shmidt, Yu A. ; Bull. Acad. Sci., USSR , Div. Chem. Sci.,4 (1953) 597-606.

91. Dubrovo, S.K. ; Bull. Acad. Sci., USSR, Div. Chem. Sci., 5 (1954) 770-777.

92. Dubrovo, S.K., Shmidt, Yu A. ; Bull. Acad. Sci..USSR, Div. Chem. Sci., 3 (1955a) 403-410.

93. Dubrovo, S.K., Schmidt, Yu A. ; Bull. Acad. Sci., USSR, Div. Chem. Sci., 4 (1955b) 603-610.

94. Warburton, R.S. and Wilburn, F.W. ; Phys. Chem. Glass. 4 (1963) 91.

95. Dimbleby, V. and Turner, W.E.S. ; J. Soc. Glass. Tech. 10 (1926) 304.

96. Tomozawa, M., Ito, S. and Molinelli, J. ; J. Non-Cryst. Sol. 64 (1984) 269-278.

97. Southard, J.C. ; J. Amer. Ceram. Soc. 63, 11 (1941) 3147-50.

98. Takahashi, K. and Yoshio, T. ; Proc. XIth Int. Cong. On Glass., Prague, vol 1 (1977b) 183-192.

99. Kanazawa, T., Kawazoe, H. and Ikeda, M. ; J. Ceram. Soc. Jpn. 78, 4 (898) (1970) 121-128.

100. Greenwood, N.N. and Earnshaw, A. ; Chemistry Of The Elements, Pergamon Press Ltd. 1st ed. 1984.

101. Simmons, C.J. and Simmons, J.H. ; J. Amer. Ceram. Soc. 69(9) (1986) 661-669.

102. Hlavac, J. ; The Technology Of Glass And Ceramics; An Introduction, Elsvier Sci. Pub. Co. Ams-Oxf-NY, 1983.

103. Gehloff, G. and Thomas, M. ; Z. Tech. Physik 6 (19250 544.

104. Scholze, H. ; Glass. Natur, Struktur und Eigenschaften, 2nd ed. Springer, Berlin-Heidelberg-New York 1977.

105. Mazurin, O.V., Streltsina, M.V. and Shvaiko-Shvaikovskya, T.P. ; Handbook Of glass Data, 3vols., Elsvier, Ams-Oxf-NY 1983.

106. Cantor, S., Ward, W.T. and Moynihan, C.T. ; J. Chem. Phys. 50 (1969) 2874.

107. Dietzel, A. and Bruckner, R. ; Glastech. Ber. 28 (1955) 455-67.

108. Napolitano, A., Macedo, P.B. and Hawkins, E.G. ; J. Res. Natn. Bur. Stand. 69A (1965) 449-55.

109. Hagy, H.E. ; J. Amer. Ceram. Soc. 46 (1963) 93-7..

110. Fontana, E.H. ; Bull. Amer. Ceram. Soc. 49 (1970) 594 -7.

111. Cox, S.M. ; J. Sci. Inst. 20 (1943) 113.

112. Hynes, M.S.R. and Rawson, H. ; Phys. Chem. Glass. 2(1) (1961) 9.

113. Douglas, R.W., Armstrong, W.L., Edward, J.P and Hall, D. ; Glass Tech. vol 6 no 2 April 1965.

114. Maikhail, M.S. ; PhD Thesis, Univ. Of Warwick, 1985.

115. Whetton, N.L. and Hall, C.R. ; Glass Tech. vol 28 no 2 Apr. 1987.

116. Loewenstein, K.L. ; The Manufacturing Technology Of Continous Glass Fibres, Elsevier, Amsterdam 1973.

117. Ostrowsky, D.B. ; Fibre And Intergrated Optics, Plenum Press, New York 1979.

118. Paul, A. ; Chemistry Of Glasses, Chapman And Hall, London, New York 1982.

CHAPTER 3 : EXPERIMENTAL TECHNIQUES

3.1 Glass Preparation

The appropriate, well mixed glass constituents (from 99% Sb_2O_3, 99% $PbCl_2$, 99% $ZnCl_2$, 99% TlCl, 98.5% $BiCl_3$) weighing about 30 gm. in total were put into an alumina crucible with a lid to reduce the losses of volatile components. Then, the mixture was melted in air in a temperature range from 1000 °C - 1200 °C depending on composition (the temperature is higher when the Sb_2O_3 content is larger). After about 5 minutes (when normally the evolution of fumes is observed), the crucible is taken out and held for about 1 - 2 minutes, and well agitated until it reaches the required viscosity. The liquid is then poured into moulds of different shapes to suit the various purposes, before being annealed at a temperature of about 250 °C for 1 hour and then being allowed to cool down to room temperature.
Approximately the same procedure was used for all glass compositions.

3.2 Thermal Analysis

The thermal characteristics of all glasses were determined by DSC (Differential Scanning Calorimetry). Experiments on powder samples were carried out with the help of a Setaram

High Temperature, HT 1000 Calorimeter with sensitivity of 10 uW at constant temperature and heating rates of 0.4 °C / min. About 1.2 gm of sample and reference (Al_2O_3 powder) were placed inside alumina holders (see figure 3.1). These could then be introduced into the calorimeter and a short time was allowed to stabilise the ambient temperature before the experiment was performed. The set temperature range was 100 °C to 500 °C. These conditions were the same for all the experiments.

A typical DSC trace can be seen in figure 3.2. The manner of experimental determination of transition temperature, Tg (endothermic), and crystallisation temperature, Tc (exothermic), are evident from that figure. The values of Tg and Tc will be shown in the next chapter.

3.3 Crystallisation Studies

3.3.1 Heat Treatment

Portions of the glass sample were heat treated at the various crystallisation temperatures Tc, for 24 hours in an electric furnace. After that, the crystallised product was characterized by X - ray diffraction and scanning electron microscopy.

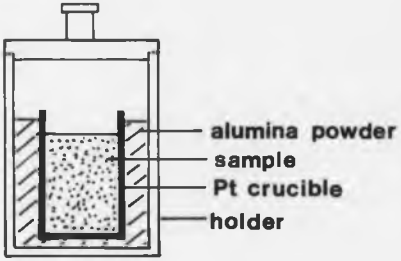

Fig. 3.1 : Sample preparation for DSC measurement.

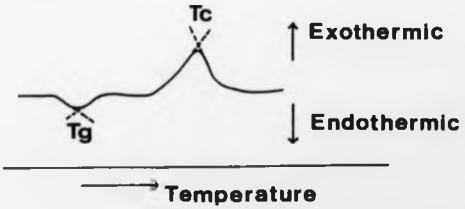

Fig. 3.2 : Typical DSC curve.

3.3.2 X - Ray Diffraction Analysis (XRD)

For X - ray diffraction purposes, a glass slide was coated evenly with a thin layer of silicone grease. The finely powdered, heat - treated sample is then evenly distributed on the grease layer. X - ray diffraction was carried out using a Philips PW 1965 / 60 Goniometer with CuKα radiation and λ = 1.5405 Å. The 2θ scan rate and time constant are the same for all the samples.

3.3.3 Scanning Electron Microscopy (SEM)

A portion of heat - treated sample was mounted in conducting bakelite. The required highly polished section was best obtained by grinding each specimen on successive grade (320, 400, 600, 800, 1000, 1200 mesh) silicon carbide grit paper and then successively diamond paste(6, 3, 1, 0.25 um) until scratch - free under an optical microscope . The specimen was coated with a thin layer of carbon by an evaporation technique. (The most serious problem with the sample is the lack of control over the thickness of the carbon coating. If it is too thin, then charging of the sample will occur and if it is too thick, the image will not be very clear). Generally, an electron accelerating voltage of 20 kv was used throughout the experiment. Any voltage higher than this, appeared to damage the samples. The micrographs were obtained using back - scattered imaging.

This process utilises atomic number contrast rather than topographical features. Thus the regions of the material containing heavy elements appear lighter in the electron micrographs than those regions containing mainly elements of low atomic number. High quality SEM images are generally difficult to obtain since there is a problem of electrical charging within the surface (1). Enlargement of some micrographs was carried out for the purpose of determining the volume fraction of the phases. The EDX (Energy dispersive X - ray analysis) spectrum of some specimens have also been taken to identify the crystal constituents. The magnifications employed were selected to be suitable for the scale of microstructure observed. Attempts have also been made to use TEM (Transmission electron microscopy) on some samples but this was not successful since the glasses were severely damaged both during preparation and in the electron beam.

3.3.4 Infra - Red Analysis (IR)

The finely powdered heat - treated sample was mixed with CsI (Caesium Iodide) powder and then made into a pellet with a thickness of about 0.12 mm. The infra - red transmission spectra were recorded at room temperature with a Perkin - Elmer type 983 I - R spectrophotometer in the region of 600 - 180 cm^{-1}.

3.4 Crystal Growth Rate

3.4.1 Heat Treatment

A portion of sample was heat - treated in an electric furnace at various temperatures around Tc (crystallisation temperature). Each composition was heat - treated at four different temperatures around Tc with four different times ranging from 4 - 20 minutes. A longer time, up to 8 hours, was also employed on one selected sample for the purpose of growth measurement at longer times.

3.4.2 Electron Microscopy

For this purpose, the procedure as given in section 3.3.3 was followed. The magnification employed was selected to be suitable for the growth rate calculation. One representative area of the specimen image was chosen for the above purpose.

3.4.3 Averaging Method

It is essential to choose a particular method in calculating the nucleation and growth of the crystal. The most common method is by using an averaging method (2). By this method, the mean crystal diameters ($\bar{X}$) of a system with N

particles (crystals) of the same shape is given by:

$$\bar{X} = \frac{\sum_i (N_i X_i)}{\sum_i (N_i)} = \frac{N_1 X_1 + N_2 X_2 + \ldots\ldots + N_n X_n}{N_1 + N_2 + \ldots\ldots + N_n} \qquad (3.1)$$

where N_1, N_2, N_3,..... are the number of particles (in this case crystals) having " diameter " X_1, X_2, X_3, ... respectively. (Note : The " diameter " is the mean length of the distance between the two tangents on opposite sides of the apparent outline of the particle parallel to an arbitrarily fixed direction, and irrespective of the orientation of each particle (3)). This equation simply means the sum of the diameters of all crystals divided by the total number of crystals. Note that the above equation is only valid for the particles of the same shape. In order to use this technique, it was assumed that the growth is uniform in three dimensions.

At time t, if growth rate is constant and all crystal growth start at t = 0, then the crystal size (x) is give by,

$$x = Ut \qquad 3.2$$

where U is the crystal growth rate. However, it should be appreciated that in SEM micrographs, the situation is complicated by two factors :-

a) The crystals are sampled at random by the sectioning technique and,

b) Not all crystals begin to grow at t = 0.

In the case of (a), it is possible to describe the average crystal diameter ($\bar{X}$) as the product of crystal size and a dimensionless shape factor k (3.4) ie;

$$\bar{X} = kx \qquad (3.3)$$

where k is a proportionality factor (4) which can be determined from the particle shape (5). Using relation (3.1) and (3.2), the mean growth rate (G) can be written as;

$$G = \frac{\sum_i N_i X_i}{t \sum_i N_i} = \frac{kx}{t} = kU \qquad (3.3)$$

Thus U can always be related to the observed mean growth rate G.

In the case of (b), this factor also leads to the observed mean growth rate G being less than U ie;

$$G = \frac{\sum_i N_i X_i}{t \sum_i N_i} = \frac{\sum_i N_i U (t - t_i)}{t \sum_i N_i} = U - \frac{\sum_i N_i t_i}{t \sum_i N_i} \qquad (3.4)$$

We have assumed that $t_i << t$ so that the second term can be neglected but it must be acknowledged that this is an approximation and is further complicated when growth deviates from linearity and becomes diffusion controlled.

It must be noted that because of the sampling technique, $U_{max} > G$ (where U_{max} is the maximum growth rate). But, since both quantities are related by a proportionality factor, the mean crystal growth measurement technique is still valid for any comparative growth rate measurement.

However, absolute values of growth would require a geometric correction.

It must also be noted that some errors could arise due to the experimental limitations such as the resolution of the microscope, uncertainties in length, incorrect counting, uncertainties in heat treatment time and so on. In most cases, these will not be the limiting factor. However the error was estimated to be less than 5 %.

There are different microstructural shapes of crystals seen in the sample depending on the composition. These include the spherical, lamellae, rod and star - like structures. The calculation of X for each type are shown in figure 3.3. All calculations of growth at a particular temperature, will be based on the above equation.

3.5 Viscosity Measurement

3.5.1 Sample Preparation

In general, any reasonably flat pieces of glass can be used. In this experiment, cylindrical pieces of glass about 1 cm. thick and 1 1/2 cm. in diameter were used in all cases.

3.5.2 Penetration Viscometer (Indentation Method)

The essential parts of the apparatus are given in figure 3.4. It is important however that the mechanism to supply

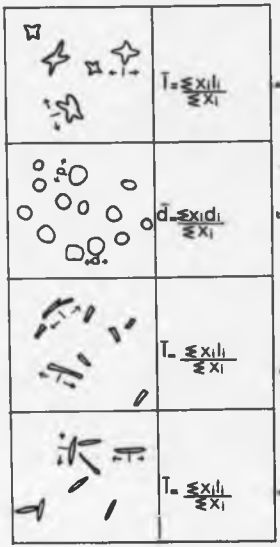

Fig. 3.3 : The overall morphology in the crystallised glass and the averaging equation involved.

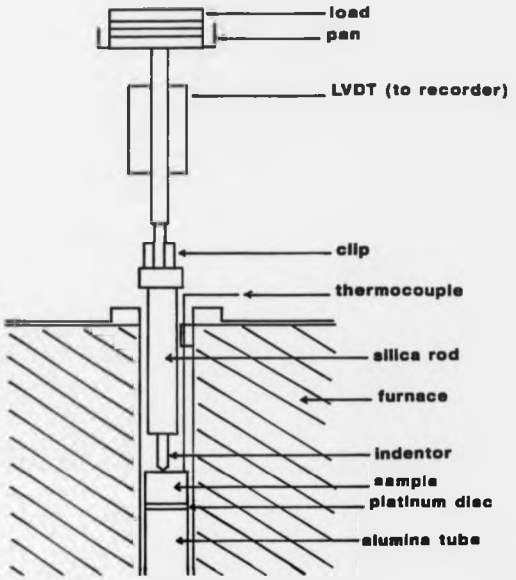

Fig. 3.4 : Essential parts of a penetration viscometer

the load must be well constructed so that its centre of gravity is well below the steel ball (indenter), thus ensuring stability. Moreover, the sample must be supported using very low thermal conductivity material so that it will not perturb the temperature condition. Before making any measurement, the temperature must equilibrate. So, a soaking time must be allowed. When the temperature reaches a constant value, contact between the upper surface of the glass and indenter can carefully be made. The rate of penetration can be read by using a scale movement attached on the upper part of the apparatus. After one determination, the indenter may be raised and another part of the glass surface may be used for another measurement at the same or higher temperature. The plot of the time taken for penetration against (penetration depth)$^{-1/2}$ will give a straight line. The line will not normally include the origin due to the zero time error. By taking the value of the gradient of the graph and inserting this value into the viscosity equation, the values of viscosities can easily be found.

Instead of using a scale movement to read the penetration displacement, the use of a Linear Voltage Displacement Transducer (LVDT) connected to the upper part of the indentor allows temperature, time taken and the penetrating displacement to be displayed simultaneously on a chart recorder.

A one kilogram load was applied to a glass sample. Before making any measurement, the sample and indenter were brought to the desired temperature and allowed about 30 minutes " soaking time ". The viscosity was measured for four different temperatures from slightly above Tg to slightly below Tc. The indenter displacement was measured using a linear voltage displacement transducer and the voltage signal sent to the chart recorder. The relation between the time t taken during the experiment and the (displacement)$^{3/2}$ at a specific temperature was plotted and the gradient of that relation was then fitted according to the equation given in section 2.5.2.4 to get the value of viscosity η. Having the values of η, the relation between viscosity (log scale) and temperature (reciprocal of absolute temperature) was then plotted.

3.6 Solubility

3.6.1 Sample Preparation

Cylindrical samples of glass with diameter = 11 mm and length = 8 mm were polished under hydrocarbon oil which is oxygen and water free in order to remove the aged surface layer and obtain a surface with no aqueous contact. The samples were then rinsed with xylene to remove the oil, ready for further experiment.

3.6.2 Distilled Water

Samples of about 4 gm in weight were immersed in 100 ml of distilled water, pH = 5.3 at 25 °C for 7 days. After that, the samples were taken out and washed thoroughly with xylene, leaving only the cleaned glass surface. Samples were then dried at 80 °C for 2 hours before being re - weighed. The ratio of weight losses per unit area were then plotted against the analysed Chlorine content of the glass.

3.6.3 100% Relative Humidity (RH)

Samples of about 4 gm in weight were left in a constant (100%) relative humidity enclosure at 25 °C for 7 days. After that, the same procedure as 3.6.2 was carried out.

3.6.4 Normal Atmosphere

Samples of about 4 gm in weight were left exposed to normal atmospheric conditions on a glass plate for 7 days at room temperature, 25 °C.After that, the same procedure as 3.6.2 was carried out.

3.6.5 pH Measurement

0.5 gm. of relatively fine glass powder were immersed in distilled water, pH = 5.3 at 25 °C. The change of pH value

was measured every 24 hours using a Kent Eil 7055 pH meter. These values were then plotted against time (days).

3.6.6 Water Permeation In Glass

A cylindrical glass sample with one polished flat surface (as in 3.6.1) was encapsulated in a transparent plastic tube so that only the polished surface was exposed. This was then connected to a flow of deionised water, pH = 5.2 at 20 °C (this value shows that there is little difference with distilled water). A measure of the water permeation of the glass was obtained by determining the position of the " diffusion " front using a vernier travelling microscope with an accuracy of ± 0.001 cm. A schematic diagram of this experiment can be seen in figure 3.5. The reading was taken every 24 hours up to 7 days. The values of water penetration distance were then plotted against the time taken.

3.6.7 Other Measurements

3.6.7.1 Measurement Of The Chloride Concentration

Chloride ion displaces thiocyanate from mercuric thiocyanate. The liberated thiocyanate is then read with ferric ion, as a measure of the chloride present.
Here, 10 ml of the sample solution containing chloride was mixed with 1 ml solution of mercuric thiocyanate in 95 %

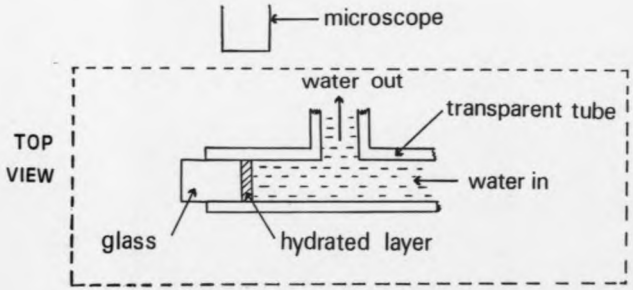

Fig. 3.5 : Schematic diagram for water permeation in glass.

ethanol. Addition of 2 ml of 6 % ferric ammonium sulphate in 1:5 sulphuric acid followed. The transmission of the solution at 460 mu was then compared with standards using a DMS 90 UV Visible Spectrophotometer. Details of the procedure are reported elsewhere (5).

3.6.7.2 Test To Identify The Presence Of Cations

Some tests to identify the presence of cations in solute water were carried out using " Spot " tests and " Flame " test. The experimental procedures are described below :

a. Spot Tests

1. Test For Pb^{2+} Or Zn^{2+}

There are two ways to spot the existence of lead or zinc in the sample solution. Both methods have been employed.

a. One spot of sample solution was added to one spot of 0.1 % dithizone. In the presence of lead or zinc, a well mixed solution will give a pink or red colour.

b. One spot of sample solution was added to one spot of 1 % HCl as well as one spot of sodium thiosulfate ($Na_2S_2O_3$). In the presence of lead, a white precipitate will be observed. If one spot of 0.1 % dithizone was added to the mixture, a magenta colour denotes the presence of zinc.

Details on the preparation of dithiazone are described elsewhere (6).

2. Test For Bi^{3+}

One spot of sample solution was added to one spot of 50 % sulphuric acid (H_2SO_4) as well as one spot of equal parts (ready mixed) of 25 % NaOH and 5 % $SnCl_2$. In the presence of Bi^{3+}, a well mixed solution will give a black precipitate.

Details of this test are available elsewhere (7).

b. Flame Test

A small amount of sample solution was put on a watch glass and mixed with concentrated HCl. A clean Platinum wire was dipped into this mixture and then inserted low down in the non - luminous outer zone of the bunsen flame. A colour of blue or green indicates the presence of antimony or thallium respectively. Details of this test are available elsewhere (8).

3.8.7.3 Quantitative Measurement Of Zn^{2+} And Pb^{2+}.

a. For Zn^{2+}, the complexometric titration method was employed. The procedure is as follows:

Dilute 25 ml of the sample solution containing Zn^{2+} to 100 ml with distilled water, add 2 ml of the buffer solution and a few drops of the indicator. Titrate with EDTA (ethylenediamine-tetra-acetic acid) solution until the colour changes from red to blue. The amount of zinc can be calculated by the factor: 1 ml, 0.1M EDTA = 6.538 mg of Zn.

Further details on the preparation of buffer solution and EDTA solution are given by Vogel (9).

b. For Pb^{2+}, the gravimetric analysis method was employed. The procedure is as follows;

10 ml of sample solution containing Pb^{2+} was diluted to 150 ml with distilled water. 4 ml of concentrated HNO_3 was added, heated, to boiling point, and then 25 ml of 6 % HIO_3 solution was slowly introduced and the mixture kept at 60 - 70 °C for 30 minutes. The mixture was then cooled to room temperature, and then filtered through a sintered glass crucible. The precipitate was washed first with 75 ml of 0.2 % HIO_3 in 1 % HNO_3, and then with three 2 ml portions of ice - cold water and finally with a little dry acetone. The precipitate was dried at 140 °C for 60 minutes and then weighed as $Pb(IO_3)_2$. The weight of Pb can be calculated by using a gravimetric factor.
Further details have been well described elsewhere (10).

3.6.8 Corrosion Rates

Seven cylindrical samples with a diameter ≈ 11 mm and length ≈ 8mm, were prepared and their weights were measured. Each sample was then immersed in 100 ml of distilled water with pH = 5.2 at 20 °C. Sample 1 was taken out in the first day and after being washed by xylene and the very white thin layer has been removed, the weight loss was measured. The corrosion rate was calculated by using the equation:

$$\text{Corrosion rates} = \frac{\Delta W}{S \cdot \Delta T} \quad (\text{gm cm}^{-1}\ \text{d}^{-1})$$

where ΔW is the weight loss, S is the total surface area and ΔT is soak time (days).

Sample 2 was taken out in the second day, third sample in the third day and so on. Everytime, the same calculation was carried out. Similar experiments were applied to other glasses.

3.6.9 Infra - Red Analysis

Some of the water - penetrated glass layer from the solubility test in 100 ml distilled water was removed and

ground into a relatively fine powder. This powder was then mixed with CsI (Cassium Iodide) and pressed into a pellet (≈ 0.12 mm thickness) for IR analysis of water content. Some of the remaining glass bulk which had undergone solubility test was also tested for the water content using the same method.

References

1. See eg: Wells, O.C. ; Scanning Electron Microscopy, Mc Graw Hill Book Co. (1974).
2. See eg: Underwood, E.E.; Quantitative Stereology, Addison - Wesley Pub. Co. (1970).
3. Herdan, G. ; Small Particle Statistic, Elsvier Pub. Co.1953 p 37 & 87.
4. DeHoff, R.T. ; Trans.AIME 230 (1964) 785.
5. Snell, F.D., Snell, F.T. and Snell, C.A. ; Calorimetric Methods Of Analysis, vol 11A, D. Van Nostrand Co. Ltd., New York, (1959) .
6. Feigl, F. ; Spot Test In Inorganic Analysis, Elsvier Pub. Co., (1958) p 473.
7. ibid, p 507.
8. Vogel, A.I., ; Macro And Semimacro Qualitative Inorganic Analysis, 4th ed. Longmans, 1962. p 145.
9. Vogel, A.I., ; Quantitative Inorganic Analysis, 3rd ed. Longmans, 1961, p434.
10. ibid, p 483.

CHAPTER 4 : RESULTS

4.1 Phase Development

4.1.1 Phase Identification

Values of Tg and Tc of most glass compositions, obtained using DSC, are given in detail in table 4.1. In some samples, more than one crystallisation temperature Tc was observed. As we can see from the table, the values of Tc - Tg are in the range from 53 °C in S_5 to 149 °C in S_{21}, showing good stability for the glass system. The values of the glass transformation range temperature Tg were in the range from 190 °C up to 318 °C. Some of the values were taken from ref. (1).

Some of the X-ray diffraction patterns of the samples when heat - treated at Tc_1 are shown in figure 4.1. Strong peaks can be observed in S_1 to S_4 and S_7 to S_{10} while only medium intensity peaks are observed in S_6 and S_{11}. A match of the calculated d spacings was made to the JCPDS index files to identify the primary crystal phases. It was found that the crystal phases that appeared were predominantly Sb_2O_3 of the valentinite type, $ZnCl_2$ and a Sillen phase based on $PbSbO_2Cl$ (2). Additionally, $PbCl_2$ occurred in the crystallised sample of S_8.

It should however be noted that the match of the phase $PbSbO_2Cl$ with the JCPDS index files is not straight forward

Samp. No.	Glass composition (mol %)	Tc (± 1) °C	Tg	Tc - Tg
A_1	0.8 Sb_2O_3 - 0.2 $ZnCl_2$	381	281	100
A_2	0.6 Sb_2O_3 - 0.4 $ZnCl_2$	411	279	132
S_1	0.7 Sb_2O_3 - 0.3 $PbCl_2$	459	318	141
		485		
S_2	0.5 Sb_2O_3 - 0.5 $PbCl_2$	315	265	50
		388		
S_3	0.6 Sb_2O_3 - 0.3 $PbCl_2$ - 0.1 $ZnCl_2$	455	306	149
S_4	0.6 Sb_2O_3 - 0.2 $PbCl_2$ - 0.2 $ZnCl_2$	393	281	111
		425		
S_5	0.5 Sb_2O_3 - 0.3 $PbCl_2$ - 0.2 $ZnCl_2$	343	283	60
S_6	0.4 Sb_2O_3 - 0.3 $PbCl_2$ - 0.3 $ZnCl_2$	332	269	63
S_7	0.3 Sb_2O_3 - 0.3 $PbCl_2$ - 0.4 $ZnCl_2$	281	235	46
		330		
S_8	0.2 Sb_2O_3 - 0.3 $PbCl_2$ - 0.5 $ZnCl_2$	243	190	53
		290		
		390		
		445		
A_3	0.4 Sb_2O_3 - 0.6 $ZnCl_2$	315	253	62

Table 4.1 : Tc, Tg and Tc - Tg values for Sb_2O_3 - $PbCl_2$ - $ZnCl_2$ glasses. (The values for S_1, S_3, S_5, S_6, S_7 and S_8 are taken from ref.1).

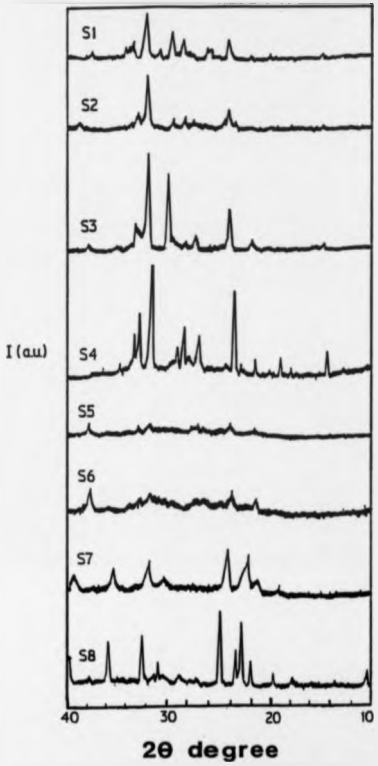

Fig. 4.1 : X - ray diffraction pattern of crystallised sample from S glasses after heat treatment at Tc1 for 24 hours.

but differs slightly by about 0.2 ° 2θ systematically, suggesting that a further examination is required in order to determine the correct phases. This task, however can be carried out by means of EDX analysis technique.

The nominal and EDX analysed compositions of the glasses are presented in table 4.2. Because of differential losses during melting (due to volatile components), the analysed components of the glass differ from the nominal. An example of the calculation to find the actual composition is given in appendix 1. From the result obtained, two ternary diagrams of nominal and actual glass composition can be drawn. They are shown in figure 4.2a and 4.2b respectively. The analysed chlorine percentage (% Cl) content of the glasses is also presented in table 4.2. The EDX results can be used to aid phase identification.

Another technique to identify the occurrence of the phases is by means of I-R analysis. Some of the I-R spectra from the samples when heat treated at T_{c_1} can be seen in figure 4.3. As can be seen, there are four types of spectra which correspond to the presence of four crystal phases in the crystallised glasses. The first phase region appears to be S_1 to S_4 , the second S_2 and S_4, the third S_3 and finally S_4. The variations of the spectra will be discussed in more detail in the next chapter.

Sample No.	Nominal (%)			Analysed (%) (± 1)			% Cl (± 0.1)
	M_1	M_2	M_3	M_1	M_{2a}	M_{3a}	
A_1	80	-	20	84	-	16	16.0
A_2	60	-	40	71	-	29	27.5
S_1	70	30	-	71	29	-	19.5
S_2	50	50	-	48	52	-	33.5
S_3	60	30	10	59	38	3	22.0
S_4	60	20	20	69	20	11	27.6
S_5	50	30	20	59	28	13	28.0
S_6	40	30	30	50	37	13	32.1
S_7	30	30	40	40	33	27	48.5
S_{8b}	20	30	50	18	42	40	59.0
A_3	40	-	60	60	-	40	34.5

Table 4.2 : The nominal and analysed constituents of S glasses (mol %).

M_1 - Sb_2O_3 M_2 - $PbCl_2$ M_3 - $ZnCl_2$

M_{2a} - Pb (O,Cl) M_{3a} - Zn (O,Cl)

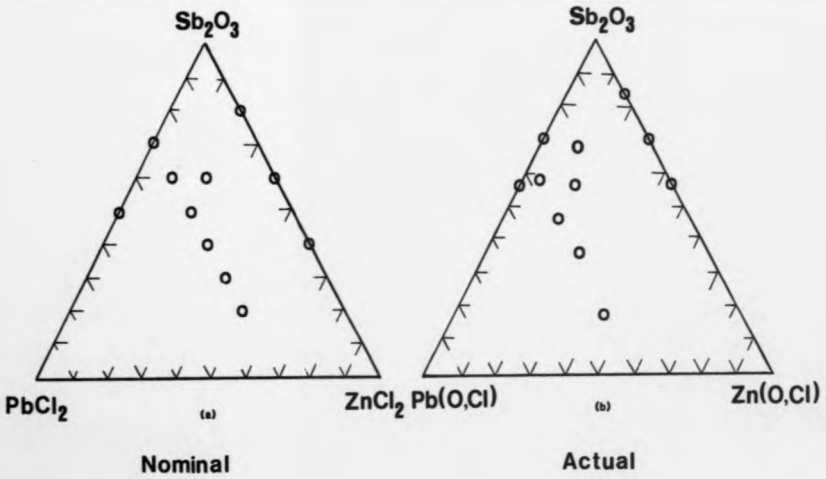

Fig. 4.2 : Ternary diagram for the composition of S glasses.

a - nominal b - actual

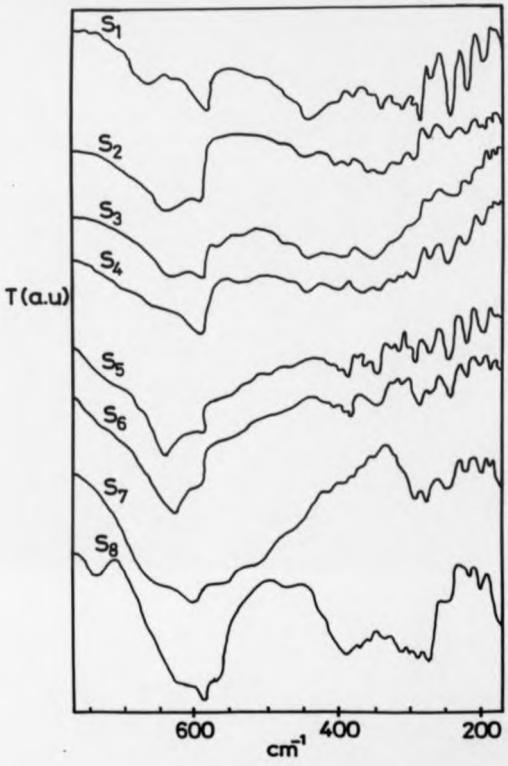

Fig. 4.3 : IR spectra with CsI powder for crystallised S glasses.

4.1.2 Phase Formation As A Function Of Composition

Phase formation in glasses which were heat - treated at T_c was primarily determined by XRD and by EDX (table 4.3). As can be seen from the table, XRD gives the major phase as $PbSbO_2Cl$ for all the $PbCl_2$ containing samples in the composition range below 50 % $ZnCl_2$. After this, the major phase is $PbCl_2$ of the coruntinite type with $ZnCl_2$ of the β type as the minor phase. Surprisingly, this is not the case when analysed by EDX. As shown, there are clearly several phases of lead antimony oxychloride with various oxygen contents, depending on the glass composition. For the glass compositions S_1 to S_4, the major phase formed was $PbSb_2O_{3.5}Cl$. Then the oxygen content of the second phase reduces systematically to $PbSb_2O_{3.0}Cl_2$ at the glass composition of S_7 while no oxide phase is formed in S8. So, as the Sb_2O_3 content is reduced and the $ZnCl_2$ content increased, the composition of the major phase is gradually changed from one with oxygen content to none. It indicates that the presence of $ZnCl_2$ might play a major role in the phase formation.

Samples of A_1, A_2 and A_3 showed no oxygen variation in the lead antimony oxychloride, ie; both $PbCl_2$ and $ZnCl_2$ are required.

Sam. No.	Tc (± 1) °C	Phase Occurrence XRD Analysis major	XRD Analysis minor	EDX Analysis major	EDX Analysis minor
A_1	381	Sb_2O_3	-	Sb_2O_3	-
A_2	411	"	-	"	-
S_1	459	$PbSbO_2Cl$	Sb_2O_3	$PbSb_2O_{3.5}Cl$	Sb_2O_3
	485	"	"	"	"
S_2	315	"	"	"	"
	388	"	"	"	"
S_3	455	"	"	"	"
S_4	393	"	"	"	"
	425	"	"	"	"
S_5	343	"	"	$PbSb_2O_3Cl_2$	"
S_6	332	"	"	"	"
S_7	281	"	"	$PbSb_2O_{2.5}Cl_3$	"
	330	"	"	"	"
S_8	243	$PbCl_2$	β - $ZnCl_2$	$PbCl_2$	β - $ZnCl_2$
	290	"	"	"	"
	390	"	"	"	"
	445	"	"	"	"
A_3	315	Sb_2O_3	-	Sb_2O_3	"

Table 4.3 : The phase occurrence in S series glasses, identified by XRD and EDX analysis after heat treatment at Tc.

4.2 Microstructure

4.2.1 Structural Morphologies

SEM micrographs show the general crystal morphologies of samples which have been heat - treated for 24 hours (except for S_4, S_7 and S_m) as summarised in table 4.4. Some of them are globular or spherical in shape, some have star - like structures, tree - like structures and some of them are irregular in shape. The crystallite structure of S_1 (figure 4.4a) is star - like while in S_2 (figure 4.4b) it is spherical. In S_3 (figure 4.4c) the crystallite structure is tree - like. This is an example of dendritic growth where the nucleation starts at the bottom of the " V " shapes and then a spike grows out from the tip and develops sideways into branch arms. The morphologies of S_5 and S_6 seem to be irregular lamellar structures (figure 4.4d). In S_{11}, the globular shapes are adopted by both phases with lead antimony oxychloride appearing much brighter than the Sb_2O_3 phase (figure 4.4e). In S_{12}, there are irregularly shaped $ZnCl_2$ crystal surrounded by lead chloride (figure 4.4f). For comparison, the microstructure of A_1 is also included (figure 5.13). The effect of chloride concentration on the crystal growth rate and other properties will be discussed in chapter 5.

Sample No.	Structural Discription
S_1	" star - like " with " stretching fibre " at the sides.
S_2	" globular " with " stretching fibre " at the sides.
S_3	" tree - like " growth.
S_4	" star - like " growth.
S_5	irregular pattern.
S_6	irregular pattern.
S_7	" globular " shapes.
S_8	" globular " shapes.

Table 4.4 : The overall morphology of some samples.

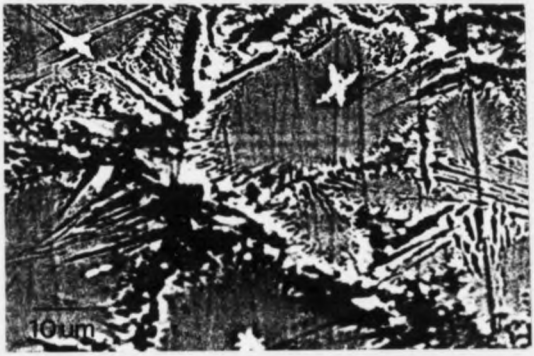

Fig. 4.4(a) : SEM micrograph of S1 glass after heat treatment at Tc = 459 °C for 24 hours.

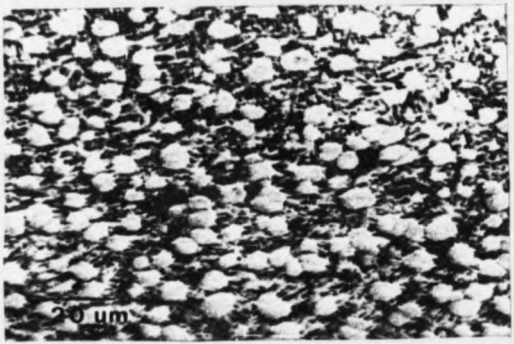

Fig. 4.4(b) : SEM micrograph of S2 glass after heat treatment at Tc = 315 °C for 24 hours.

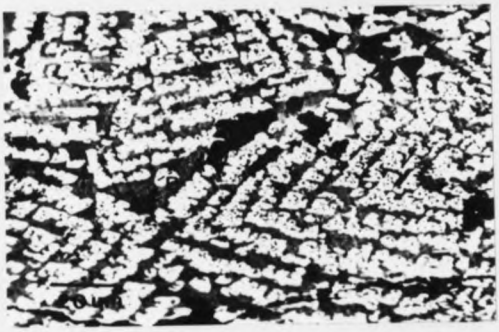

Fig. 4.4(c) : SEM micrograph of S3 glass after heat treatment at Tc = 455 °C for 24 hours.

Fig. 4.4(d) : SEM micrograph of S5 glass after heat treatment at 400 °C for 20 min.

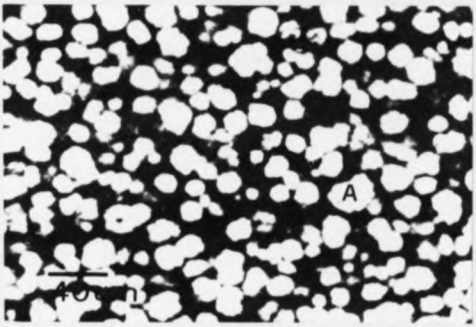

Fig. 4.4(e) : SEM micrograph of S7 glass after heat treatment at Tc = 280 °C for 8 minutes, showing phases:-

A - $PbSb_2O_{2.5}Cl_3$ B - Sb_2O_3

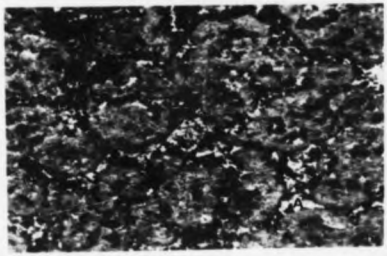

Fig. 4.4(f) : SEM micrograph of S8 glass after heat treatment at Tc = 320 °C for 20 min., showing phases:-

A - $PbCl_2$ (white)

B - B - $ZnCl_2$ (dark)

4.2.2 Volume Fraction

The volume fractions of the various crystal phases were determined to show how phase development in a series of glasses varies as a function of composition. Such assessment is very important especially in the study of quantitative stereology.

The volume fraction of each phase has been calculated using areal analysis (3). Relatives areas can be determined from a tracing of the micrograph by cutting out the phase of interest and weighing all the pieces, then comparing to the total weight. For improved accuracy, measurement has to be carried out on several micrographs. The results of this measurement are displayed in table 4.5. In order to relate these results to glass composition, a plot of volume fractions of the phase of interest ie; lead antimony oxychloride, with nominal percentage of $ZnCl_2$ was made and the plot is presented in figure 4.5. The relation to the analysed chlorine content is also shown.

4.3 Measurement Of Growth Rate

4.3.1 Growth Versus Time

The growth of crystals in the glass was determined by thermal exposure for a certain time which in this case is about 4 - 20 minutes. However, a long time exposure is

Volume Fraction (%)

Sample No.	$PbSb_2O_{3.5}Cl$	Sb_2O_3	Residual Glass
S_1	2.5	48.5	49.0
S_2	33.2	63.7	3.1
S_3	52.8	38.0	9.2
S_4	70.5	28.0	1.5
	$PbSb_2O_5Cl_2$ +	Sb_2O_3	
S_5	88.0		12.0
S_6	91.0		9.0
	$PbSb_2O_{2.5}Cl_3$	Sb_2O_3	
S_7	82.0	7.0	11.0
	$PbCl_2$	$ZnCl_2$	
$S_{8,9}$	52.1	30.2	17.7

Table 4.5 : Volume fractions of phases calculated using the areal analysis method.
(After heat treated at Tc_1 for 24 hrs.)
(Error ± 3%)

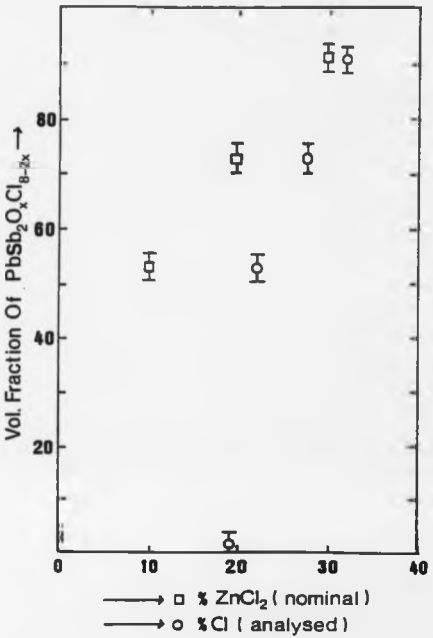

Fig. 4.5 : The variation of the volume fraction of $PbSb_2O_xCl_{8-2x}$ with $ZnCl_2$ and chlorine content.

needed to complete the growth curve. The mean size of the crystal is then measured using the method described in the previous chapter. The results of both measurements for S_1 can be seen in figure 4.6a and 4.6b for short and long times respectively. At short time, the graph is linear but curvature is apparent after about 1 hour exposure time. For glasses S_3, S_5, S_4, S_7 and S_8, only short time exposures were applied. The results of these measurements are displayed in figures 4.7 to 4.11. Except for S_8 and S_4, where the phases were not distinguishable, the glasses exhibit separate growth curves for each phase. In S_6, the growth of $ZnCl_2$ is impossible to measure since the phase is extremely small and irregular.

In some samples such as S_1, at higher temperature, the growth of the minor phase seems larger than the major phase, while in S_7, all the growth curve for the minor phase lie below that of the major phase.

4.3.2 Growth Rate Versus Temperature

From the variation of crystal size with time, then the rate of growth can be calculated by dividing the growth (mean size of the crystals as measured by microscope) by the time of exposure. Figures 4.12 to 4.17 represent the growth rate - temperature curves of S_1, S_2, S_3, S_4, S_7 and S_8 respectively. Most of the major phase curves show a maximum

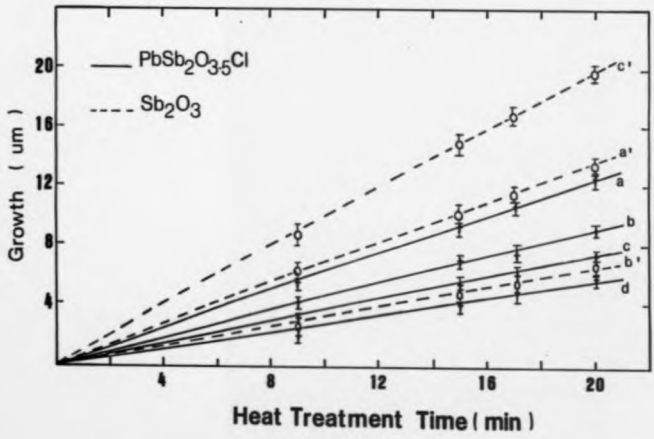

Fig. 4.6(a) : Growth of S1 for short heat treatment time.
(a = a' = 470 °C, b = b' = 450 °C, c = c' = 490 °C, d = 430 °C).

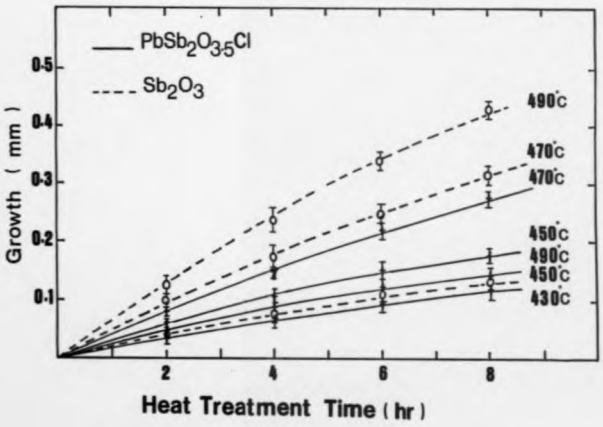

Fig. 4.6(b): Growth of S_1 for longer heat treatment time and temperature.

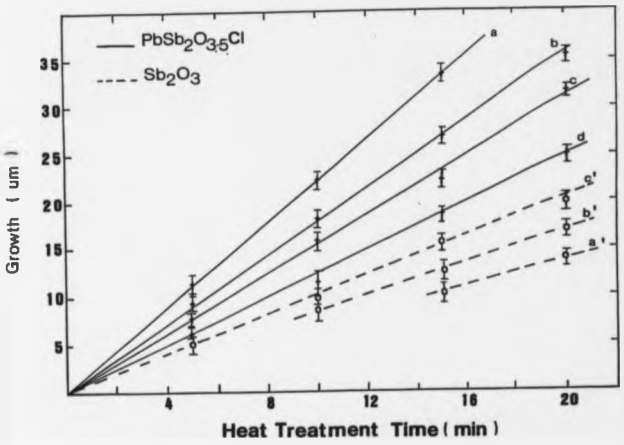

Fig. 4.7 : Growth versus time for 53 glass.
(a = a' = 440 °C, b = b' = 470 °C,
c = c' = 500 °C, d = 400 °C) .

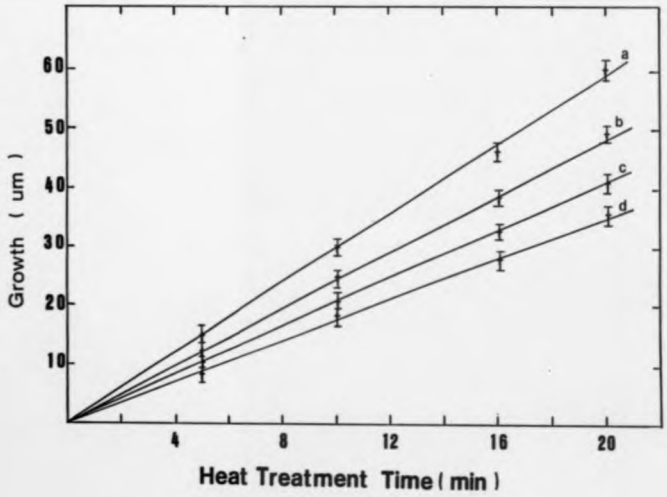

Fig. 4.8 : Growth versus time for S5 glass.
(a = 380 °C, b = 400 °C, c = 360 °C
d = 340 °C). The graph corresponds to
the growth of $PbSb_2O_3Cl_2$ + Sb_2O_3 .

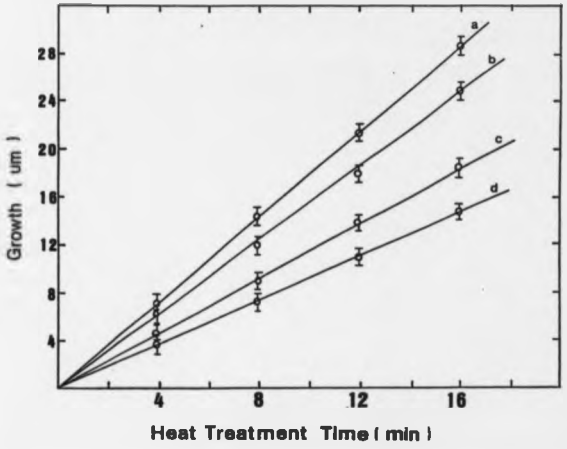

Fig. 4.9 : Growth versus time for S_6.
(a = 340 °C, b = 360 °C,
c = 300 °C, d = 280 °C).
The graph corresponds to the
growth of $PbSb_2O_3Cl_2$ + Sb_2O_3.

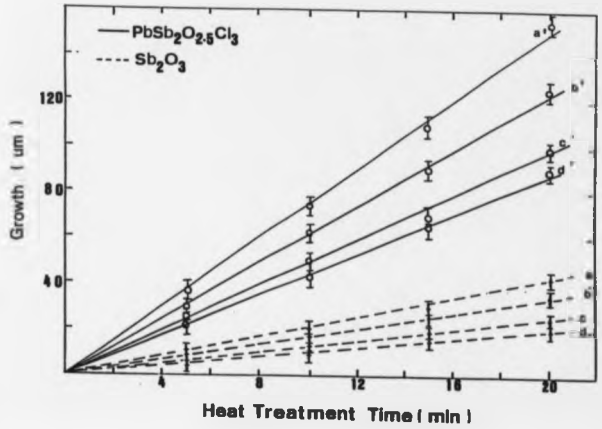

Fig. 4.10 : Growth versus time for S_7.
(a = a' = 300 °C, b = b' =
360 °C, c = c' = 380 °C, d =
d' = 280 °C) .

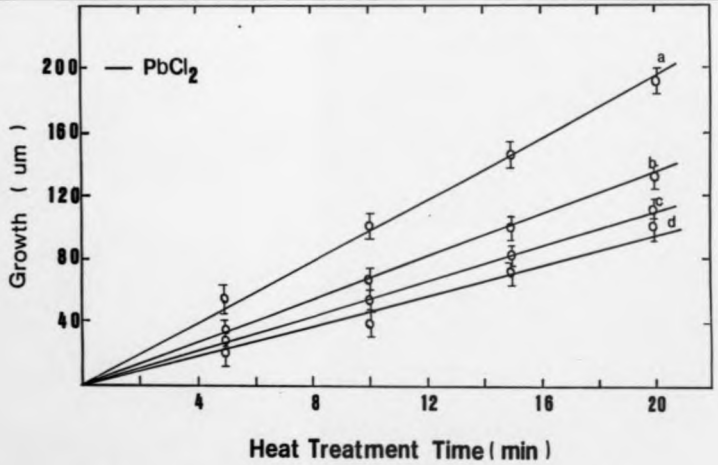

Fig. 4.11 : Growth versus time for S8 glass. Only the growth of $PbCl_2$ is shown. (a = 320 °C, b = 360 °C, c = 280 °C, d = 400 ° C) .

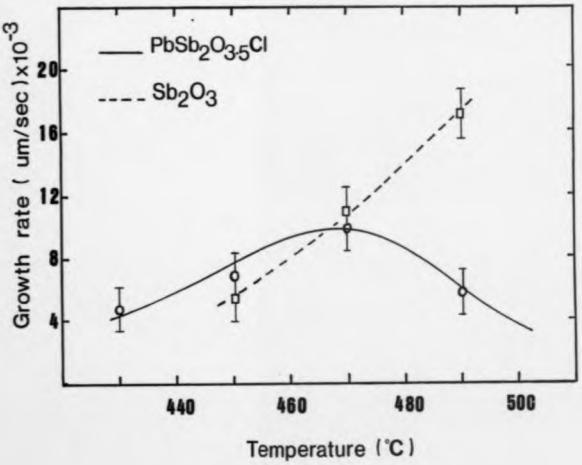

Fig. 4.12 : Growth rate - temperature curve for S_1.

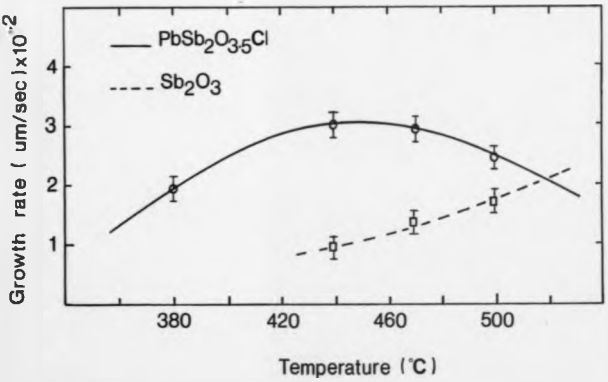

Fig. 4.13 : Growth rate - temperature curve for S3.

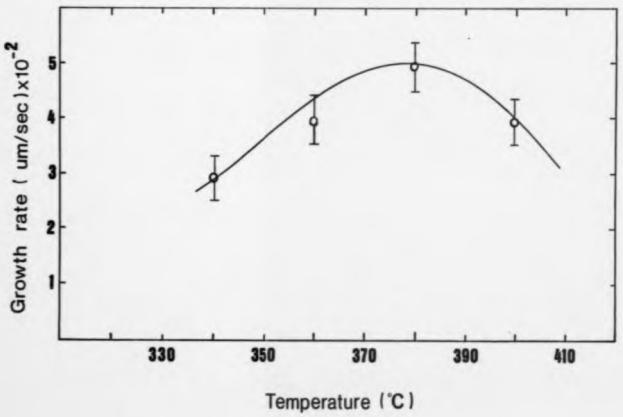

Fig. 4.14 : Growth rate - temperature curve for S_5.

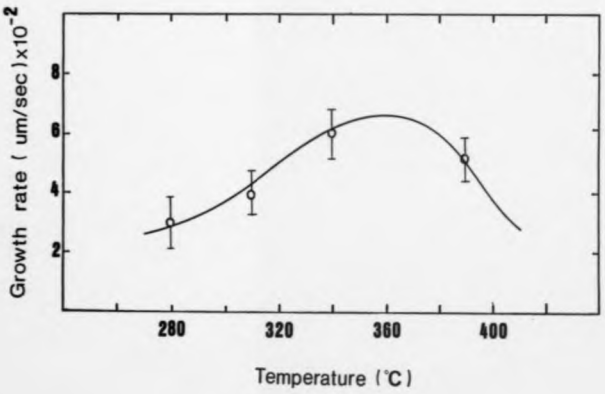

Fig. 4.15 : Growth rate - temperature curve for S_6.

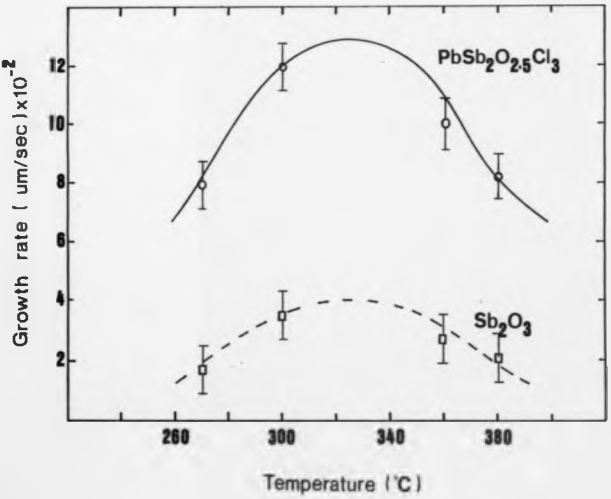

Fig. 4.16 : Growth rate - temperature curve for S_7.

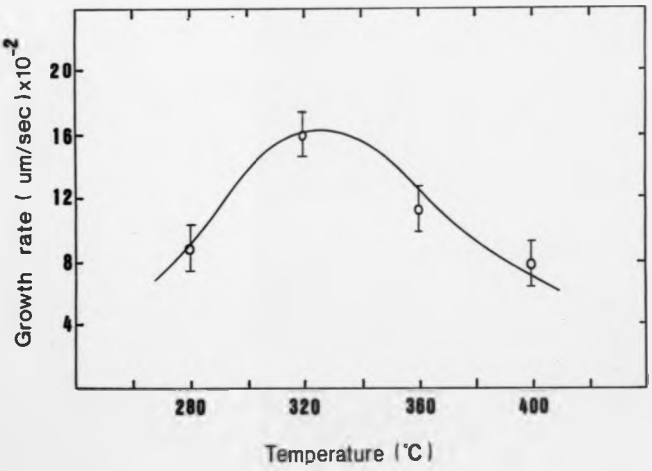

Fig.4.17 : Growth rate - temperature curve for Sn.

whereas the second phase often only shows the first part of the growth rate - temperature curve.

4.3.3 Maximum Growth Versus Chlorine Content

From the curves of growth rates (figure 4.12 - 4.17), the maximum growth rate ie; the highest point where the curve gradient was zero, can be taken. These points can then be plotted against the analysed chlorine content of each sample. This relation is presented in figure 4.18. As can be seen, the relation between these two parameters give a straight line ie; as the percentage of chlorine increases, the maximum growth rate increases.

4.3.4 $T_{...}$ Versus Chlorine Content

As can be seen from the growth rate curves, the maximum growth rate occurs at a certain heat treatment temperature, $T_{....}$ Taking all $T_{...}$ values, the plot against the analysed percentage of chlorine content of each sample can be made. The result of this plot can be seen in figure 4.19. The figure shows that, when the chlorine content increases, the maximum temperature decreases slowly.

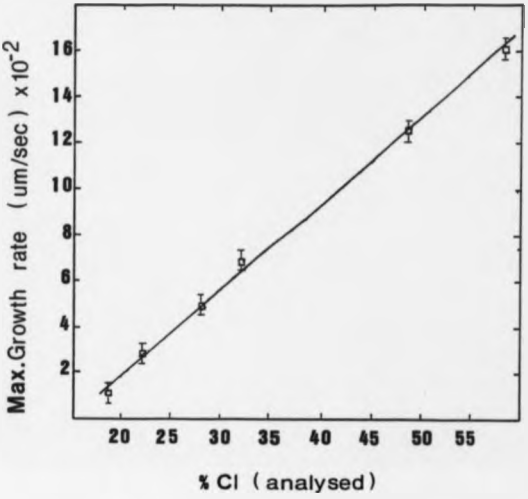

Fig. 4.18 : Maximum growth rate versus chlorine content.

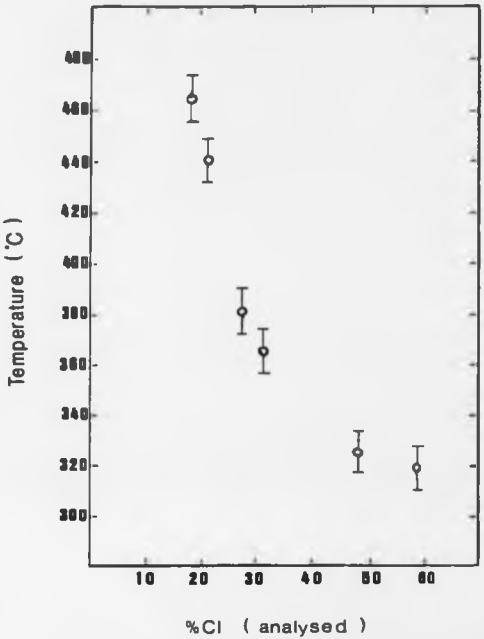

Fig. 4.19 : The relation between T_{max} (temperature corresponding to maximum growth rate) and chlorine content.

4.4 Measurement Of Viscosity

4.4.1 Log η Versus Temperature

The relation between viscosity and temperature is presented as the log scale of viscosity against the reciprocal of absolute temperature in Kelvin. Figure 4.20 shows that the parameters are related by a straight line. The range of viscosity which has been covered is about 10^{6} P to 10^{13} P with an accuracy of about ± 2 % .

4.4.2 Log η Versus Chlorine Content

Log viscosity versus analysed percentage chlorine content of each sample is plotted in figure 4.21. It is clear from the figure that, as the chlorine content increases, the log viscosity slowly decreases.

4.5 Measurement Of Chemical Durability

4.5.1 Weight Loss / Area Versus Chlorine Content

The weight loss per unit area of samples when exposed to 100 % relative humidity (RH) and when immersed in 100 ml of distilled water (for 7 days in both cases) are plotted against the analysed percentage chlorine content in figures 4.22 and 4.23 respectively. Both plots show a significant

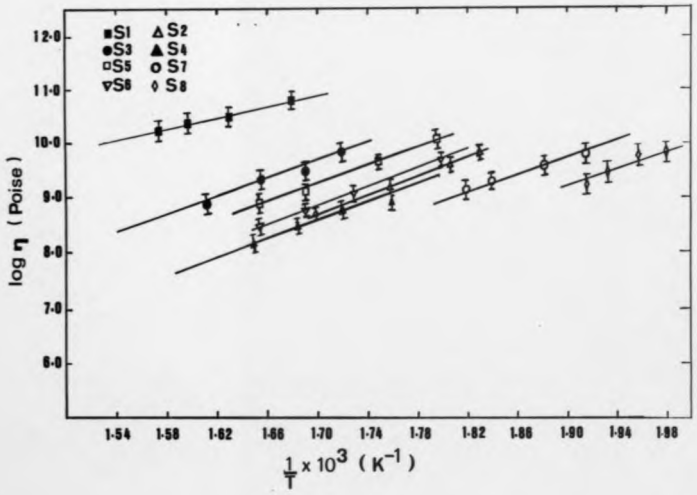

Fig. 4.20 : Log viscosity against reciprocal of absolute temperature.

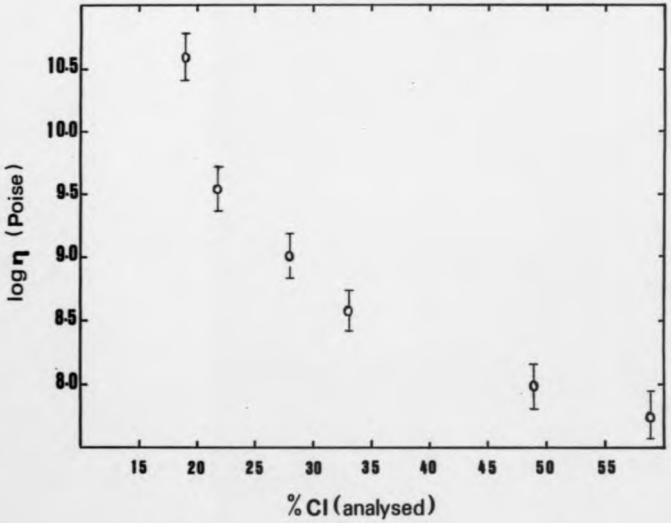

Fig. 4.21 : Log viscosity at 322 °C against the analysed chlorine content.

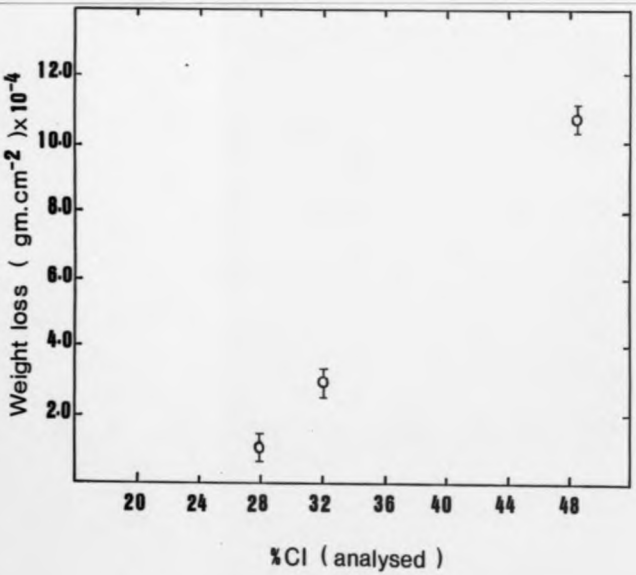

Fig. 4.22 : Weight loss versus chlorine content for S glasses when exposed to distilled water, pH = 5.2 at 20 °C for 7 days.

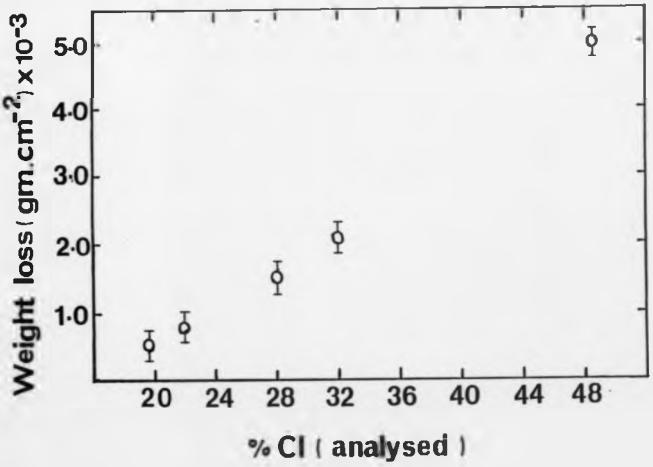

Fig. 4.23 : Weight loss versus chlorine content for S glasses when exposed to distilled water, pH = 5.2 at 20 °C for 7 days.

loss of weight, especially for those samples with high chlorine content .

The result of the solubility experiment under normal atmospheric condition is displayed in table 4.6. As can be seen, the glasses with lower chlorine content experience very low losses, while the glasses with higher chlorine content are relatively rapidly attacked.

4.5.2 Corrosion Rate Versus Chlorine Content

By dividing the weight loss per unit area with the exposure time (days), the corrosion rate was obtained. These values were then plotted against the soak time and against the analysed percentage of chlorine in figures 4.24 and 4.25 respectively.

4.5.3 Water Permeation Test

4.5.3.1 Penetration Depth Versus Time

The depth of penetration of the glass surface by water was measured using a travelling microscope. The penetration depths were then plotted against the exposure time and the results are displayed in figure 4.26. From this figure, it is clear that the depth increased with exposure time. The relation was linear with time $t^{1/2}$ up to several days. For

Samp. No	Weight loss (gm cm-2)
S_1	$< 10^{-6}$
S_2	$< 10^{-6}$
S_3	$< 10^{-6}$
S_4	$< 10^{-6}$
S_5	$< 10^{-6}$
S_6	1.5×10^{-5}
S_7	2.3×10^{-5}

Table 4.6 : Weight loss per unit area S glasses when exposed to normal atmosphere for 7 days at 25 °C.
(Error ± 10%).

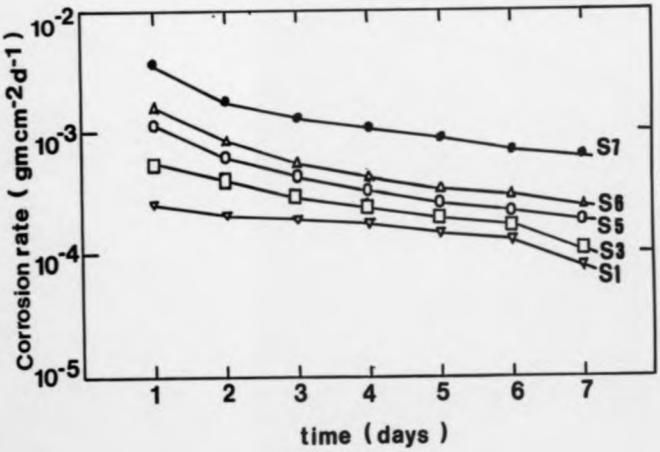

Fig. 4.24 : Corrosion rate versus time for S glasses.

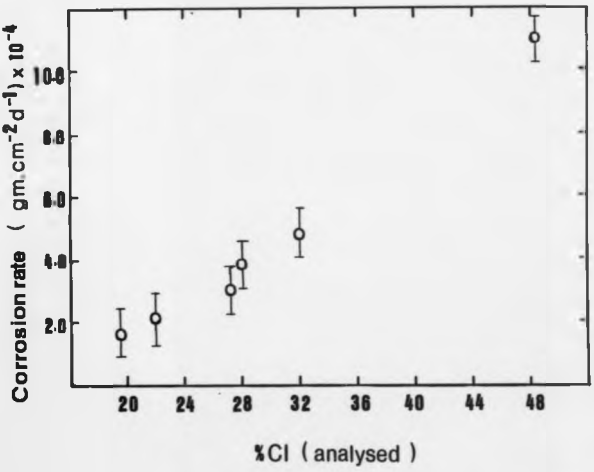

Fig. 4.25 : The relation between corrosion rate (4 days in distilled water) and chlorine content.

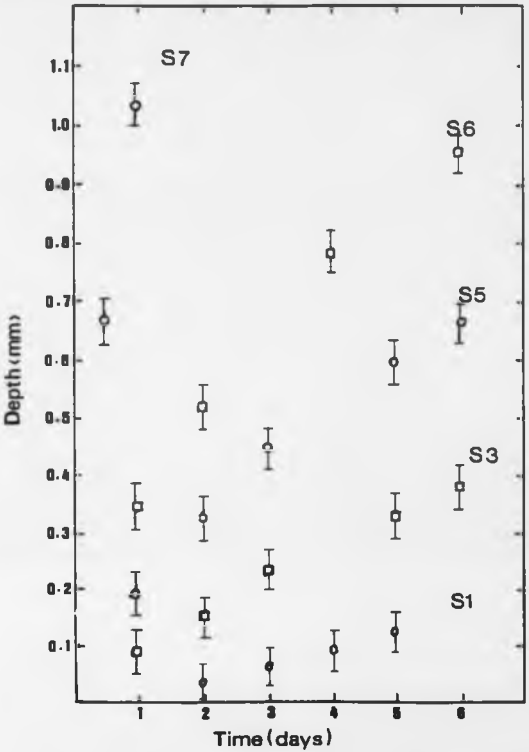

Fig. 4.26 : Penetration depth versus time for S glasses.

sample S_1, the depth only became measureable after being exposed for about 1.5 days.

4.5.3.2 Penetration Depth Versus Chlorine Content

Figure 4.27 shows the relation between the penetration depth after 4 days exposure time and the analysed percentage of chlorine. The relation shows a steady increase in penetration as the chlorine content becomes higher.

4.8.4 Solution pH

The change in pH of the solution may provide an indicator of the corrosion mechanisms and therefore pH measurement was conducted up to 7 days. The temporal variation of solution pH for glasses S_1, S_2, S_3, S_4 and S_7 is presented in figure 4.28. All show a marked decrease in pH from 5.0 to 3.0 over several days. The tests were conducted in static conditions.

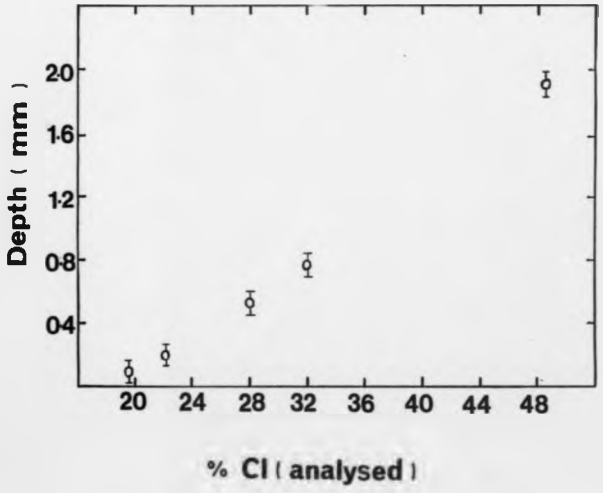

Fig. 4.27 : The relation between penetration depth after 4 days and chlorine content.

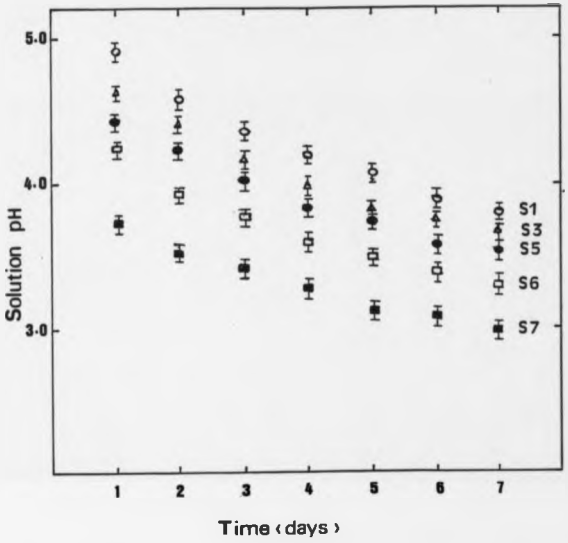

Fig. 4.28 : The temporal variation of solution pH for 5 glasses after being immersed in distilled water for various times.

References

1. Ahmed, M.M and Holland, D. ; Glass Tech. 28 (1987) 141.

2. JCPDS Data Card, Entrance File Number; 17-469.

3. Underwood, E.E. ; Quantitative Stereology, Addison - Wesley Pub. Comp. ,1970.

CHAPTER 5 : DISCUSSION

5.1 Introduction

In the present chapter we will discuss all the experimental results which have been presented in the previous chapter and include the effect of adding $BiCl_3$ and TlCl to the glass composition. As in the previous sections, this section will examine the effect of such materials on thermal stability, phase occurrence, crystal growth rate, viscosity and the chemical durability of the glass.

5.2 Thermal Characteristics

All the values of glass transformation temperature (T_g), glass crystallisation temperature (T_c) and glass stability range ($T_c - T_g$) are displayed in chapter 4. The results show that the stability range of up to 149 °C was obtained. This value decreases however when the nominal concentration of $ZnCl_2$ is increased. It is found that the analysed chlorine content controls most of the thermal characteristics of the glass. This is perhaps due to the ability of the chlorine to disrupt the glass network. Other thermal properties including the thermal expansion coefficient have been discussed and reported elsewhere (1).

5.3 Analytical And Microstructural Study

As have been mentioned earlier, the X - ray diffraction indicates a phase in the crystallised glass which is found to be in fact a family of phases from the results given by EDX analysis. In order to confirm this identification, the lattice parameters for the unknown crystal phases were calculated from the X - ray data. This was carried out using a method suggested by many workers (see eg. ref. 2). The calculated results can be seen in table 5.1. They show that the phase Sb_2O_3 (valentinite) is close to the JCPDS material as the lattice parameters of this standard are a = 4.9 Å , b = 12.4 Å , c = 5.42 Å with orthogonal symmetry. The other phase is clearly a tetragonal phase of lead antimony oxychloride. This is in contrast to the identification of $PbSbO_2Cl$ as an orthorhombic structure (3). So, the phase is not simply $PbSbO_2Cl$ but a lead antimony oxychloride with a variation in stoichiometry. This is consistent with the study using Raman Scattering Spectroscopy reported by Dubois et al.(4) which also found that the structure is not orthorombic but tetragonal. If the value of a_o of this system is plotted versus the " sample number " (i.e. increasing nominal content of $ZnCl_2$), this produces the graph as shown in figure 5.1. From this figure, it is evident that from S_1 to S_4 (Zone A), one phase exists, whilst other phases occur at Zone B, Zone C and Zone D. This is consistent with the phase analysis by EDX which

Sa. No.	Ph.No.	Lattice Parameters (Å) (± 0.01)			System
		a	b	c	
$S_{1.}$	1	6.32	-	11.80	T
	2	4.82	12.30	5.45	O
$S_{2.}$	1	6.38	-	11.95	T
	2	4.80	11.95	5.30	O
$S_{1.}$	1	6.19	-	10.90	T
	2	4.82	11.9	5.48	O
$S_{4.}$	1	6.33	-	12.13	T
	2	4.74	11.70	5.50	O
S_{5}	1	7.90	-	12.90	T
	2	4.74	12.00	5.41	O
S_{6}	1	7.90	-	12.90	T
	2	4.82	12.90	5.41	O
$S_{7.}$	1	8.50	-	12.90	T
	2	4.82	12.90	5.20	O
$S_{8.}$	1	7.45	9.13	4.54	O

Table 5.1 : Calculated lattice parameters and the crystal system of some samples.

T - Tetragonal O - Orthogonal

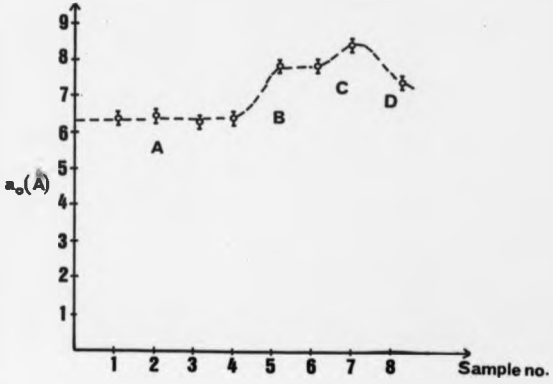

Fig. 5.1 : The lattice parameter (a_o) versus sample number, showing four distinctive phase zones.

shows that there are four types of lead antimony oxychloride. In addition, if the ratio of Oxygen : Chlorine is calculated from EDX analysis, the results show that there are four distinct ratios which correspond to the four types of phase. The results of these calculations can be seen in table 5.2. If these ratios are plotted against the sample number as seen in figure 5.2, it can be clearly seen that there are four zones in the figure which again supports the above evidence. So, the variation in Oxygen : Chlorine ratio and lattice parameters are both consistent with EDX analysis. This confirms that the analysis was correct.

As further confirmation, the samples were investigated by using I - R spectrophotometry. The results of this investigation have been displayed in figure 4.3. An examination of this figure shows that the I - R spectra are similar for S_1 to S_{11}, a different pattern occurs for S_{12} to S_{14}, another for S_{15} and another for S_{16}. These results show that there are four slightly different phases present in the samples. This is also consistent with the previous discussion.

We believe that the absorption bands between 460 cm^{-1} - 670 cm^{-1} in S_1 to S_5 are dominated by the Sb-O-Sb stretching vibration and the bands between 180 cm^{-1} - 460 cm^{-1} are due to the existence of various compounds of lead antimony oxychloride. However, more detailed analysis is required.

Sample No.	Oxygen - Chlorine Ratio (± 0.01)	
	Calculated	Expected
$S_{1a,b}$	3.32 , 3.56	3.50
$S_{2a,b}$	3.30 , 3.00	3.50
S_3	3.00	3.50
$S_{4a,b}$	3.00 , 3.10	3.50
S_5	1.60	1.50
S_6	1.90	1.50
$S_{7a,b}$	0.65 , 0.84	0.83
S_8	0.16	0.00

Table 5.2 : Calculated O:Cl ratio of the crystal phase from EDX and expected ratio from the phase formation.

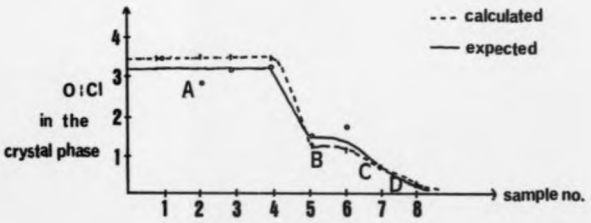

Fig. 5.2 : The relation between O : Cl ratio and sample number.

---- Calculated from EDX analysis

____ Calculated from the phase formulae

Calculation of volume fractions of the phases (see table 4.5 and figure 4.5), clearly indicates that as the nominal or analysed percentage of $ZnCl_2$ and Cl respectively, increase, the volume fraction of the Sillen type phase increases as well. At 40 % $ZnCl_2$ (nominal) or 48.5 % Cl (analysed), the volume fraction decreases. This decrease may correspond to the changes in major phase occurrence. Therefore from a microstructural point of view, there are also changes reflecting the EDX analysis results.

The microstructures of S_1 and S_2 (figure 4.4a and 4.4c respectively) are significantly different although only 10 % of $ZnCl_2$ was added to the latter composition. While in S_1 the structure is star - like, in S_2 there is a tree - like structure or dendritic structure. The characteristic growth for the latter type has been reported in detail by Chalmers (5). This indicates that $ZnCl_2$ might play some role in determining the crystal morphology.

A higher magnification of S_1 and S_2 shows that the growth morphology of Sb_2O_3 takes the form of " stretching fibres ". This can be seen in figure 5.3a and 5.3b respectively. This is probably due to the depletion of Pb or Cl which is necessary to the growth of lead antimony oxide - chloride at the centre followed by Sb_2O_3. If the percentages of Pb and Cl (using EDX analysis across the area shown) are plotted, the result in figure 5.4 is obtained. From this figure, it

Fig. 5.3(a) : SEM micrograph of S1, showing the " stretching fibre " morphology of Sb_2O_3 after heat treatment at Tc = 485 °C for 24 hours. The spectrum is also displayed.

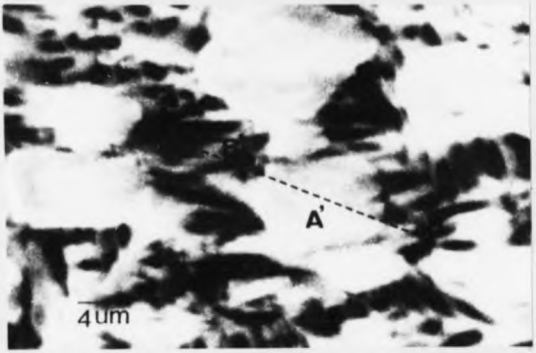

Fig. 5.3(b) : SEM micrograph of S2, showing the " stretching fibre " morphology of Sb_2O_3. (Marked F).

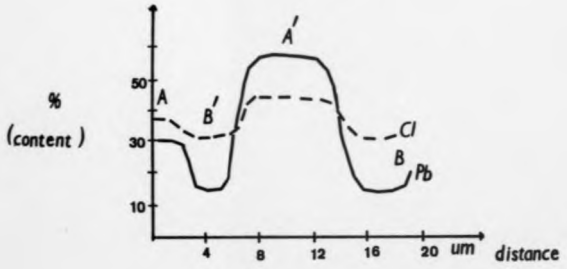

Fig. 5.4 : The variation in the percentage of Pb and Cl content across a crystallised area of S2 (see fig. 5.3(b)). There are two clear areas A' and B' where Pb and Cl play a major part.

is obvious that there are two distinct compositional areas. In area A', the percentage content of Pb and Cl are increased reflecting the growth of lead antimony oxychlorides. In area B', Pb and Cl are deficient and thus this is the area where the nucleation and growth of Sb_2O_3 occurs.

Although the amount of $ZnCl_2$ might be important in influencing the volume fraction as discussed earlier, it seems that Zn itself does not take significant part in the nucleation and growth. If the cross - section from figure 4.4c is made, again by EDX analysis, the negligible variation of this element can clearly be seen (figure 5.5(a)). It is clear from this figure that there is little variation in the percentage of Zn content compared to Pb and Cl.

The cross - sectional analysis of one particle from S_4 (see figure 4.4d) shows little variation in any of the glass components. This is perhaps why it was found difficult to distinguish the major and minor phases in this sample. This variation can be seen in figure 5.5(b).

Adding 10% more of $ZnCl_2$ at the expense of $PbCl_2$ to S_3 (to give S_4) produces different microstructure, ie; from dendritic to " star - like " structure. The latter type can

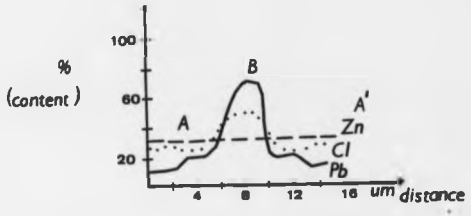

Fig. 5.5(a) : Composition variation across S3 (see fig. 4.4(c)) from A to A'.

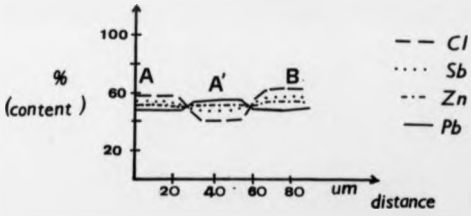

Fig. 5.5(b) : Composition variation across S5 (see fig.4.4(d)) from A to B. Only small depletion range occurs. This is the area where separate phases cannot be distinguished.

be seen in figure 5.6. Two phases are present and are indicated in the figure as well as their spectra.

The surface layers of glasses of composition of more than 40 % $ZnCl_2$, hydrated noticeably in air after about one week. It is known that these materials are very hygroscopic (1), so preservation of their structure ready for SEM is very difficult. As seen in figure 5.7, the morphologies of both phases were irregular. Attempts to use TEM (Transmission Electron Microscopy) have been made but without success since the sample easily melts.

Taking these various results altogether, a tentative picture of the phase stability region of the system can be drawn. This is shown in figure 5.8 where $PbSb_2O_3Cl_3$ and the substituted $PbSb_2O_{3-x}Cl_3$ are situated near the boundary of the glass forming region.

5.4 Crystal Growth Rate

The results of growth measurement have been given in the previous chapter (figure 4.6 to 4.17) and the microstructure of the crystals from these multicomponent glasses can be seen in figures 5.9 to 5.12 which represent the growth of S_1, S_2, S_3 and S_4 respectively, after certain times at temperature.

Fig. 5.6 : SEM micrograph of S4 glass after heat treatment at Tc = 393 °C for 24 hours, showing a " star - like " structure. The spectrum of both phases are also displayed. (Sb_2O_3 and $PbSb_2O_{3.5}Cl$).

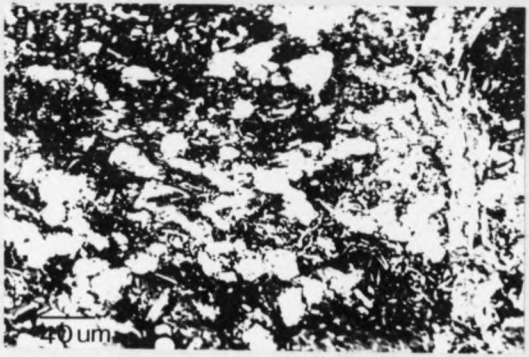

Fig. 5.7 : SEM micrograph of S8 after heat treatment at Tc = 290 °C for 24 hours, showing irregular crystal shapes.

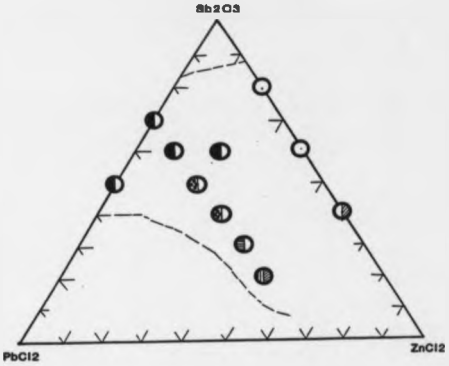

Fig. 5.8 : Phase stability region in Sb_2O_3 - $PbCl_2$ - $ZnCl_2$ ternary glasses.

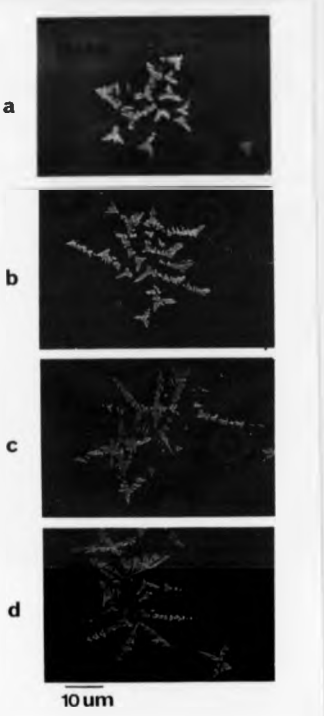

Fig. 5.9 : Crystal growth of S3 after heat treatment at 440 °C for various times. (a = 5 min. b = 10 min., c = 15 min., d = 20 min.).

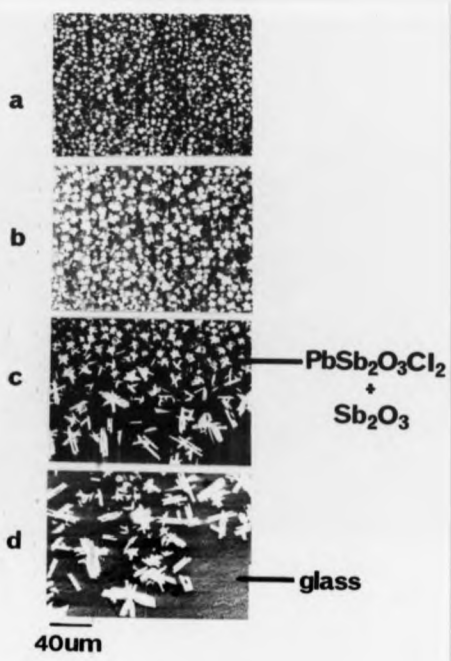

Fig. 5.10 : Crystal growth of S5 after heat treatment at 400 °C for various times. (a = 3 min. b = 6 min., c = 15 min., d = 20 min.).

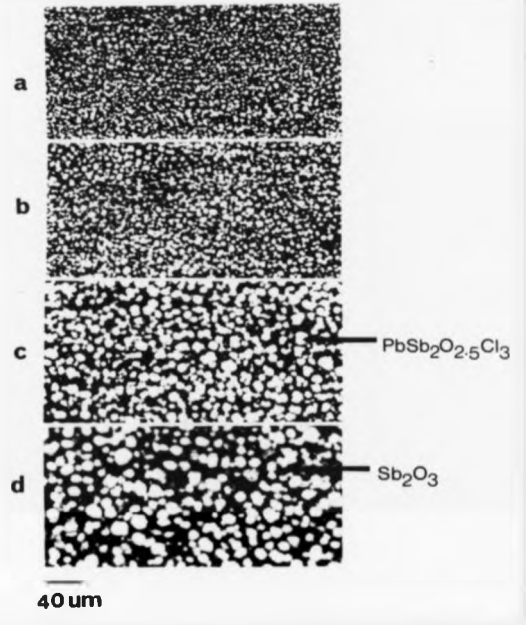

Fig. 5.11 : Crystal growth of S7 after heat treatment at 280 °C for various times. (a = 5 min., b = 10 min., c = 15 min., d = 20 min.) .

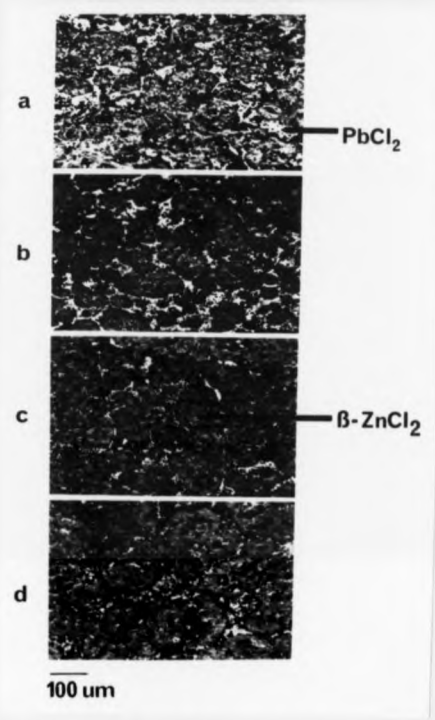

Fig. 5.12 : Crystal growth of S8 after heat treatment at 320 °C for various times. (a = 5 min. b = 10 min., c = 15 min., d = 20 min.) .

In all cases where the crystal growth had been measured at short time, the relation between growth and time was found to be fairly constant until the specimen was almost devitrified. At short times of crystallisation, there are still sufficient components which can be brought to crystal growth fronts by diffusion processes to develop the crystal sites. Under this condition, the growth rate seems to be time independent. However at longer times (figure 4.6(b)), diffusion processes can no longer replenish crystal growth components. As a result, the growth is much slower and will saturate after certain time of heat treatment. This is why it was found that at about 4 hours of heat treatment, the relation between growth and time is no longer constant but started to show curvature and finally, stops.

It should also be noted here that, the assumption has been made that the crystal growth follows the normal growth model as mentioned in chapter 3.

From examination of the crystal growth rate - temperature curve of S_1 (see figure 4.12), it is clear that there are two types of growth. The initial phase which developed at temperature around 400 °C is $PbSb_2O_{3.5}Cl$. The maximum growth rate of this phase was about 0.01 μm sec^{-1}, and was obtained at approximately 470 °C. The growth then steadily reduces with increasing temperature. The second crystal phase is Sb_2O_3. It starts to develop only at about 440 °C

and then steadily increases as temperature increases. This reflects the presence of two distinct values of Tc for the glass with $PbSb_2O_{3.5}Cl$ formation giving rise to the lower Tc phase and Sb_2O_3 the higher Tc phase.

The inclusion of 10 % $ZnCl_2$ in S_1 (ie; S_2, see figure 4.13) increases the maximum growth rate up to around 0.03 μm sec^{-1} and reduces the maximum temperature T_{max} down to around 430 °C. Another effect that can be seen is the earlier development of the phase Sb_2O_3 (around 400 °C). The reduction of Sb_2O_3 to 50 % and the inclusion of 20 % $ZnCl_2$ has a significant effect on morphology as the growth of Sb_2O_3 and $PbSb_2O_3Cl_2$ were not separable. This can be seen in figure 4.14. In addition, the " common " growth rate is increased up to 0.05 μm sec^{-1} and T_{max} is reduced to about 380 °C. A similar case occurs with S_4 where 30 % $ZnCl_2$ was included in the compositon. Here the growth rate is increased to about 0.07 μm sec^{-1} and T_{max} further reduced to about 360 °C.

With the inclusion of 40 % $ZnCl_2$ (ie; S_7, see figure 4.16), two simultaneous crystal growths namely $PbSb_2O_{3.5}Cl$ and Sb_2O_3 are now resolved with different growth rate but the same T_{max}. The maximum growth rate of the former was found to be about 0.13 μm sec^{-1} and T_{max} around 325 °C.

The addition of more $ZnCl_2$ up to 50 % (S_{50}, see figure 4.18), results in the increase of growth rate to 0.16 μm sec^{-1} at a T_{max} around 300 °C.

The increase (at lower temperatures) and reduction (at higher temperatures) in growth rate of samples are as described by equation (2.4) and (2.5) respectively, discussed earlier in chapter 2. While the latter is thermodynamic controlled, the former is determined by many kinetic factors. However, both of them are expected to be chloride dependent and it has been seen that the growth rate is increased by inclusion of $ZnCl_2$ at the expense of Sb_2O_3. These results indicate that it is the chloride concentration which affects crystallisation. This effect can be seen clearly by plotting the maximum growth rate against the analysed percentage of chlorine (figure 4.18). From this figure, the growth rate increases almost linearly with % Cl (analysed) inspite of the fact that the phase produced is changing in stoichiometry.

Another result that can be deduced from the growth rate - temperature curve is that the T_{max} is reduced by increase in $ZnCl_2$ content. If this temperature is plotted against the analysed Cl content, the relation displayed in figure 4.19 is obtained. This graph shows that the maximum growth temperature steadily decreases as the % Cl (analysed) increases. The point at 59 % (S_0) now corresponds to growth of $PbCl_2$.

The other thing is that the growth morphology of A_1 glass (figure 5.13), is almost the same as found in S_1, ie; a dendritic growth. This behaviour is surprising in view of the different phase concerned but may be controlled by the total amount of Cl (analysed) in the sample which is the same for S_1 and A_1. However they do show different growth rates (figure 5.14(a) and (b) and figure 5.15(a) and (b)). Examination of the growth morphology of S_1 glass (figure 4.4b) shows spherical structures whereas the growth morphology of S_1 (figure 4.4a), shows " star - like " structures. We therefore conclude that there may be some effect of heavy metal chloride on changing the crystal morphology. This change may well affect the growth rate measurement (figure 5.16(a) and (b)). The effect of heavy metal chloride on this behaviour however will be discussed in more detail with the inclusion of heavy metal chloride components such as $BiCl_3$ and TlCl in the systems in a later section.

The role of viscosity in the crystallisation behaviour will be discussed in the following section.

5.5 Viscosity

The relation between viscosity and the reciprocal of the absolute temperature can be seen in figure 4.20. From that figure, it can be seen that a linear relationship is obtained for all the samples . The measurement covers a

Fig. 5.13 : Growth morphology of A2 glass when heat treated at Tc = 410 °C for 24 hours, showing dendritic growth.

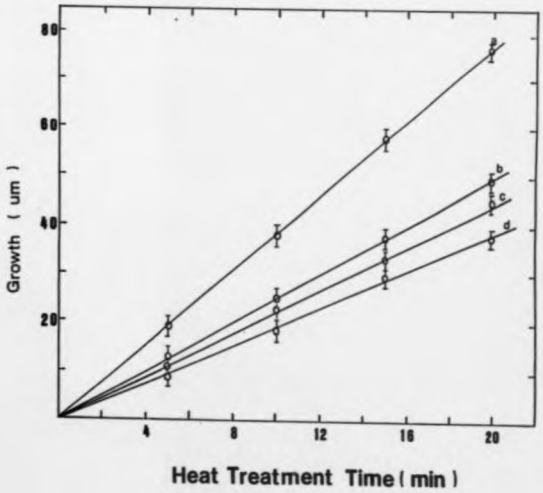

Fig. 5.14(a) : Growth versus time for A2 glass at various temperatures. (a = 410 °C, b = 440 ° C, c = 360 °C, d = 330 °C) .

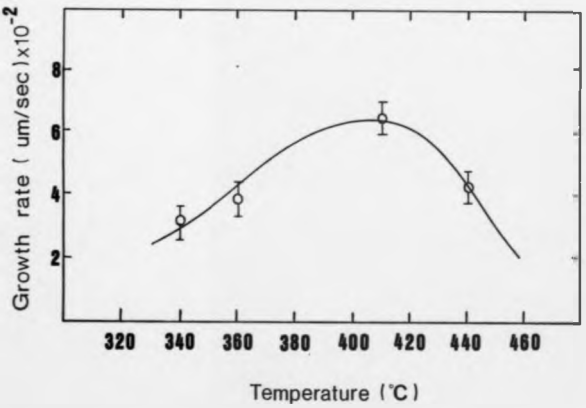

Fig. 5.14(b) : Growth rate - temperature curve for A2 glass.

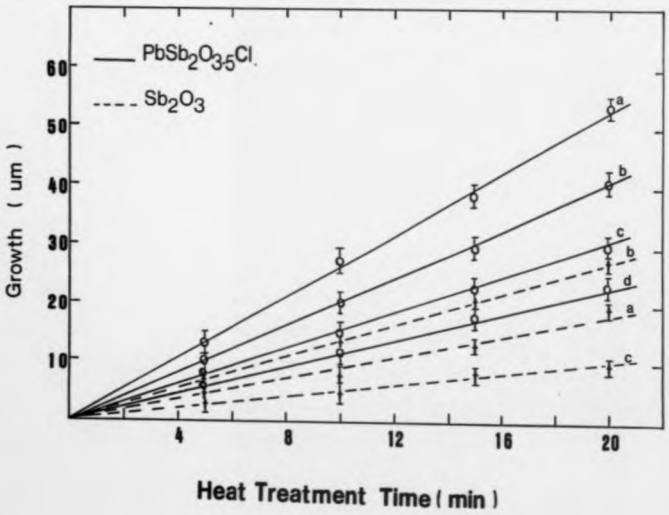

Fig. 5.15(a) : Growth versus time for S4 glass at various temperatures. (a = a' = 410 °C, b = b' = 430 °C, c = c' = 390 °C, d = 370 °C).

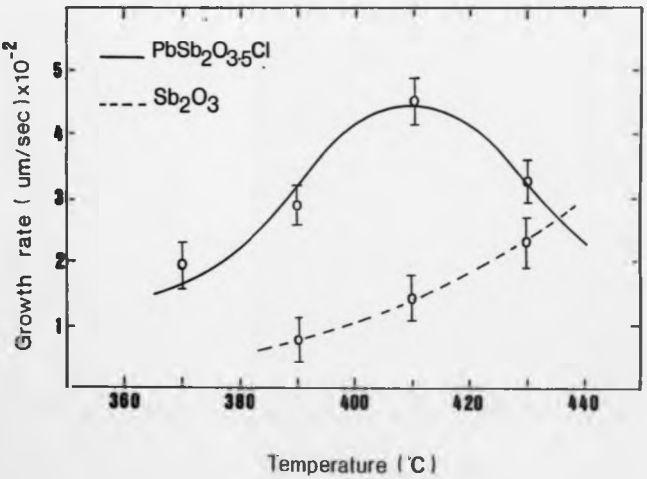

Fig. 5.15(b) : Growth rate - temperature curve for S4 glass.

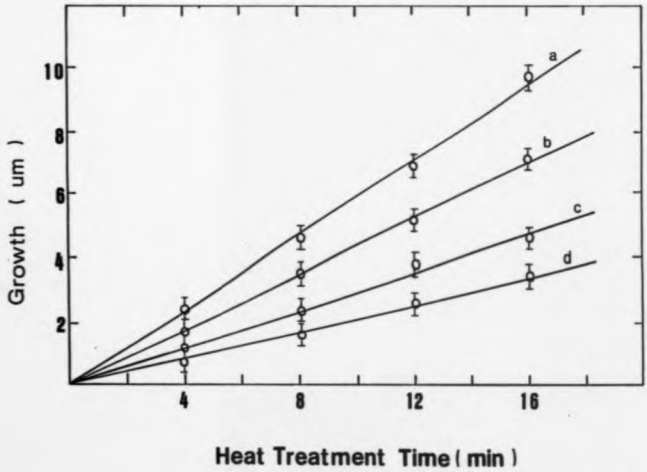

Fig. 5.16(a) : Growth versus time for S2 glass at various temperatures.

(a = 400 °C, b = 440 °C, c = 360 °C, d = 330 °C).

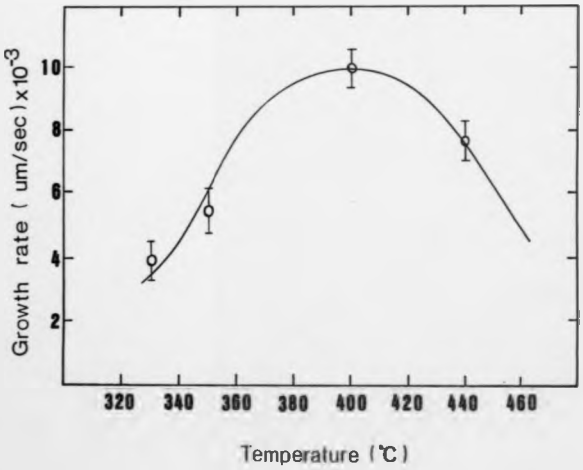

Fig. 5.16(b) : Growth rate - temperature curve for S2 glass.

viscosity range from 10^{4} P to 10^{13} P and thus the activation energy does not change over the temperature range which has been used during the experiment. If a fixed temperature is chosen (in this case 322 °C) and the corresponding viscosity values plotted against the analysed percentage of chlorine (figure 4.21), the results show that there is a variation of viscosity with % Cl which arise from the influence on the parameter A (ie; $\eta = A \exp (B/T)$ where T is temperature, B is related to activation energy (37)) which is related to glass structure, and not from changes in activation energy. It clearly shows that the viscosity decreases steadily as the % Cl increases reflecting the disruption of the glass network.

The increases in growth rate with chlorine content can thus be related to be the reduction of viscosity. As the viscosity decreases, the atoms in the glass are more mobile and can therefore more easily rearrange themselves to the periodic order of the crystal resulting in increased growth rate. This has long been recognised (8). In conclusion, one can say that, as the Cl content increases, the viscosity reduces and therefore enhances the crystal growth rate.

A close examination of figure 4.20 shows that the inclusion of more $ZnCl_2$ will reduce the viscosity. This effect has been described elsewhere (7). Other possible effects which have not generally been taken into account in this study are

the effects of impurities such as hydroxyl ions (OH^-) which might be present in the glass system. These ions are present in practically all oxide components and halide components, particularly in ZnCl, since this material is very hygroscopic (8). The effect of this ion in promoting growth rates as well as reducing the viscosity of a glass has been studied by McMillan et al. (9) and further studies were reported by Gonzales - Oliver et al. (10).
Obviously more detailed work needs to be done with respect to these effects. It will be discussed again later when the effects of $BiCl_3$ and TlCl are examined.

5.8 Chemical Durability

5.8.1 Effects Of Atmospheric Moisture

Table 4.6 shows the weight loss per unit area of samples exposed to normal atmosphere for 7 days. The samples with less than a nominal concentration of 20 % $ZnCl_2$ experienced no significant weight losses. This shows that the glasses are relatively unreactive in normal atmospheric conditions. However, glasses with more than 30 % $ZnCl_2$ show weight losses and there is evidence of some corrosion around the glass surface.
When the glasses were exposed to an atmosphere with 100 % Relative Humidity (RH) for 7 days, it was found that glasses with less than 28 % Cl (analysed) content were not

affected by the humidity (figure 4.22). The glasses with more than this amount of chlorine experienced significant weight losses. These results demonstrate that there are some compositions which have sufficient durability to have some practical usage.

5.6.2 Effects Of Distilled Water

The effects on the glasses exposed to distilled water for 7 days can be seen in figure 4.23. The results indicate that although some of the glasses resist attack under atmospheric condition, most of them were reactive in the present of water. The degree of reactivity, as might be expected, increases with analysed chlorine content (figure 4.25).

Addition of more $ZnCl_2$ at the expense of Sb_2O_3 has an obvious effect, that is, increasing the corrosion rates, reflecting the higher solubility of $ZnCl_2$ (11,12).

Examination of figure 4.23 and figure 4.25 shows the corrosion rates of the glasses (for 7 days) are in the range of (0.2 - 1.0) x 10^{-4} $gm.cm^{-2}.d^{-1}$. In comparison, these values are an order of magnitude lower than those for fluorozirconate based glasses under similar conditions reported by Simmons and Simmons (13).

5.6.3 Water Permeation In Glass

The relationship between penetration depth and immersion time is displayed in figure 4.26. The penetration depth of the samples increases linearly with $t^{1/2}$. These relations suggested that the process is diffusion controlled. Using the relation $x = (Dt^{1/2})$ (14) where t is the time taken for penetration, x is the penetration depth , the diffusion coefficient D can be estimated. Plotting the values of x against $t^{1/2}$ (see figure 5.17), it was estimated that the diffusion coefficient increases from 0.5 to 20 x 10^{-8} cm^2 sec^{-1} with increased chlorine content. For the glass of S_1 where the diffusion controlled process was not observed, the diffusion coefficient could be estimated as follows. At time t_c where the transition from the initial diffusion controlled process to the time dependent takes place, both $x = (Dt^{1/2})$ and $x = At + B$ where A and B are constants, should be satisfied. This implies that $(Dt_c^{1/2}) = At_c + B$. Thus from the gradient and the interception of linear portion, D can be calculated. D was estimated to be less than 0.2 x 10^{-13} cm^2 sec^{-1}. The values of D were then plotted against the Cl (analysed) and the result are presented in figure 5.18. This indicates that the diffusion coefficient associated with corrosion is greater for samples with higher chlorine content. This result also suggests that corrosion is a diffusion controlled process with chlorine being a diffusion controlling species.

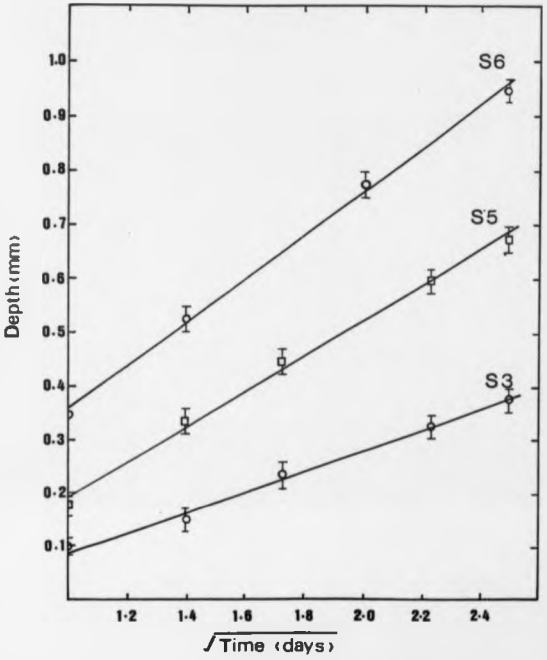

Fig. 5.17 : Penetration depth versus (time)$^{\frac{1}{2}}$ for S glasses.

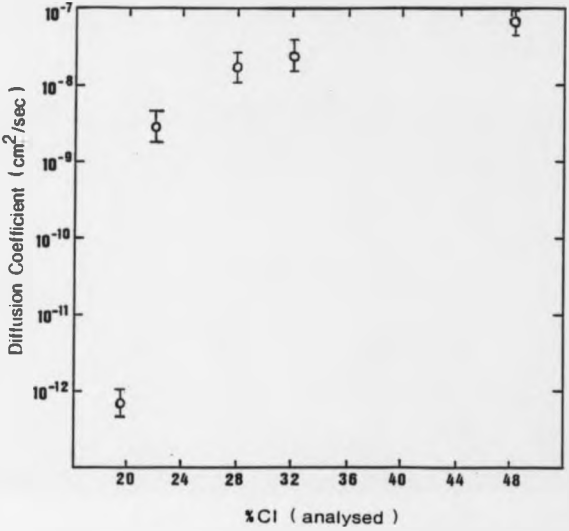

Fig. 5.18 : Diffusion coefficient, D versus Cl content.

The effect of other glass components and H_2O species on the corrosion process is examined in the next few sections.

5.6.4 pH Drift Behaviour

Figure 4.28 shows the temporal variation of solution pH for the five oxychloride glasses. All show a marked decrease in pH from 5.0 to 3.0 over 7 days. A test was conducted by soaking fine powder in distilled water at a pH = 5.2 under static conditions. The decrease in pH could result from the diffusion of H^+ and Cl^- from the glass (g) into the solution (s) as a result of a reaction between the glass matrix and water molecules in the glass. The simplified corrosion mechanism may be expressed as follows :

$$M\text{-}Cl\ (g) + H_2O\ (g) \longrightarrow M\text{-}OH\ (g) + Cl^-\ (g) + H^+\ (g) \qquad (5.1)$$

$$Cl^-\ (g) \xrightarrow{\text{diffusion}} Cl^-\ (s) \qquad (5.2)$$

$$H^+\ (g) \xrightarrow{\text{diffusion}} H^+\ (s) \qquad (5.3)$$

In order to confirm this reaction, measurement of chloride concentration in the water was carried out (refer to section 3.6.9). Furthermore, the hydrogen ion concentration

in the solution was also calculated from the pH data in figure 4.28 and applying the equation $pH = -\log_{10}[H^+]$. If $[H^+]$ and $[Cl^-]$ are plotted versus corrosion rate (figure 5.19), the results indicate that $[Cl^-]$ and $[H^+]$ increase approximately linearly as the corrosion rate increases. Comparison with figure 4.25 (corrosion rate versus % Cl), shows that both H^+ and Cl^- increase as the amount of chlorine in the glass (presented as H-Cl in the equation) increases. Equation 5.1 to 5.3 do not give the full picture since it was found that the concentration of chloride ions is twice that of hydrogen ions. This result will be discussed in detail in the corrosion mechanism section.

In conclusion, the pH behaviour of the solution is strongly dependent on the % Cl content. The hydroxyl group which appears in equation (5.1) also needs a further examination.

5.8.5 Surface Water Content

For all glasses, the measurement of infrared absorption shows that the same OH stretching and HOH bending vibration occurred around 3500 cm^{-1} and 1616 cm^{-1} respectively. This had been reported elsewhere (1). One method used to study the presence of water content as OH groups or H_2O molecules is IR Spectroscopy (15). Figure 5.20 represents the results of IR absorption by the hydrated layer on S_1 after exposure to distilled water for 4 days. From this figure, it was found

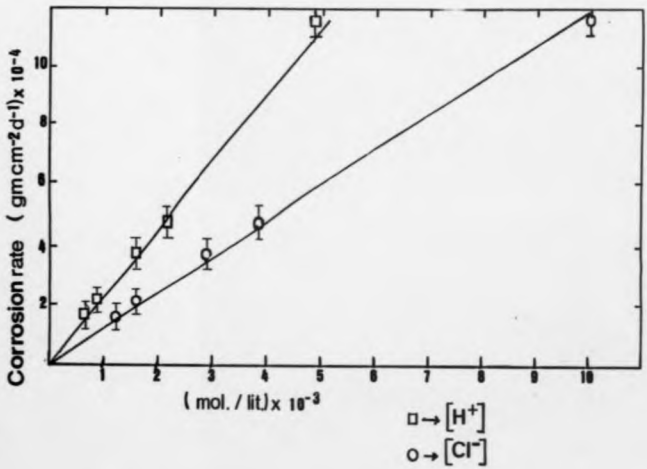

Fig. 5.19 : Corrosion rates of S glasses versus the concentration of hydrogen and chloride ions, showing a linear relationship. (after 4 days soak time).

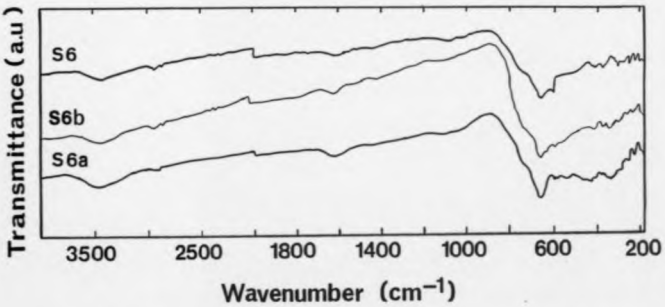

Fig. 5.20 :IR spectra with CsI of hydrated layer from S6 after being exposed to distilled water pH = 5.2 at 20 °C for 4 days.

a - sample dried in normal atmosphere.

b - sample dried in the oven.

that the absorption peak intensity of both OH positions were increased relative to the parent glass. The peaks, particularly of the OH stretching vibration, are broadened considerably. If the integrated peak areas are calculated (18), it is found that the OH vibration peak grows slightly faster than the HOH bending peak. This indicates the presence of hydroxide groups in the hydrated layer. This result is consistent with the M-OH groups in equation (5.1). Furthermore, the peaks around 600 cm^{-1} which are due to the Sb-O-Sb stretching vibration (17) were also found to be disturbed. This may also be indicated by formation of another obvious absorption peak around 350 cm^{-1} which did not exist in the uncorroded glass. Maroni et al. (18) and Odgen et al. (19) have reported that this peak arises from complexes of the tetrahedral unit of $Pb(OH)_4^{--}$. This evidence thus supported the suggestion that at least some metal hydroxide is present in the corroded glass.

The intensities of the 3500 cm^{-1} and 1616 cm^{-1} absorption bands of S_a (dried in air for 24 hours) are much higher than in S_b (dried in the oven for 24 hours) (figure 5.20) , presumably due to more rapid evaporation of water at higher temperature. Similar results have been reported in the case of fluoride glasses both in air (20) and at higher temperature (21,16). In addition, it was also observed that the integrated peak area of the absorption peak around 350 cm^{-1} which represent the M-OH vibrational frequency was in

the order of $S_{4.4}$ > $S_{4.8}$. Thus, dehydration also involves removal of hydroxyl ion from the glass.

Figure 5.21 shows the results of IR spectroscopy investigation on the hydrated layer of S_4 after being exposed in distilled water for 4 days In addition to the results observed in S_4 glass, another striking absorption peak occurs around 250 - 300 cm^{-1}. Lippincott et al. (21) reported that the peak around 290 - 300 cm^{-1} belongs to the tetrahedral units $(Zn(OH)_4)^{2-}$ while Clark et al. (22) show that the 280 - 295 cm^{-1} absorption arises from the tetrahedral units $(ZnCl_4)^{2-}$ and an absorption peak at 285 cm^{-1} from the Zn-Cl network (1). These again indicate the presence of metal hydroxide in the corroded glass.
However, further experiments are needed to clarify the exact mechanism.

5.8.6 Microscopic Appearance Of Surface

Scanning electron microscopic observations of the corroded surface were carried out and some micrographs are presented in figure 5.22 and 5.23 for S_4 glass, exposed for 4 days in distilled water at 25 °C, in static condition. The micrograph show " unwashed " and " washed " with xylene respectively. The " unwashed " sample appeared severely cracked due to dehydration of the corrosion layer by heating in the oven for a few hours. There are precipitated crystal

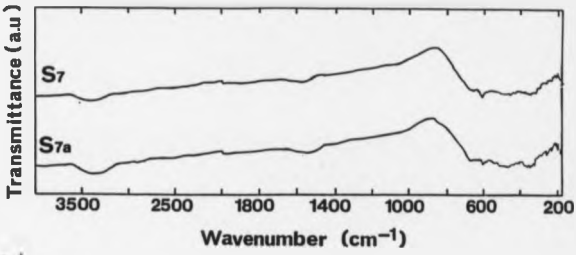

(a)

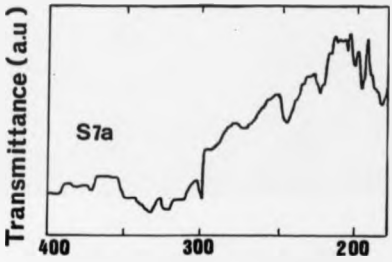

(b)

Fig. 5.21 : a. IR spectra with CsI of hydrated layer from S7 after being exposed in distilled water, pH = 5.2 at 20 °C for 4 days.

b - Enlargement of S7a from 180 cm^{-1} to 400 cm^{-1}.

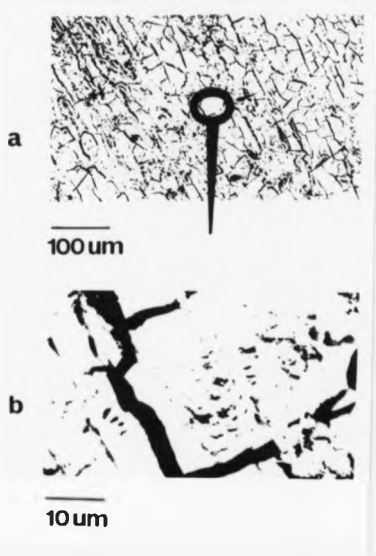

Fig. 5.22 : The " unwashed " corroded glass surface of S5 after being exposed to distilled water, pH = 5.2 at 20 °C for 4 days.

a - sample after drying in the oven, showing some cracks.

b - a magnification of (a), showing crystal precipitates.

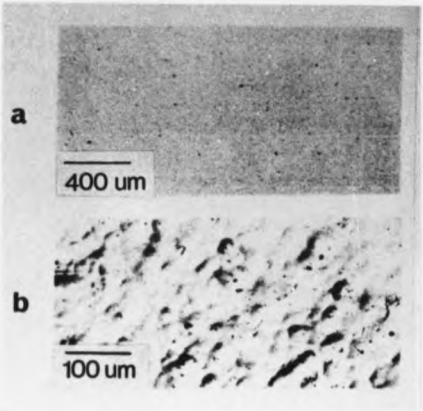

Fig. 5.23 : The " washed " corroded glass surface of S5.

a - as polished

b - " washed " showing the surface under the corroded layer.

deposits over the top of the glass surface as can be seen in figure 5.22. After the glass was washed to remove the precipitated crystal deposits from the vitreous part, a further micrograph was taken. The micrograph (see figure 5.23) shows that the surface was very rough which represents the corroded surface. The precipitated crystal deposit was identified by X - ray diffraction. The results are shown in figure 5.24. In general, most of the samples (S_1 to S_4) show a similar diffraction pattern to the crystallised glass except for S_1 and S_6 where slight differences in phase occurrence were observed. The phases for S_1 to S_4 as expected were found to be Sb_2O_3 and " $PbSbO_2Cl$ ". In S_1 and S_6 the phases were found to be " $PbSbO_2Cl$ " and surprisingly a new phase $Zn_4(OH)_6Cl_2$. The results are summarised in table 5.3.

Further, it is worth noting that the X - ray diffraction pattern of the hydrated layer and crystallised glass differ by about 0.05 Å in d spacing for S_1 to S_4 but only slightly for S_1 and S_6. This difference might be caused by the presence of OH groups as suggested by the IR Spectroscopy investigation. It is therefore suggested that the phase should (instead of $PbSbO_2Cl$) be in the form of " $PbSbO_{2-x}(OH)_{2x}Cl$ " or " $PbSbO_2Cl.nH_2O$ ". The latter form is not dominant since it indicates the presence of H_2O molecules which is contrary to the IR findings. However, since EDX results show that the crystallised glass contains a compound

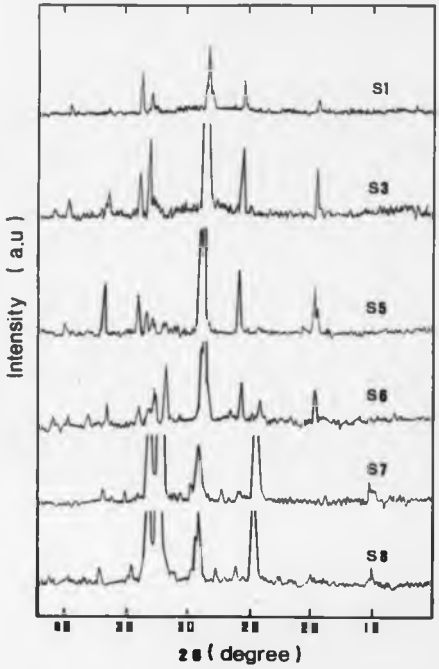

Fig. 5.24 : X - ray diffraction patterns of the corroded layers for S glasses.

Sample No.	Phase Occurrence			
	Crystallised Glass		Corroded Layer	
	Major	Minor	Major	Minor
S_1	$PbSbO_2Cl$	Sb_2O_3	Sb_2O_3	$PbSbO_2Cl$
S_3	"	"	"	"
S_5	"	"	"	"
S_6	"	"	"	"
S_7	"	"	$PbSbO_2Cl$	$Zn_5(OH)_8Cl_2$
S_8	$PbCl_2$	$ZnCl_2$	"	"

Table 5.3 : The occurrence of phases on the corroded layer of some samples when identified by X - ray diffraction analysis.

with varying oxygen - chlorine ratio, it is suggested that the corrosion deposits consist of $PbSb_2O_{n-1}(OH)_nCl$, where n has a value which depends on the chlorine content.

Figure 5.25 shows an " unwashed " corroded layer from S_7 glass after 4 days in static distilled water at 25 °C. From this figure the typical crystal deposits on the glass surface can clearly be seen. There are two distinct crystal deposits. One is a sphere - like structure and the other is a white precipitate spread over the whole area. EDX analysis show that the former is composed mainly of the elements Zn and Cl while the latter contains Pb, Sb and Cl. The higher chlorine contents of S_7 and S_8 suggest that the corrosion phases should be of the form $PbSb_2O_{n-1}(OH)_nCl_n$ and $Zn_5(OH)_{8-n}CL_{2n}$ for the major and minor phase respectively. This result is consistent with the XRD investigation on the hydrated layer of S_7. Unfortunately, O and H cannot be measured by EDX because of their low atomic number.

5.8.7 Corrosion Mechanisms

The combination of the above results, when carefully manipulated begin to yield some understanding of the corrosion process in oxychloride glasses. This process is best examined in the context of and in comparison with known

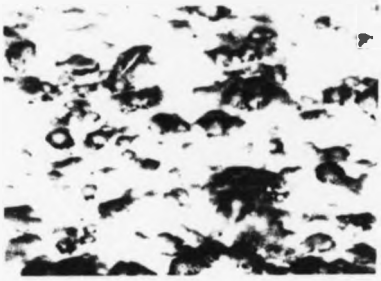

Fig. 5.25 : Typical crystal deposits at the surface of S7 glass after being exposed to distilled water, pH = 5.2 at 20 °C for 4 days.

leaching processes such as in silicate or fluorozirconate glasses.

In well - mixed or flowing solutions, the amount of silica removed from durable silicate glasses generally increases, first according to a $t^{1/2}$ law due to the rate - controlling interdiffusion of alkali metal ions and H^+ or H_3O^+ ions and then as t , due to the matrix dissolution through a steady state dealkalised layer (13,24,25). In other words, silicate glasses leach through a process of ion exchange followed by a matrix dissolution. Both of these processes control the leaching rate, pH solution and other chemical properties.

In fluorozirconate based glasses, the corrosion process occurs initially by selective extraction followed by matrix dissolution and undergoes very little ion exchange (13). The low water resistance and aqueous solution of these glasses have been discussed in detail by Seddon (28). Most of the systems such as ZrF_4, AlF_3 and BeF_2 based glasses show a similar leaching process.

In oxychloride glasses, the results show that the water penetration depth generally increases with $t^{1/2}$ which indicates that the corrosion is diffusion controlled. However, whether it involves the diffusion of HOH, H_3O^+, H^+, Cl^- or other species, including some cations into the solution is somewhat unclear.

In the earlier section, it has been showed that the concentration of H^+ increases as the concentration of Cl^- increases. An interesting question to be asked, is whether cations such as Pb^{2+}, Sb^{3+} or Zn^{2+} are present in the solution. The existence of these cations can be determined qualitatively by using a Spot test or a Flame test (27). The results can be seen in table 5.4. The test results show that some cations such as Pb^{2+} and Zn^{2+} are present in the solution while others are not. These results indicated the need for further experiment. Consequently, quantitative analysis of Pb^{2+} and Zn^{2+} was conducted by means of chemical analysis (29). The results, shown in table 5.5, indicates that equation (5.1) needs some modifications. It also suggests that the corrosion mechanism involves destruction of the glass structure involving the Zn network as well as Pb network. The former might come from the destruction of $ZnCl_4$ tetrahedra (30) while the latter might come from the PbO_4Cl_2 octahedra (31). It should also be noted that, from the data shown in table 5.5, the calculated ratio of Cl^- : H^+ : Pb^{2+} was approximately 4 : 2 : 1. Using this knowledge, the schematic corrosion equation for the glasses of S_1 to S_5 may be expressed as;

Sample	Cations				
	Pb^{2+} *	Sb^{3+} *	Zn^{2+} *	Tl^{+} *	Bi^{3+}
S_1	Y	N	-	-	-
S_2	Y	N	-	-	-
S_3	Y	N	-	-	-
S_4	Y	N	-	-	-
S_7	Y	N	Y	-	-
S_8	Y	N	Y	-	-
T_1	Y	N	-	N	-
T_2	Y	N	-	N	-
T_3	Y	N	-	-	N
T_4	Y	N	-	-	Y

Table 5.4 : Qualitative analysis for the presence of cations in the solution of S series and T series glasses using Spot tests and Flame tests (*).

Y - Detected N - Undetected

Sample No.	Concentration (mol / litre) x 10^{-4}			
	* Cl^-	H^+	* Pb^{2+}	* Zn^{2+}
S_1	12.4	6.3	3.3	-
S_3	15.4	8.5	4.7	-
S_5	28.9	16.0	6.3	-
S_6	41.9	22.0	10.0	-
S_7	101.9	49.0	12.0	15.2

Table 5.5 : Quantitative analysis of some anions and cations present in the solution of S series glasses after 4 days soak time.

* - Spectroscopy method (28)

$ - Chemical analysis method (29)

$$
\begin{array}{lll}
 & O & \\
Cl & | & Cl \\
 & > Pb < & (g) \quad + \quad 4\ H_2O\ (g) \\
Cl & | & Cl \qquad \text{------>} \quad 4\ Cl^-\ (s) + 2\ H^+\ (s) \\
 & O & \qquad\qquad + Pb^{2+}\ (s) + 6\ [OH]\ (g)
\end{array}
$$

(5.4)

and for the glasses of S_7 to S_8 where Zn^{2+} was detected, instead of equation (5.4), an additional corrosion equation should be involved, ie;

$$
\begin{array}{lll}
Cl & & Cl \\
 & > Zn < & (g) \quad + \quad 2\ H_2O\ (g) \text{ ----> } 4\ Cl^-\ (s) + 2\ H^+\ (s) \\
Cl & & Cl \qquad\qquad + Zn^{2+}\ (s) + 2\ [OH]\ (g)
\end{array}
$$

(5.5)

In other words, the glass first reacts with the water in the glass matrix and as a consequence releases the Cl^-, H^+, Pb^{2+} and Zn^{2+} to the solution by a diffusion process leaving some [OH] bonded to the corroded glass surface.

One however should bear in mind that the left hand side of the equations is by no means intended to show the exact structure of glass involved during corrosion. It is only a representation of the corrosion mechanism which fits the experimental evidence. As can be seen from the equation, it

shows that for every mole of $PbSbO_2Cl_4$ octahedra corroded, 4 mol of chloride ions, 2 mol of hydrogen ions and 1 mol Pb^{2+} will be released to the solution (S_1 to S_4). In the case of S_7 and S_8, 1 mol of Zn^{2+} and Pb^{2+} will be released. However, the amount of Zn^{2+} is higher than Pb^{2+}, indicating that in the glasses with $ZnCl_2$ as the major component, the second mechanism will finally dominate the corrosion.

The final remark that can be made is the existence of [OH] groups in the corroded layer for both of the mechanisms. As has been suggested before, these hydroxyl groups are predominantly in the form of metal hydroxides. However, it is still not clear whether dominant groups are Pb-OH or Zn-OH or a mixture with other species such as Sb or Cl to form a compound. It is still a mystery.

The corrosion of oxychloride glasses depends largely on the amount of chloride available to react with water in the glass matrix thus destroying the glass structure.

5.7 EFFECT OF TlCl AND $BiCl_3$

5.7.1 Thermal Properties

The nominal and analysed (by EDX) compositions of these glasses can be seen in table 5.6. By examining this table, it can be seen that some loss of chlorine occurs presumably due to hydrolysis of the materials, but there is an increase in chlorine content over the parent glasses. The basic thermal properties of the glass were measured by DSC and the results of Tg, Tc and Tc - Tg are presented in table 5.7. As can be seen, values of Tc - Tg up to 101 °C can be obtained. Comparison of T_1, T_2, T_3 and T_4 with S_1 shows that substitution for Sb_2O_3 reduces the glass stability but substitution of TlCl in the ternary has less effect. Comparison of T_1, S_1 and T_4 gives the destabilising effect of chloride addition in the order TlCl > $BiCl_3$ > $ZnCl_2$. Assuming that the analysis of $BiCl_3$ is reliable, the changes in chlorine level do not follow the molar added quantities. Hence, there must be a significant loss of chlorine during preparation which differs through the series. This is not simply related to the chlorine content and may indicate the different roles of cation in the network. In the case of T_4 and S_2, the all $ZnCl_2$ glass is less stable than if 10% is replaced by TlCl but composition changes make discussion speculative.

S.No.	Nominal (%) / Analysed (%) (± 0.1)					% Cl (± 0.1)
	Sb_2O_3	$PbCl_2$	$ZnCl_2$	TlCl	$BiCl_3$	
S_1	70 / 71.0	30 / 29.0	-	-	-	19.5
T_1	65 / 67.1	30 / 27.3	-	5 / 2.6	-	22.7
T_2	60 / 60.5	30 / 28.3	-	10 / 11.2	-	26.8
S_2	60 / 59.0	30 / 38.0	10 / 3.0	-	-	22.0
T_3	65 / 66.0	30 / 29.5	-	-	5 / 4.5	27.2
T_4	60 / 64.5	30 / 26.7	-	-	10 / 8.8	27.8
S_4	40 / 50.0	30 / 37.0	30 / 13.0	-	-	32.1
T_5	35 / 33.4	30 / 34.5	30 / 29.2	5 / 2.8	-	38.0
T_6	30 / 34.5	30 / 32.5	30 / 26.8	10 / 7.2	-	44.0
S_7	30 / 40.0	30 / 33.0	40 / 27.0	-	-	46.5

Table 5.6 : The nominal and analysed (mol %) of the T glass compositions with % Cl (analysed) content.

Samp. No.	Tg (°C) (± 1)	Tc (°C) (± 1)	Tc - Tg (°C) (± 1)
S_1	318	459	141
		485	
T_1	270	340	70
		418	
		450	
T_2	264	326	62
		379	
		450	
		457	
S_3	306	455	149
T_3	272	345	73
		442	
		458	
T_4	264	340	76
		420	
		444	
S_4	269	332	63
T_5	266	367	101
		405	
T_6	273	362	89
		390	
		410	
S_7	235	281	46

Table 5.7 : The Tg, Tc and Tc - Tg values of T series glasses.

5.7.2 Crystallisation Studies

The crystallisation studies were carried out as before. The X- ray diffraction pattern of the samples after heat - treatment at T_{c_1} for 24 hours are displayed in figure 5.26.

As in the case of S series glasses, the XRD analysis indicates only the parent phase. So, analysis by EDX is needed to complete the phase identification. The results from EDX analysis are displayed in table 5.8. In T_1 and T_3, in addition to the two phases previously identified in S series glasses, another phase occurs. This phase is identified as $Pb_2Tl_3Cl_5$ or Thallium lead chloride. The occurrence of this phase is expected to be a major cause of destabilisation of the glass. In T_2 and T_4 there are two inseparable phases, similar to those of S_2 and S_4 in the S series glass. In T_5 and $T_{4'}$ two distinguishable phases occurred. One is Sb_2O_3 and another is lead antimony oxychloride with the reduction of oxygen content, similar to those found in S glasses.

It is of particular interest to make a comparison of the crystallisation behaviour of glasses S_1, T_3, T_4, S_3, S_5 and T_5 (chosen in such a way that the effect of an addition of heavy metal chloride as well as the chlorine content can be seen). This comparison is displayed in table 5.9. One point to notice is the occurrence of the crystal phases. By

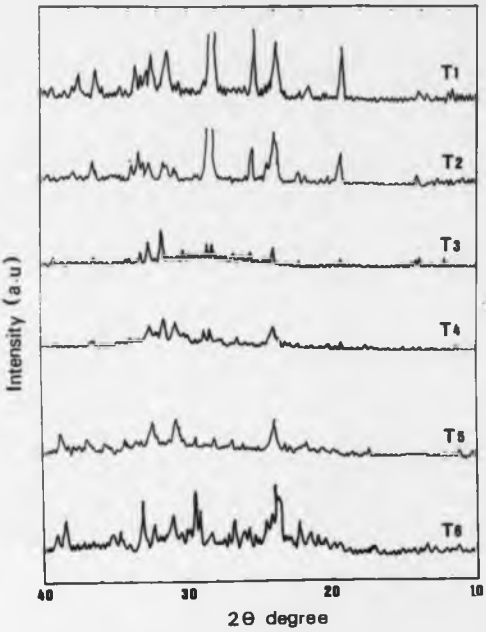

Fig. 5.26 : X - ray diffraction patterns of crystallised glasses from I series.

S.	XRD Analysis			EDX Analysis		
No.	Ph1	Ph2	Ph3	Ph1	Ph2	Ph3
T_1	Sb_2O_3	Pb_2TlCl_3	$PbSbO_2Cl$	Sb_2O_3	Pb_2TlCl_3	$PbSb_2O_{3.5}Cl$
T_2	"	"	"	"	"	"
T_3	"	$PbSbO_2Cl$	-	"	+ $PbSb_2O_{3.5}Cl$	-
T_4	"	"	-	"	+ "	-
T_5	$PbSbO_2Cl$	Sb_2O_3	-	$PbSb_2O_2Cl_3$	Sb_2O_3	-
T_6	"	"		"	"	-

Table 5.8 : The occurrence of phases identified by XRD and EDX analysis.

Sam. No.	% Cl (± 0.1)	Phase Occurence Ph1	Ph2	Ph3	Structural Description
S_3	22.0	$PbSb_2O_{3.5}Cl$	Sb_2O_3	-	Star-like
T_2	26.8	Sb_2O_3	Pb_2TlCl_3	$PbSb_2O_{3.5}Cl$	Rod and Irregular
T_4	27.8	Sb_2O_3	$PbSb_2O_{3.5}Cl$	-	Lamellae
S_5	28.0	" +	$PbSb_2O_3Cl_2$	-	Irregular
T_6	44.0	$PbSb_2O_3Cl_2$	Sb_2O_3	-	Spherical
S_7	48.5	$PbSb_2O_{3.5}Cl_3$	Sb_2O_3	-	Spherical

Table 5.9 : Comparison of phase occurrence, crystal morphology and % Cl (analysed) content.

replacing 10 % of $ZnCl_2$ (S_1) with 10 % of TlCl (T_3), the phase occurrence is totally different, ie: from two to three crystal phases. On the other hand, replacing it with 10 % of $BiCl_3$ (T_4) resulted in no change of crystal phase. Both $BiCl_3$ and TlCl increase the amount of % Cl content although as might be expected the latter contributes slightly less.

If the comparison was now made between samples of S_{11}, S_7 and T_4 , it can be seen that the phase occurrence in T_4 is surprisingly similar to S_8 although, judging from the % Cl content , the phases in T_4 should be similar to S_7. This result suggested that the amount of chlorine content itself is not sufficient to explain the crystallisation behaviour of oxychloride glasses.

The heat - treated samples were also examined by IR Spectroscopy. The results of this investigation are displayed in figure 5.27. Judging from the spectra, it can be concluded that there are three groups of phases. One is in T_1 and T_2 , one in T_3 and T_4 and finally the group of T_5 and T_6. These results are consistent with the previous analysis.

5.7.3 Growth Rate

The crystal growth rate was measured as before. The growth and morphology of the samples T_{11}, T_3 and T_4 are displayed in figure 5.28 to 5.30 respectively. As can be seen, some of

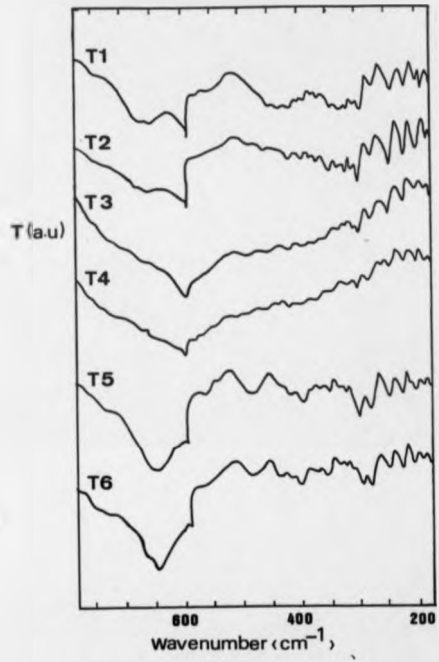

Fig. 5.27 : IR spectra with CsI of crystallised T glasses.

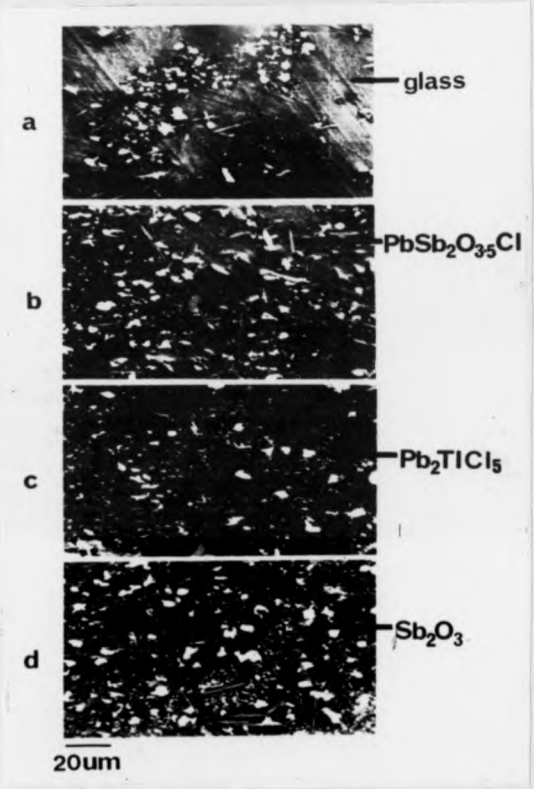

Fig. 5.28 : Growth morphology of T2 glass after heat treatment at 390 °C for various times. (a = 5 min., b = 10 min., c = 15 min., d = 20 min.) .

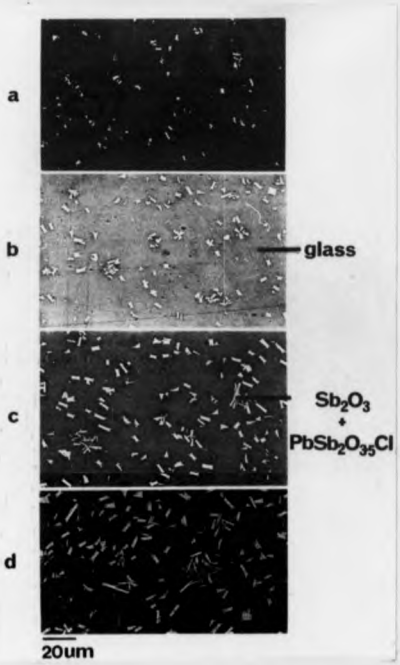

Fig. 5.29 : Crystal growth of T3 after heat treatment at 360 °C for various times. (a = 5 min., b = 10 min., c = 15 min., d = 20 min.).

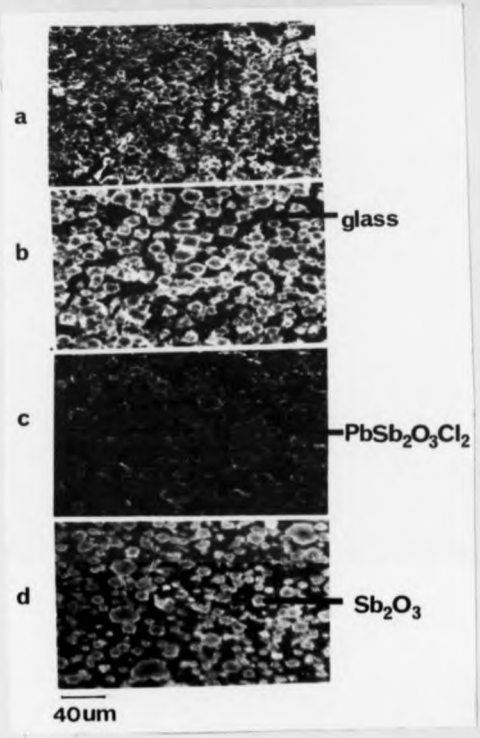

Fig. 5.30 : Crystal growth of T5 after heat treatment at 390 °C for various times. (a = 5 min., b = 10 min., c = 15 min., d = 20 min.).

them are rod shapes, lamellae, spherical and irregular shapes. In T_1 and T_2, the crystals of Sb_2O_3 and Pb_2TlCl_5 were small and irregular so that it was difficult to measure when using the normal scale. Only the growth of $PbSb_2O_{3.5}Cl$ is comfortably measured. In T_3 and T_4, because the crystal phases are not separable, the growth which has been measured actually represents the growth of both phases. In T_5 and T_6, there is a clear boundary between the phases so that growth can be measured separately. The growth of T_1, T_2, T_3, T_4, T_5 and T_6 at different temperatures can be seen in figures 5.31 to 5.36 respectively. By dividing the growth by time, the growth rate - temperature curve can be plotted. These results can be seen in figures 5.37 to 5.39.

If the comparison is made between pairs of glasses of T_1 and T_2, T_3 and T_4 or T_5 and T_6, it is found that increasing the chloride content results in increased growth rate. The full results for these glasses can be seen in table 5.10. It also interesting to note that by adding 5 % more TlCl to T_1 (to give T_2), the maximum growth rate suddenly doubles whereas adding 5 % more of $BiCl_3$ to T_3 (to give T_4), increases the maximum growth rate less. This indicates that in terms of destabilisation of the glass structure, TlCl is more effective than $BiCl_3$. This is consistent with the results on the study of thermal stability of the glasses. It is believed that the heavy metal chloride as well as Cl

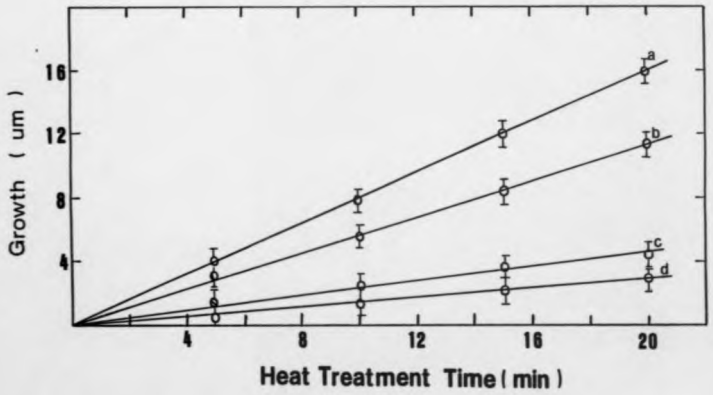

Fig. 5.31 : Growth versus time for T1 glass at various temperatures.

(a = 390 °C, b = 420 °C, c = 360 °C, d = 330 °C).

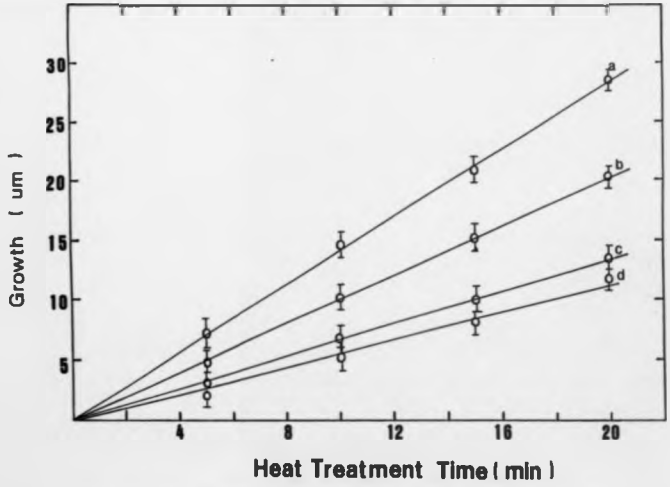

Fig. 5.32 : Growth versus time for T2 glass at various temperatures.

(a = 390 °C, b = 430 °C, c = 340 °C, d = 310 °C) .

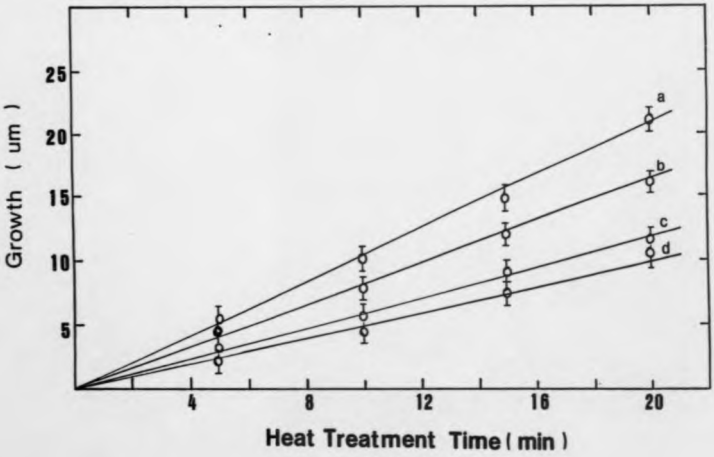

Fig.5.33 : Growth versus time for T3 glass at various temperatures.

(a = 360 °C, b = 390 °C, c = 330 °C, d = 300 °C) .

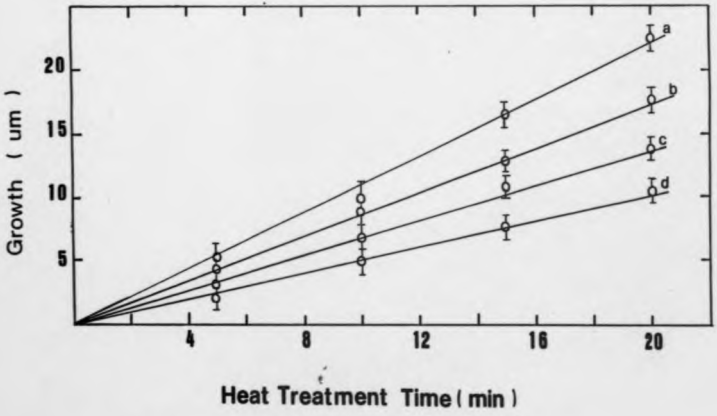

Fig.5.34 : Growth versus time for T4 glass at various temperatures.

(a = 360 °C, b = 390 °C, c = 330 °C, d = 300 °C) .

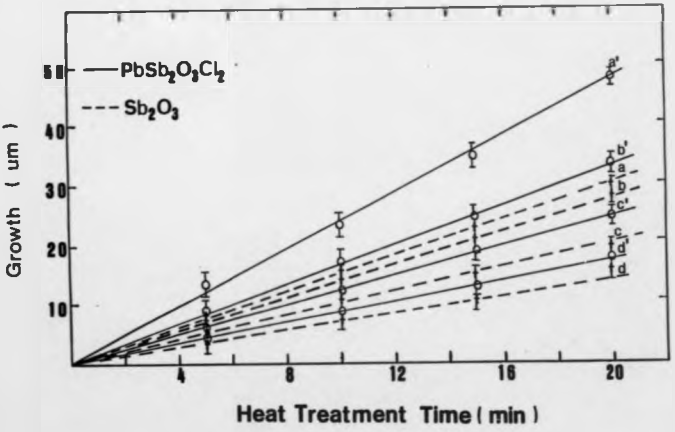

Fig.5.35 : Growth versus time for T5 glass at various temperatures.

(a = a' = 360 °C, b = b' = 390 °C, c = c' = 330 ° C,

d = d' = 300 °C) .

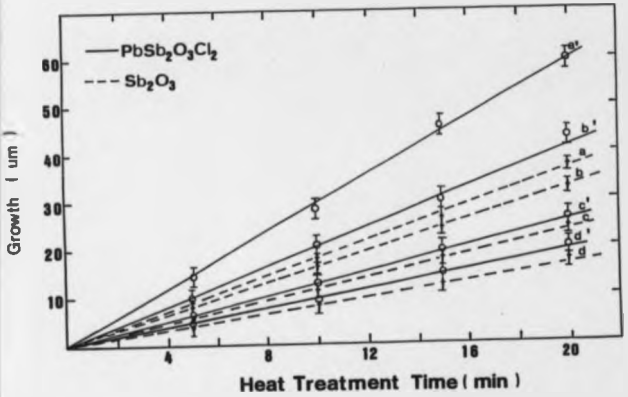

Fig. 5.36 : Growth versus time for T6 glass at various temperatures.
(a = a' = 360 °C, b = b' = 390 °C, c = c' = 330 °C,
d = d' = 300 °C).

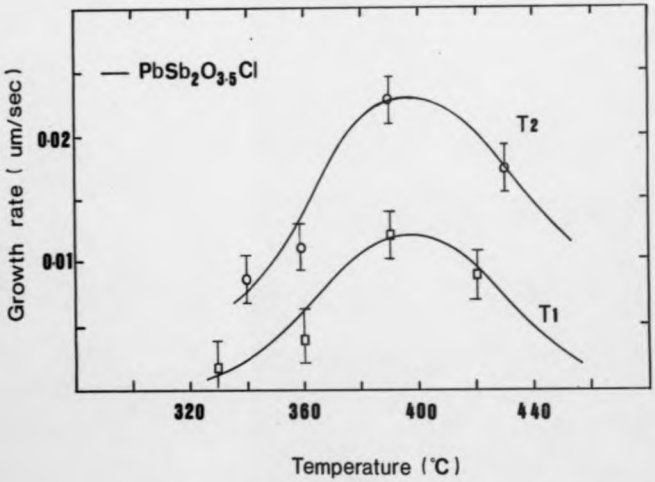

Fig. 5.37 : Growth rate - temperature curve for T1 and T2 glasses showing only the growth rate of $PbSb_2O_{3\cdot5}Cl$.

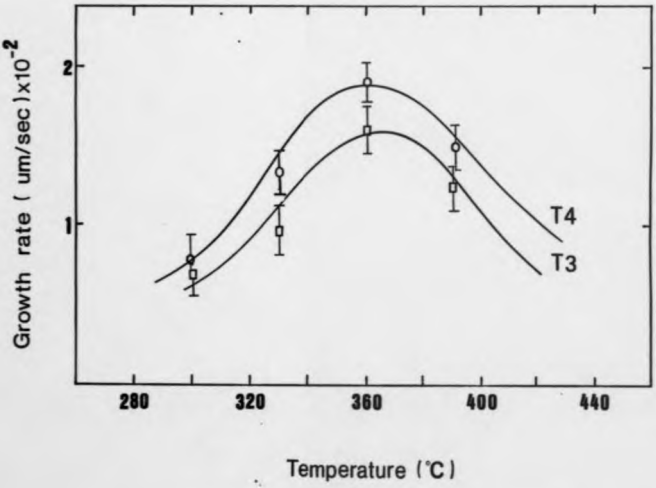

Fig. 5.30 : Growth rate - temperature curve for 13 and 14 glasses.

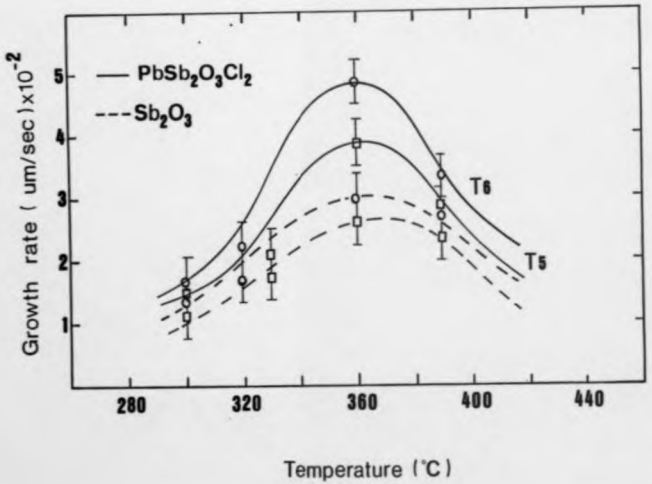

Fig. 5.39 : Growth rate - temperature curve for 15 and 16 glasses.

Sam. No.	% Cl (± 0.1)	Maximum growth rate (± 0.001) (μm sec^{-1})	log viscosity (± 0.1) (at 315 °C)
T_1	22.7	0.013	9.8
T_2	26.8	0.023	9.3
T_3	27.2	0.016	9.1
T_4	27.8	0.019	9.0
T_5	36.0	0.039	8.8
T_6	44.0	0.050	8.8

Table 5.10 : The maximum growth rates, viscosities and % Cl content for T glasses.

content act as important factors in determining the growth rate.

Another point that can be made is that the heavy metal chloride also might play a role in determining crystal morphology. This can be seen by judging the crystal shapes in figure 5.28 and 5.29 shown earlier for T_1 and T_2 respectively. However, other factors described by Holland (32) must also be involved.

Finally, from the occurrence of crystal phases observed, a tentative phase diagram of the glass stability region can be drawn. This diagram is presented in figure 5.40(a) and (b) for the glass involving $BiCl_3$ and TlCl respectively.

5.7.4 Viscosity

The viscosity was measured over the temperature range from just above Tg to slightly below Tc. The viscosity range from 10^8 P to 10^{13} P was thus measured. The relation between log viscosity and the reciprocal absolute temperature is presented in figure 5.41. As can be seen from that figure, a linear relationship between these parameters was obtained for all the glasses. It was also observed that the viscosity values were reduced with increasing " sample number ". If this result was related to the growth rate measurement (see table 5.10), it can be deduced that as the viscosity

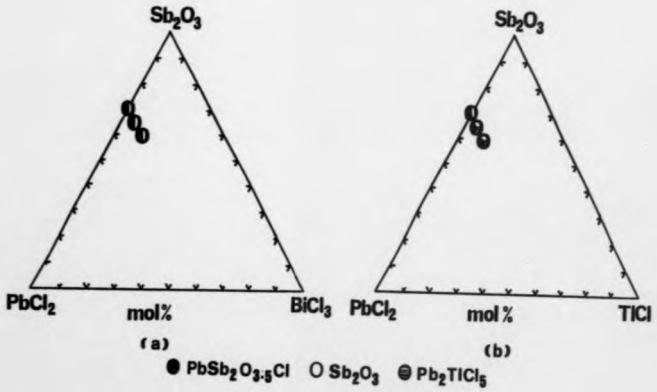

Fig. 5.40 : Phase stability region of:-

a - Sb_2O_3 - $PbCl_2$ - $BiCl_3$

b - Sb_2O_3 - $PbCl_2$ - TlCl

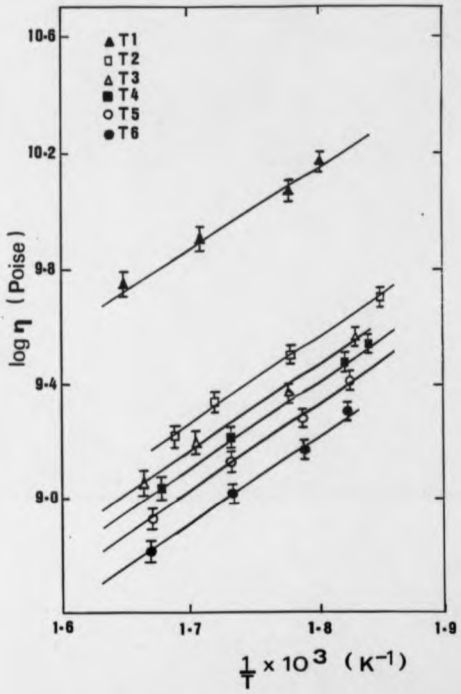

Fig. 5.41 : Log viscosity versus reciprocal of absolute temperature for T glasses.

decreases the growth rate increases. This conclusion was in agreement with the S series glass. Also, the viscosity is generally higher than in S series glasses (except for S_1). This again might be one of the effects of heavy metal chloride.

The plot of log viscosity at 315 °C against the % Cl content can be seen in figure 5.42. As the % Cl increases, the viscosity slowly decreases. As in the S series glasses, this might be due to the disruption of the glass network.

5.7.5 Chemical Durability

5.7.5.1 Effect Of Atmospheric Moisture

In general, most of the glasses without $ZnCl_2$ were moisture resistant and were not affected when exposed in normal atmospheric condition for 7 days. Only the glasses with $ZnCl_2$ were affected. The complete observations and measurements can be seen in table 5.11. In T_3 and T_4 where the % Cl was high, a very thin white layer was seen on the glass surface. This might be due to the presence of $ZnCl_2$ as well as the amount of % Cl content. This behaviour was similar to those of S series glasses. Further examination is however required.

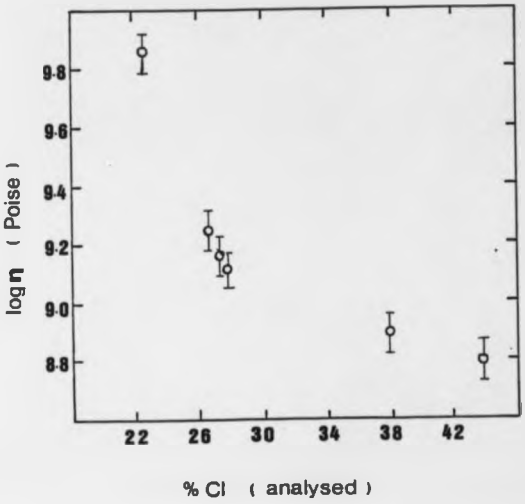

Fig. 5.42 : Log viscosity versus chlorine content for I glasses at 315 °C.

Samp. No.	Weight loss (gm cm^{-2})
T_1	$< 10^{-6}$
T_2	$< 10^{-6}$
T_3	$< 10^{-6}$
T_4	$< 10^{-6}$
T_5	1.8×10^{-5}
T_6	2.3×10^{-5}

Table 5.11 : Weight loss per unit area of T glasses when exposed to normal atmosphere for 7 days. (Error = ± 10%).

Sample No.	at % Cl (0.1)	Weight loss (gm cm^{-2})
T_1	22.7	$< 10^{-6}$
T_2	26.8	2.0×10^{-5}
T_3	27.2	5.0×10^{-5}
T_4	27.8	9.0×10^{-5}
T_5	38.0	70.0×10^{-5}
T_6	44.0	110.0×10^{-5}

Table 5.12 : Weight loss per unit area of T glasses when exposed to 100 % RH after 7 days at 25 °C. (Error = ± 10%).

When the glasses were exposed to 100 % RH, most of them were affected except for T_1. Glasses of T_2 and T_4 were affected by the condition, a medium white layer was observed and weight loss measurement shows that the glass experienced a weight loss for about 2 x 10^{-3} gm cm^{-2} over 7 days. The more detailed results are displayed in table 5.12. A few points can however be made here. If the comparison is made with a glass of S series with a comparable % Cl content, it is found that these glasses (of T series) were affected in a similar manner to the S series glasses. These results indicate that the amount of Cl plays the dominant role in the glass durability. Another point is that the glass with $BiCl_3$ seems less durable than the one with TlCl composition. This is of particular interest since, as has been discussed earlier, the glass with $BiCl_3$ gives better thermal stability than the latter composition. This result needs further attention.

5.7.5.2 Effect Of Distilled Water

In the previous section, the effect of heavy metal chloride in stabilising or destabilising the glasses has been discussed. In particular, $BiCl_3$ reduces the growth rate as well as increasing the viscosity. In this section, the effect of distilled water on the T series glasses will be examined.

When the glasses were immersed in 100 ml of distilled water with pH = 5.2 at 25 °C for 7 days, all of the glasses experienced weight lossess. The losses were higher with the glasses of higher % Cl content. The relation of these two parameters can be seen in figure 5.43. If the individual composition of the glass was examined, it was found that the glass with BiCl$_3$ seems affected more severely than the glass with TlCl. Furthermore, both of these glasses were more affected than the one with ZnCl$_2$ composition (see table 5.13). This indicates that the heavy metal chlorides lessen the glass durability.

The corrosion rates of these glasses can be seen in figure 5.44. As expected, the glass with higher chlorine content leached at a higher rate. A similar pattern was observed for all the samples ie; the corrosion front move inwards with diffusion control kinetic ie; depth α t $^{1/2}$, and hence is likely to be controlled by OH diffusion. If the comparison is made between these glasses with those of S series glasses with a comparable chlorine content, it is found that, in general, the T series glasses corroded at a higher rate than the former glasses. This may indicate that the heavy metal chloride increases the glass solubility, although the exact mechanism is not yet known, and this is somewhat at odds with the effect on thermal stability.

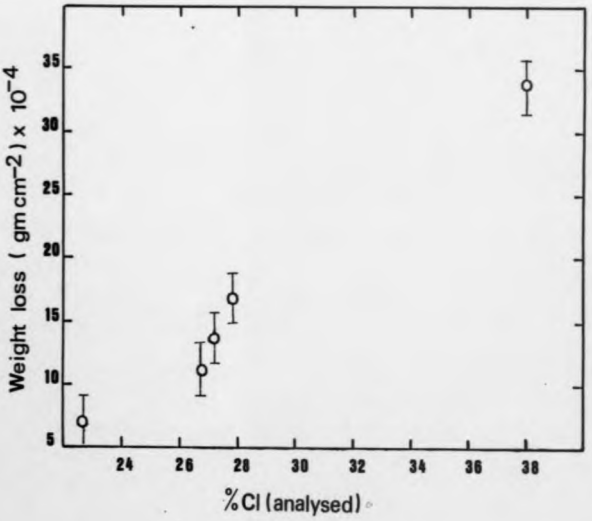

Fig. 5.43 : Weight loss versus chlorine content for I glasses when exposed to distilled water, pH = 5.2 at 20 °C for 7 days.

Samp. No.	at % Cl (± 0.1)	Weight loss (gm cm^{-2})
S_3	22.0	8.0×10^{-4}
T_2	26.8	11.0×10^{-4}
T_4	27.8	17.0×10^{-4}

Table 5.13 : Effect of heavy metal chloride on glass durability for some samples when immersed in distilled water, pH = 5.2 at 20 °C for 7 days.

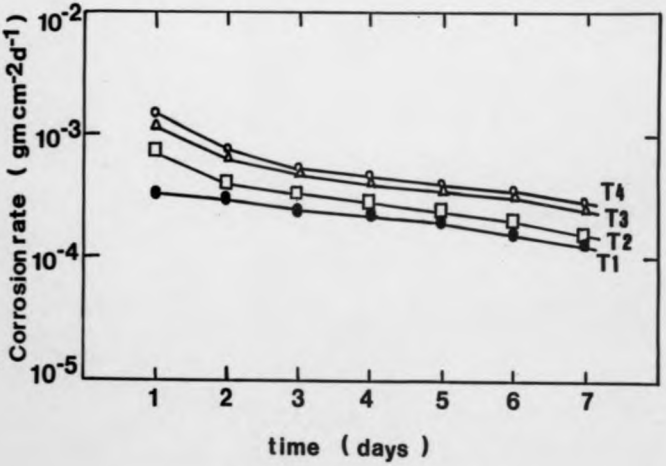

Fig. 5.44 : Corrosion rates versus time for T glasses.

5.7.5.3 Effect On Water Permeation

As in the previous study, the data suggest that the permeation of these glasses is diffusion controlled. Figure 5.45 and 5.46 show that the penetration depth increases with $t^{1/2}$. As in the case of S series glasses, the diffusion coefficient can be calculated from that graph. The detailed results can be seen in table 5.14 where the values of D are comparable with those of S_4 and S_5 glasses at about 2.2 x 10^{-8} cm^2 sec^{-1} and 6.0 x 10^{-8} cm^2 sec^{-1} respectively (see figure 5.18) but with less % Cl content. This indicates that the reaction of glass with water is not only affected by chlorine content but also the presence of heavy metal chlorides such as Bi and Tl. Replacing $ZnCl_2$ with $BiCl_3$ increases the value of D more than replacement by TlCl (table 5.14(a)). Also, the addition of $BiCl_3$ contributes more chlorine content than TlCl, thus increasing the diffusion rate.

In conclusion, the addition of $BiCl_3$ decreases the glass durability more than TlCl.

5.7.5.4 Effect On Solution pH

The temporal variation of solution pH with exposure time of the samples to distilled water pH = 5.2 at 20 °C is shown in figure 5.47. The pH values decrease rapidly at first from

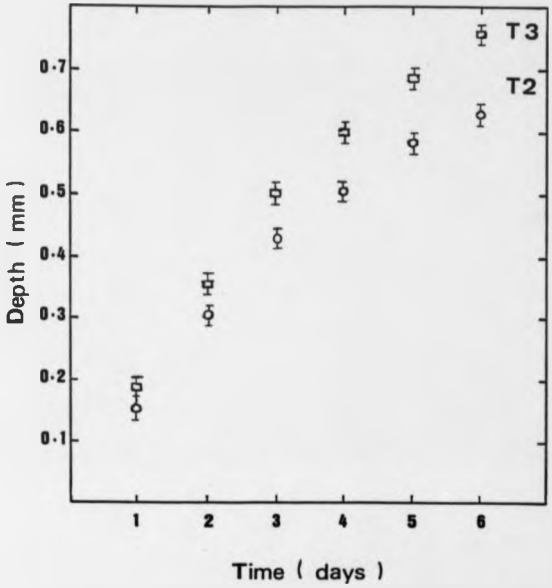

Fig. 5.45 : Penetration depth versus time for T glasses.

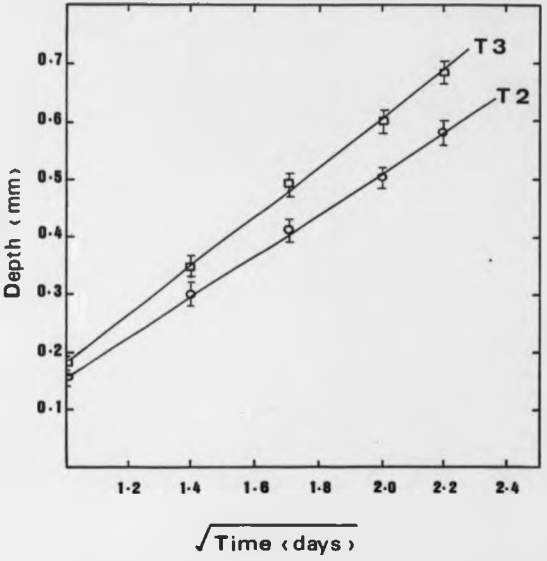

Fig. 5.46 : Penetration depth versus (time)$^{\frac{1}{2}}$ for T glasses.

Samp. No.	Diffusion Coefficient, D x 10^{-8} (cm^2 sec^{-1})
T_2	2.0
T_3	5.0

Table 5.14 : The calculated diffusion coefficients, of T glasses.

Samp. No.	at % Cl (± 0.1)	D x 10^{-8} (cm^2 sec^{-1})
S_3	22.0	0.72
S_4	26.0	1.80
T_2	26.8	2.00
T_3	27.2	5.00

Table 5.14(a) : Effect of heavy metal chloride on diffusion coefficient, D.

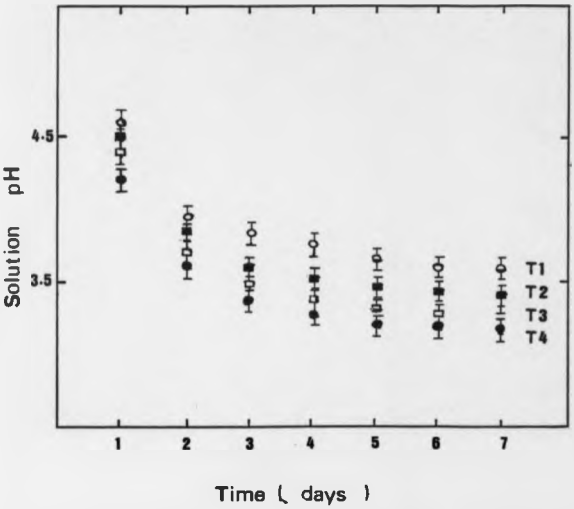

Fig. 5.47 : Temporal variation of solution pH of T glasses when exposed to static distilled water for different times (days) .

about (4.7 - 4.3) in the first day to (4.0 - 3.6) in the second day and then begins to plateau (3.6 - 3.2) in the seventh day (the pH values refers to T_1 to T_4). The reduction of the pH was expected, and was due to the increase in the H^+ concentration in the solution arising from the diffusion of H^+ to the solution during the corrosion process. In comparison to the S glasses, the pH values of T glasses decrease faster indicating that the diffusion rate is faster. It has been proposed that the major factor that contributes to the pH drop is disturbance of glass network releasing Cl^- and H^+ to the solution. The question now is how much amount of Cl^- correspond to the amount of H^+ diffused into the solution. This will be discussed in the later section.

5.7.5.5 Effect On The Surface Water Content

The infrared examination of the corroded layer of glasses from T_2 and T_3 (represented by $T_{2'}$ and $T_{3'}$ respectively) are shown in figure 5.46. From this, it is obvious that the absorption around 3500 cm^{-1} which is due to OH stretching vibration appears as a broad peak in both glasses. As in the case of S series glasses, the data indicate that OH stretching band grows faster than the one by HOH bending vibration. As in S glasses, the existence of an absorption peak around 350 cm^{-1} is due to lead (II) hydroxyl groups. Also, this peak seems more striking in the glass with high

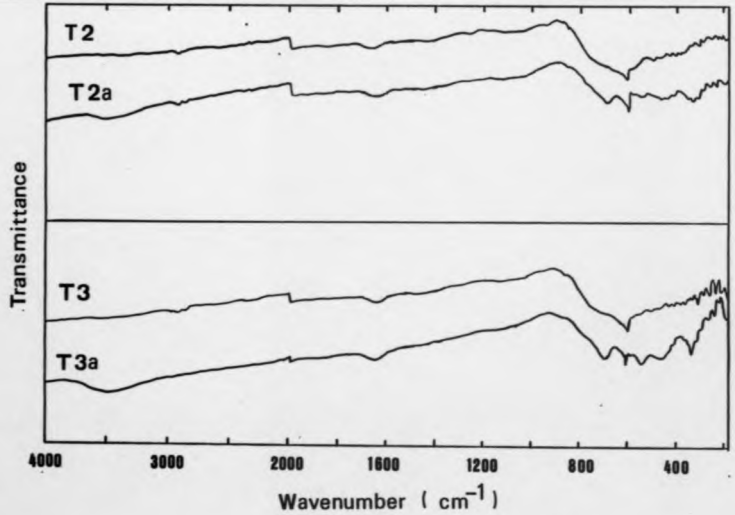

Fig. 5.48 : IR spectra with CsI of the corroded layer (labelled " a ") of T2 and T3 glasses after being exposed to distilled water, pH = 5.2 at 20 °C for 7 days.

chlorine content. This may indicate that this peak is due to a compound of metal hydroxyl chloride.

5.7.5.6 Effect On Surface Structure

Again, the technique of Scanning Electron Microscopy (SEM) has been employed to assess the appearance of the corroded glass surface. These microstructures are displayed in figures 5.49 and 5.50 for glasses T_2 and T_3 respectively. Both of the glasses were immersed in 100 ml of static distilled water for 7 days at 20 °C. Figure 5.49 shows a corroded glass layer (A) with a clear crystal precipitate on the surface. This precipitate consists of crystals spread over the surface (B). When the corroded layer was removed (C), the surface still shows effect of corrosion but no crystal deposit is seen. Figure 5.50 shows the glass T_3 surface before the corrosion test was conducted (as polished) (A), and (B) is the glass surface after corrosion took place. The crystal precipitate on the corroded layer can be seen to cover the entire surface.

Both glasses show similar crystal shapes distributed all over the surface. These deposits were identified by means of XRD as well as EDX analysis. The XRD results (see figure 5.51) show that the corroded layer consist of two crystal phases. The phases were found to be Sb_2O_3 and " $PbSbO_2Cl$ " with again different lattice parameter from the crystallised

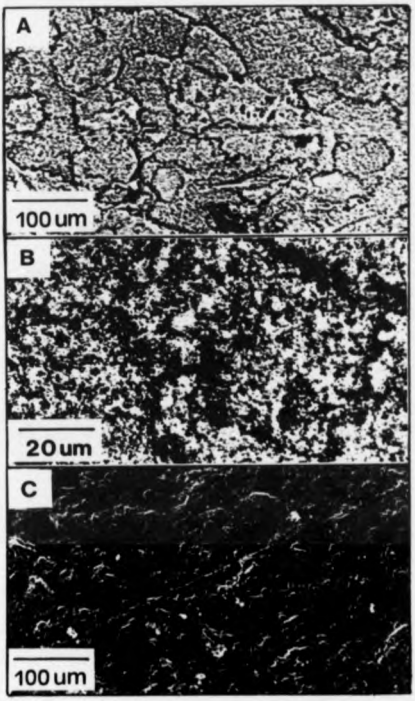

Fig. 5.49 : Microscopic appearance of water attacked surface layer of T1 glass.

A - Corrosion surface and crystalline layer.

B - Magnified corroded surface showing crystal deposits

C - Surface after removal of corroded layer.

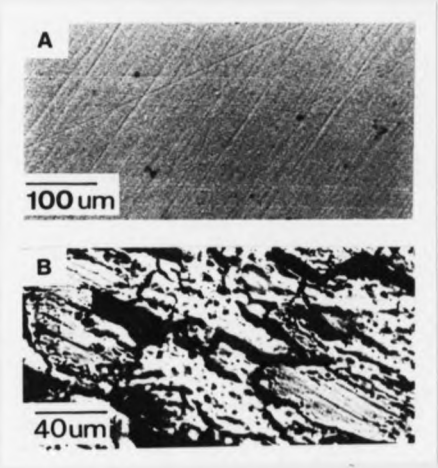

Fig. 5.50 : Micrograph of T3 glass .

A - as polished

B - corroded layer with crystal deposits.

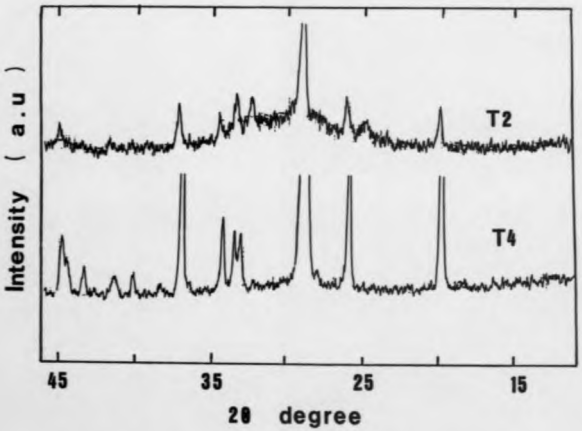

Fig. 5.51 : X - ray diffraction pattern of the corroded layer of T glasses.

with again different lattice parameter from the crystallised glass, differences, again suggesting that other groups such as OH must be involved. EDX analysis shows that the crystal precipitates are Sb_2O_3 and $PbSb_2O_{6-x}Cl$. Assuming that OH groups are involved in the process (as for S glasses), it is suggested that the corroded layer consists of $PbSb_2O_{6-x-n}(OH)_nCl$, where n has a values which depends on the chlorine content. The full results are given in table 5.15. The existence of this compound is also consistent with the IR Spectroscopy analysis discussed earlier. The corroded layer was very thick and porous and was seen to experience some cracking due to dehydration in the oven for a few hours.

One point that should be noted here is that the phase Pb_2TlCl_5 was not observed in the surface corrosion product. This may mean that the heavy metal chloride shows greater chemical durability. Another thing is that both glasses of T and S series show a similar type of corrosion and give a similar crystal precipitation. This means that the chemical durability of the glasses still depend much on the % Cl content.

5.7.5.7 Effect On Corrosion Mechanism

To determine the exact process which occurs during corrosion is very difficult. Only for silicates is the corrosion mechanism largely understood (14,15,24,25). Others,

Sam. No.	XRD Analysis		EDX Analysis		Suggested	
	Major	Minor	Major	Minor	Major	Minor
T_1	$PbSbO_2Cl$	Sb_2O_3	$PbSb_2O_{3.5}Cl$	Sb_2O_3	$PbSb_2O_3(OH)Cl$	Sb_2O_3
T_2	"	"	"	"	"	"
T_3	"	"	"	"	"	"
T_4	"	"	"	"	"	"
T_5	"	"	$PbSb_2O_3Cl_2$	.	$PbSb_2O_2(OH)_2Cl_2$	"

Table 5.15 : The phase occurrence in corrosion deposits identified by XRD and EDX analysis. The last column represents the suggested phase. (Note : No Bi was detected (negligible) during EDX analysis).

including fluoride or fluorozirconate or oxyhalide glasses are unclear or still in the stage of modelling. However, the collection of data obtained from the experiment on the corrosion layer will at least give some supportive evidence to the corrosion mechanism which will be presented below.

As in the S glasses, T glasses also experience the water permeation which is diffusion controlled (penetration depth increases with $t^{1/2}$). A decrease in pH indicates the diffusion of H^+ into the solution and it was also found that Cl^- diffuses into the solution.

Chloride concentration was measured spectroscopically (28), the concentration of hydrogen ions using a pH electrode and cation of Pb^{2+} by chemical analysis (29). The results can be seen in table 5.16. Calculation shows that the ratio of Cl^- : H^+ : Pb^{2+} is approximately 4 : 2 : 1. Using these results, the reactions mechanisms in glasses without $BiCl_3$ (T_1 and T_2 glasses) might be expressed as in equation (5.4) for the S glasses. No Tl^+ was detected, therefore the glass structure involving Tl can be omitted in the equation.

Glasses containing $BiCl_3$ (T_3 and T_4) are quite interesting. Spot tests had shown that no Bi^{3+} was detected when the mol % of $BiCl_3$ was small. However, when the $BiCl_3$ content was increased, the Bi^{3+} was suddenly detected (see

Sample No.	Concentration (mol / litre) x 10^{-4}		
	* Cl^-	H^+	* Pb^{2+}
T_1	21.8	10.9	5.1
T_2	28.2	14.8	6.3
T_3	38.7	19.2	8.8
T_4	52.9	26.0	13.2

Table 5.16 : Quantitative analysis of some ions present in solution after 4 days soak time of T series glasses.

* - Spectroscopy method (28)

* - Chemical analysis method (29)

Spot Test in table 5.4). This suggests another reaction mechanism involving Bi - Chlorine polyhedra.

The crystal structure of $BiCl_3$ consists of a bismuth atom closely associated with three chlorine atoms in the shape of a distorted trigonal pyramid, with five other chlorine atoms at bridging distances. The geometry of this eightfold coordination is best described as a trigonal biprism with six chlorine atoms at its corner, and with two more chlorine atoms in face - bridging position (33). It is reported that the IR cut off in $BiCl_3$ - KI glasses is due to the asymmetric stretching frequency for the quasi - lattice subunits of $BiCl_{4}^{-}$ (34). Thus, the reaction mechanisms should involve this structure. It is however very difficult to measure the amount of Bi^{3+} in the present of Pb or Zn since they chemically belong to the same group. Also, very little Bi (negligible) was detected by EDX analysis on the corroded layer which suggests that the corrosion reaction must resulted in no Bi^{3+} in the corroded layer.

For glass containing $ZnCl_2$ as in T_5, the corrosion mechanism is expected to be as in the S series glasses since both Zn^{2+} and Pb^{2+} were detected and TlCl was not.

The OH groups which are products of both equations are found to be associated with metal hydroxide groups rather than

belonging to HOH bending groups. This was also indicated by IR Spectroscopy.

From the above discussions, it is clear that the heavy metal chloride has some effect on the corrosion mechanism and thus on glass durability. Of particular interest is the role of $BiCl_3$ which not only acts as a contributor to the chloride content in the glass but is also directly involved in the corrosion mechanism. Unlike TlCl (where Tl itself apparently does not play an important role in durability), a certain amount of $BiCl_3$ (in this case 10 mol %) seems able to reduce the durability of glass. The effect of heavy metal chloride in reducing the durability, can be ranked in the order of Bi > Pb > Tl. In other words, the higher the atomic number, the less durable the glass will be. It partly reflects the greater contribution to the % Cl content.

The above results show that addition of a more heavy chloride to the glass will reduce the solution pH and increases the weight losses resulting from a low durability , lower than the S series glasses with similar amounts of chlorine.

5.8 SILLEN PHASE COMPOSITIONS

The Sillen phases have the general formula ABO_2X where A is Pb or alkali-earth atom and B is Sb, X being halogen (in this case Cl) (35). Our results show some modification to the phase formula with a systematic change in Sillen phase from $PbSb_2O_{3.5}Cl$ to $PbSb_2O_{4.5}Cl_3$ being observed with increasing chlorine content of the glass. The occurrence of the different phases as a function of oxygen : chlorine ratio in the glass is indicated in table 5.17.

Over O:Cl of 3.6, the only crystal phase is Sb_2O_3 which is orthorhombic and contains $[SbO_3]$ pyramidal units. Hasegawa et. al (36) suggested that the glass also contains chains of $[SbO_3]$ pyramids.

For O:Cl ratio between 3.00 and 3.60, the phase $PbSb_2O_{3.5}Cl$ is formed. This is now tetragonal and it has been suggested that the Sillen phase contains $[SbO_4]$ square pyramidal units.

For O:Cl ratio between 1.8 and 1.9, the phase is $PbSb_2O_3Cl_3$ and for a ratio from 0.65 to 0.84, the phase is $PbSb_2O_{4.5}Cl_3$. It would appear that there is no gradual change in stoichiometry of these phases. Further work is needed to study the crystal structure of these Sillen phases in detail and additionally to relate the structural units in the crystal to those which may occur in the glass.

Sillen Phase	O:Cl ratio +	O:Cl ratio *
Sb_2O_3	-	> 3.60
$PbSb_2O_{3.5}Cl$	3.50	3.00 - 3.60
$PbSb_2O_3Cl_2$	1.50	1.60 - 1.90
$PbSb_2O_{2.5}Cl_3$	0.83	0.65 - 0.84
$PbCl_2$	0.00	< 0.16

Table 5.17 : Sillen phase as a function of O:Cl ratio.

\+ - From crystal phase formulae.

* - From glasses where crystal phase formed.

References

1. Ahmad, M.M. and Holland, D. ; Glass. Tech. vol.28,no 3 (June 1987).
2. Azaroff, L.V. : Elements of X-ray Crystallography, Mc Graw Hill, New York (1968).
3. JCPDS Data Card ; Entry number : 17 - 469.
4. Dubois,B., Videau, J.J., Couzi, M. and Portier, J. ; J. Non - Cryst. Sol. 88 (1986) 355-365.
5. Chalmers, B. ; The Principal Of Solidification, Wiley New York (1964).
6. Hillig, W.B. and Turnbull, D. ; J. Chem. Phys. 24 (1956) 4.
7. Ahmad, M.M. and Holland, D. ; Mat. Sci. Forum, 19-20 (1987) 87.
8. Goldstein, M. and Nakonecznyj, M. ; Phys. Chem. Glasses 6 (1965) 126.
9. McMillan, P.W. ; Glass - Ceramics, 2nd ed., Acad. Press (1979) p 54.
10. Gonzales - Oliver, C.J.R., Johnson, P.S. and James, P.F. ; J. Mat. Sci. 14 (1979) 45-48.
11. Zhonghong, J., Xinyuan, H. and Lisong, H. ; J. Non - Sol. 80 (1986) 543-549.
12. Gorre, L.E. and Pastor, R.C. ; Mat. Res. Bull. vol. 18 (1983) 1391-1398.
13. Simmons,C.J. and Simmons, J.H. ; J. Amer. Ceram. Soc. 69 (9) (1986) 681-689.

14. Tomozawa, M., Ito, S. and Molenelli, J. ; J. Non - Cryst . Sol. 64 (1984) 269-278.

15. Scholze, H. ; Naturwiss. 47 (1960) 226.

16. Toulloc, M.L., Simmons, C.J. and Simmons J.H., ; J. Amer.Ceram. Soc. 71 4 (1988) 219-224.

17. Miller, P.J. and Cody, C.A. ; Spectrochim. Acta 38A (1982) 555.

18. Maroni, V.A. and Spiro, T.G. ; J. Amer. Chem. Soc. 89, 1 (Jan. 4, 1967) 45-48.

19. Ogden, J.S. and Ricks, J.M.; J. Chem. Phys., vol.56, no. 4, (Feb. 1972) 1658.

20. Loehr, S.R., Bruce, A.J., Mossadegh, R., Doremus, R.H. and Moynihan, C.T. ; Mat. Sci. Forum, 5 (1985) 311.

21. Lippincott, E.R., Psellos, J.A. and Tobin M.C. ; J. Chem. Phys. 20 (1952) 536.

22. Clark R.J.H. and Dunn, T.M. ; J. Chem. Soc. (1963) 1198.

23. Simmons, C.J. , Sutter, H., Simmons, J.H. and Trans, D. C., ; Mat. Res. Bull., 17 (1982) 1203.

24. Scholze, H. ; J. Non - Cryst. Sol. 52 (1982) 91-103.

25. Tomozawa, M. ; J. Non - Cryst. Sol. 73 (1985) 197-204.

26. Seddon, A.B. ; Fluoride Glasses, ed. by: Alan E. Comyn (chapter 7). John Wiley & Sons, (1989).

27. Feigl, F. ; Spot Test in Organic Analysis, Elsvier Pub. Comp., Lond. (1956).

28. Snell, F.D., Snell, C.T. and Snell, C.A. ; Calorimetric Methods Of Analysis, vol 11A, D. Van Nostrand Co. Ltd. New York, 1959.

29. Vogel, A.I. ; Quantitative Inorganic Analysis, 3rd ed. Longmans, 1961.

30. Baldwin, C.M., Almeida, R.M. and Mackenzie, J.D. ; J. Non - Cryst. Sol. 43 (1981) 309-344.

31. Rao, B.G. and Rao, K.J. ; Phys. Chem. Glasses, vol. 25, no.1 (Feb. 1984) 11-15.

32. Holland, D. ; Physics World, (Oct. 1988) p41.

33. Nyburg, S.C., Ozin, G.A. and Szymanski, J.T. ; Acta Cryst. B27 (1971) 2298.

34. Angell, C.A. and Zeigler, D.C. ; Mat. Res. Bull. vol.16, (1981) 279-283.

35. Sillen, L.G. ; Naturwissensch 30 (1942) 420.

36. Hasegawa, H., Sone, M. and Imaoka, M. ; J. Phys. Chem. Glasses, vol 19, no 2 (1978) 28-33.

37. Paul, A. ; Chemistry Of Glasses, Chapman And Hall (1982) p 81.

CHAPTER 6 : CONCLUSION

6.1 INTRODUCTION

In this chapter, some of the conclusions that can be made will be summarised. The conclusion will be divided into three parts: the thermal studies; crystallisation and microstructural studies; and finally the chemical durability studies.

6.2 Thermal Studies

Stable oxychloride glasses from the system of Sb_2O_3 - $PbCl_2$ - $ZnCl_2$ have been studied. The glass composition of 70 % Sb_2O_3 - 30 % $PbCl_2$ up to 20 % Sb_2O_3 - 30 % $PbCl_2$ - 50 % $ZnCl_2$ have been prepared. Additions of a fourth component such as $BiCl_3$ and TlCl have been made successfully. From these studies, some conclusions can be summarised as follows;

1. A thermal stability range (Tc - Tg) up to 148 °C can be achieved. This range is greater than some known fluorozirconate glasses (1).

2. Introducing more chloride into the system reduces the thermal stability range. The values of Tg and Tc were also reduced. This effect was also observed in the system PbO -

GeO_2 - $PbCl_2$ (2). Other properties such as thermal expansion were also affected (3).

3. Addition of a heavier metal chloride such as TlCl or $BiCl_3$ as the fourth component does not affect the thermal stability except that the chlorine content is increased.

4. Judging from the Tc - Tg gap, it seems that the addition of $BiCl_3$ stabilises the glass more than TlCl. In quaternary systems of 35 % Sb_2O_3 - 30 % $PbCl_2$ - 30 % $ZnCl_2$ - 5 % TlCl, Tc - Tg > 100 °C were achieved.

6.3 Crystallisation And Microstructural Studies

1. The study of the crystallisation process in these oxychloride glasses shows that there are two major phases produced. One is Sb_2O_3 of valentinite type and the other based on $PbSbO_2Cl$ of the Sillen type phase. These results are consistent with those of Dubois et al. (4) except that EDX analysis shows that the second phase is in the form of $PbSb_2O_xCl_{5-x}$ with x = 3.5 to 2.5. That is, there is a variation in oxygen content as well as the chlorine. This result was supported by the IR investigation.

2. $ZnCl_2$ only acts as a chlorine source for crystal growth. Zn itself does not participate in crystallisation.

3. Glasses without $ZnCl_2$ show a morphology with the form of a " stretching fibre " while the others show various morphologies. For more than 40 % $ZnCl_2$, crystal structure determination is hampered by chemical attack.

4. The addition of heavy metal chloride affects the crystallisation process. The occurrence of Pb_2TlCl_5 provides an example. Although the concentration of chlorine is a crucial factor, the role of a heavy cation must also be taken into account.

6.4 Growth Rates And Viscosity

1. All glasses show constant crystal growth rates for times < 1 hour. After that, the rate decreases and growth ceases after about 4 hours of heat treatment time. The maximum growth rate increases with chlorine content from 0.01 $\mu m\ sec^{-1}$ up to 0.18 $\mu m\ sec^{-1}$ and T_{max} (the temperature corresponding to maximum growth rate) decreases as chlorine content increases. The inclusion of heavy metal chloride produces an increase in growth rate by virtue of the increase in chlorine content.

2. Viscosity is an obvious chlorine controlled process. As the chlorine content increases, the viscosity decreases. However, there are indications that the inclusion of heavy

metal chloride increases the viscosity. This requires further investigation.

3. The decrease in viscosity leads to an increase in growth rates,in agreement with many studies (5). Other factors such as the presence of impurities including OH^- ions in the glass composition cannot be neglected.

6.5 Chemical Durability

1. Most glasses without $ZnCl_2$ were practically moisture resistant.

2. Most glasses experienced weight losses when immersed in distilled water. The glass with $BiCl_3$ was the most severely affected, more than the glass with TlCl or $ZnCl_2$.

3. Unlike silicate glasses where the corrosion process occurs by competing mechanisms of ion exchange and matrix dissolution (8) and fluorozirconate glasses where the process is dominated by matrix dissolution and little influenced by ion exchange (7), the data here suggest that the oxychloride glasses corrode by the diffusion of H^+ and Cl^- ions, as well as cations, from the glass bulk to the solution(thus decreasing the solution pH). The diffusion rate (indicated by the diffusion coefficient) was higher in the glass with high chlorine content (except for glasses

with heavy metal chloride). However, the durability of these glasses were slightly better when compared to poor soda silicates (see figure 6.1) and to those of Ba - Th based glasses (8).

4. The corrosion rates depend on the chlorine content and increase as the % Cl increases. Also, the corrosion rate is relatively faster in the first day and gradually becomes slower after a few days (see figure 6.2).

5. Under static conditions, the corroded glass was covered by corrosion product. This layer acts as a partial diffusion barrier and reduces the corrosion rate. The highly porous, thick hydrated layer situated on the uncorroded glass surface is identified by XRD technique as a mixture of Sb_2O_3 and " $PbSbO_2Cl$ " of the Sillen type phase.

6. The schematic corrosion mechanisms for the glasses can generally be written as:

$$M\,[\,PbO_2Cl_4 + 4\,H_2O\,]\,(g) \longrightarrow 4M\,Cl^-\,(s) + 2M\,H^+\,(s) + M\,Pb^{++}\,(s) + 6M\,[OH]\,(g).$$

and the glasses with Zn^{++} show the additional process:

$$M\,[\,ZnCl_4 + 2\,H_2O\,]\,(g) \longrightarrow 4M\,Cl^-\,(s) + 2M\,H^+\,(s) + M\,Zn^{++}\,(s) + 2M\,[OH]\,(g).$$

g - glass s - solution

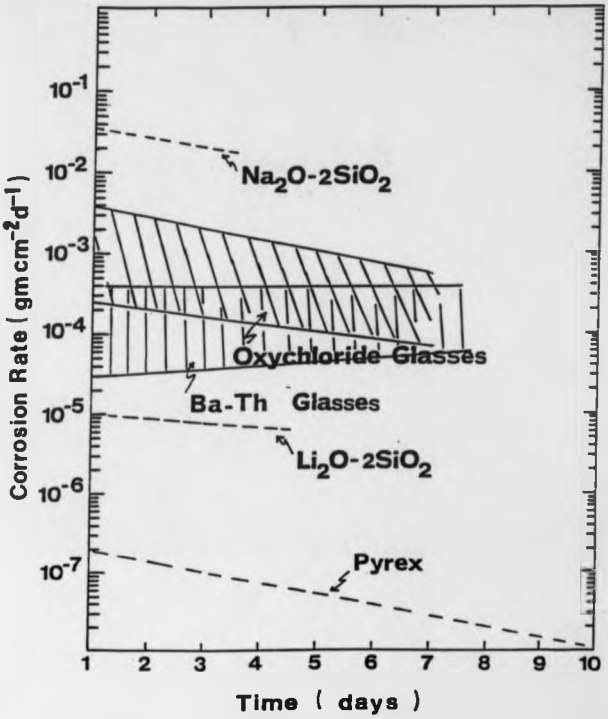

Fig. 6.1 : Comparison of the glass durability for some known glasses (7), showing the position of oxychloride glasses.

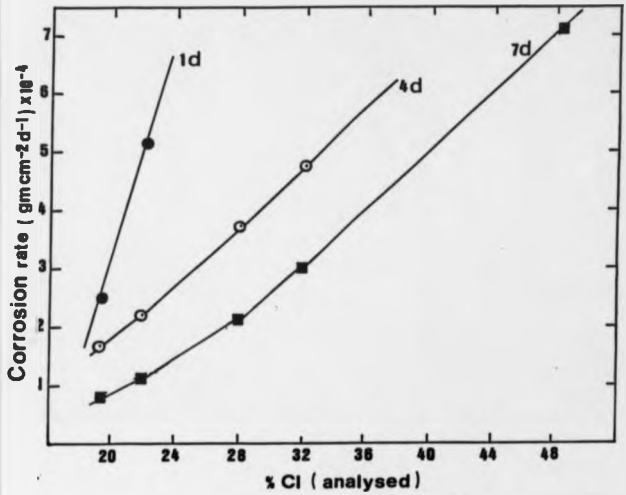

Fig. 6.2 : Corrosion rates versus chlorine content for different soak times (days). The corrosion rates decreased after the first day and was strongly dependent on the chlorine content.

7. The schematic corrosion equations show that [OH] bonded remains on the corroded glass surface. IR investigation shows that it is in the form of metal hydroxyl groups rather than molecular HOH. This was supported by the appearance of the lead (ii) hydroxide absorption bands near 350 cm^{-1} as well as $(Zn(OH)_4)^{2-}$ in the region of (250 - 300) cm^{-1}. Thus, it was believed that the units present are of the form of $PbSb_2O_{6-x}(OH)_xCl_x$ and $Zn_n(OH)_{2n-x}Cl_{x+1}$ (for S_7 and S_8) where n depends on the chlorine content. This conclusion was supported by XRD and EDX analysis.

8. Although the addition of heavy metal chloride does not seems to affect the thermal stability, it does affect the chemical durability. Other factors, including the presence of impurities such as OH^- or water in the glass composition will also reduce the durability as suggested by Tomozawa et al. (9).

References

1. Parker, J.M., Saddon, A.B. and Clare, A.G. ; Phys. Chem. Glasses, vol. 28, no 1 (Feb. 1987) 4-10.
2. Ahmed, M.M. and Holland, D. ; Mater. Sci. Forum, vol.5 (1985) 175-188.
3. Ahmed, M.M. and Holland, D. ; Glass Tech., vol 28, no 3 (June 1987) 141-144.
4. Dubois, B., Videau, J.J., Couzi, M. and Portier, J. ; J. Non - cryst. Sol. 88 (1986) 355-365.
5. Hillig, W.B. and Turnbull, D. ; J. Chem. Phys. 24 (1956) 4.
6. Scholze, H. ; J. Non - Cryst. Sol. 52 (1982) 91-103.
7. Simmons, C.J. and Simmons, J.H. ; J. Am. Ceram. Soc. 69, 9 (1986) 661-668
8. Simmons, C.J., Sutter, H., Simmons J.H. and Tran D.C. ; Mat. Res. Bull. vol 17 (1982) 1203-1210.
9. Tomozawa, M., Takata, M., Acocella, J., Watson, E.B. and Takamori, T. ; J. Non - Cryst. Sol. 56 (1983) 343.

CHAPTER 7 : FUTURE WORK

One of the aims of this thesis is to suggest future work to find more evidence to support the conclusion of this work and also to extend measurements to other glass compositions. The suggestions may be summarised as follows;

1. Since these glasses have shown fairly wide formation ranges and some reasonable thermal as well as optical properties, it is suggested that the TeO_2 and GeO_2 analogue to Sb_2O_3 system should be studied. These compositions might give glasses with higher IR transmission and could improve optical properties. Quaternary systems should also be further explored.

2. A detailed study of the kinetics of nucleation and crystallisation of the glasses in relation to chlorine content is suggested. This study will provide more information about the thermal stability of the glasses.

3. The dependence of the kinetics of hydrated surface layer development on glass composition and its correlation with the dissolution rate of the glass should be studied. This will give information on corrosion mechanisms and their dependence on composition.

4. The effect of solution pH on glass corrosion has not been covered in the present study. This is important since glass applications may require a range of ambient conditions.

5. Magic angle spinning NMR may be used to study the OH and H_2O environments in the glass during corrosion and hence give further indication of the corrosion mechanism.

Appendix 1

Example of the calculation to find the composition of the actual glass from the EDX data.

e.g. Nominal glass composition : 70% Sb_2O_3 - 30% $PbCl_2$

Actual glass	:	Pb^{2+}	Sb^{3+}	Cl^-	O^{-2}
Atomic percentage (from EDX)	:	13.48	64.65	19.8	100.56*

* - calculation

By assuming that Pb and Sb have valencies 2^+ and 3^+ respectively and then balancing the formal charges for anions and cations we require 100.56 oxygen atoms to be present in the system.

a. Assuming oxygen atoms are preferentially attracted to Sb atoms.

64.65/2 Sb formed ---> 32.32 molecules of Sb_2O_3.

Thus, 32.32 x 3 = 96.96 oxygen atoms have been used

and Σ O left = 100.56 - 96.96 = 3.6

b. Pb ---> O

3.6 O present as 3.6 PbO i.e. used 3.6 Pb

thus, Σ Pb left = 13.48 - 3.6 = 9.88 Pb.

Thus, 9.88 Pb present as 9.88 $PbCl_2$.

So, the actual glass is :

(32.32 / (32.32 + 9.88 + 3.6) x 100% = 70.56% Sb_2O_3

and 29.44% Pb(O,Cl)